Advances in designing of polymeric micelles for biomedical application in brain related diseases

Jaskiran Kaur[a], Monica Gulati[a,b], Bhupinder Kapoor[a], Niraj Kumar Jha[b], Piyush Kumar Gupta[c], Gaurav Gupta[d], Dinesh Kumar Chellappan[e], Hari Prasad Devkota[f], Parteek Prasher[g], Md Salahuddin Ansari[h], Faris F. Aba Alkhayl[i,j], Mohammed F. Arshad[k], Andrew Morris[l], Yahya E. Choonara[m], Jon Adams[b], Kamal Dua[b,n], Sachin Kumar Singh[a,b]*

[a]*School of Pharmaceutical Sciences, Lovely Professional University, Phagwara 144411 Punjab, India*

[b]*Faculty of Health, Australian Research Centre in Complementary and Integrative Medicine, University of Technology Sydney, Ultimo, NSW 2007, Australia*

[b]*Department of Biotechnology, School of Engineering & Technology (SET), Sharda University, Plot No.32-34 Knowledge Park III Greater Noida, Uttar Pradesh, 201310, India*

[c]*Department of Life Sciences, School of Basic Sciences and Research, Sharda University, Plot no. 32 - 34, Knowledge Park III, Greater Noida - 201310, Uttar Pradesh, India*

[d]*School of Pharmacy, Suresh Gyan Vihar University, Mahal Road, Jagatpura, Jaipur, India*

[e]*School of Pharmacy, International Medical University, Bukit Jalil, 57000, Kuala Lumpur, Malaysia*

[f]*Graduate School of Pharmaceutical Sciences, Kumamoto University, 5-1 Oehonmachi, Kumamoto 862-0973, Japan*

[g]*Department of Chemistry, University of Petroleum & Energy Studies, Energy Acres, Dehradun-248007, India*

[h]*Department of Pharmacy Practice, College of Pharmacy, Shaqra University, Aldawadmi, Saudi Arabia*

[i]*Department of Pharmaceutical Chemistry and Pharmacognosy, College of Dentistry and Pharmacy, Buraydah Colleges, Buraydah, Kingdom of Saudi Arabia*

[j]*Department of Medical Laboratories, College of Applied Medical Sciences, Qassim University, Buraydah, Kingdom of Saudi Arabia*

[k]*Department of Research and Scientific Communications, Isthmus Research and Publishing House, New Delhi, 110044, India*

[l]*Swansea University Medical School, Room 262, 1st Floor, Grove Building, Swansea University, Singleton Park, Swansea, Wales, SA2 8PP*

[m]*Wits Advanced Drug Delivery Platform Research Unit, Department of Pharmacy and Pharmacology, School of Therapeutic Sciences, University of Witwatersrand, 7 York Road, Parktown, Johannesburg 2193, South Africa*

[n]*Discipline of Pharmacy, Graduate School of Health, University of Technology Sydney, Ultimo, NSW 2007, Australia*
***Corresponding Author:** Name: Sachin Kumar Singh; Address: School of Pharmaceutical Sciences, Lovely Professional University, Phagwara - 144411, Punjab, India. **E-mail address**: singhsachin23@gmail.com

Abstract

In recent years, unique physicochemical properties of amphiphilic block copolymers have been utilized to design the polymeric micelles for brain-specific delivery of drugs, proteins, peptides and genes. Their unique properties such as nano-size, charge-switching ability, stimuli-responsive cargo release, flexible structure, and self-assembly enable them to overcome limitations of conventional dosage forms that include rapid drug release, drug efflux, and poor brain bioavailability, and poor stability. These limitations hinder their therapeutic efficacy in treating brain diseases. Their ease of functionalization and enhanced penetration and retention effect make them suitable nanocarriers for the diagnosis of various brain diseases. In this context, the present manuscript provides an insight into the progress made in the functionalization of micelles such as the incorporation of stimuli-sensitive moieties in copolymers, conjugation of cargo molecules with the core-forming block via responsive smart linkers, and conjugation of active ligands and imaging moieties with the corona forming block for brain targeting and imaging. Further, the review also expounds on the role of polymeric micelles in delivering neurotherapeutic to the brain. Some patents related to polymeric micelles formulated for brain delivery are also enlisted.

Keywords: Amphiphilic polymers; Brain targeting; Functionalization; Polymeric micelles

Table of contents

1. Introduction

The brain is a delicate organ of the central nervous system (CNS) that interprets the senses, initiates body movements, controls cognitive functions, considers learning and memory as well as maintains active functions [1,2]. As per WHO, neurological disorders are considered a detriment to public health, across the globe [3]. The prevalent CNS disorders are Alzheimer's disease, Parkinson's disease, epilepsy, glioma, brain traumatic injury, schizophrenia, and many more [4,5]. Certain factors including aging, lifestyle habits, physical injuries, environmental factors, mutation, and exposure to chemicals or toxins are supposed to be responsible for neurological disorders [5–8]. As a result, these disorders cause structural and functional deficiencies that require additional medical treatment and prolonged care [9].

Therefore, the effective management of CNS diseases is a challenging task due to various physiological barriers that impede the delivery of payloads. These physiological barriers include blood-brain barriers (BBB), blood-cerebrospinal fluid (CSF), blood-retinal barrier, and blood-spinal cord barrier [9,10]. Among all the barriers, BBB appears as a stronger one that hinders the passage of harmful and noxious substances from the bloodstream and maintains

brain homeostasis [11,12]. It is a semi-permeable barrier composed of astrocytes, endothelial cells, tight junctions, neurons pericytes, and basal membrane [11,13]. The various transport pathways that are involved in the delivery of the aforementioned substances across BBB are presented in Fig 1. Such transport pathways work in both directions i.e., blood to brain and brain to blood [14]. However, for drug delivery, blood to the brain transport system is more promising than other transport systems [15,16].

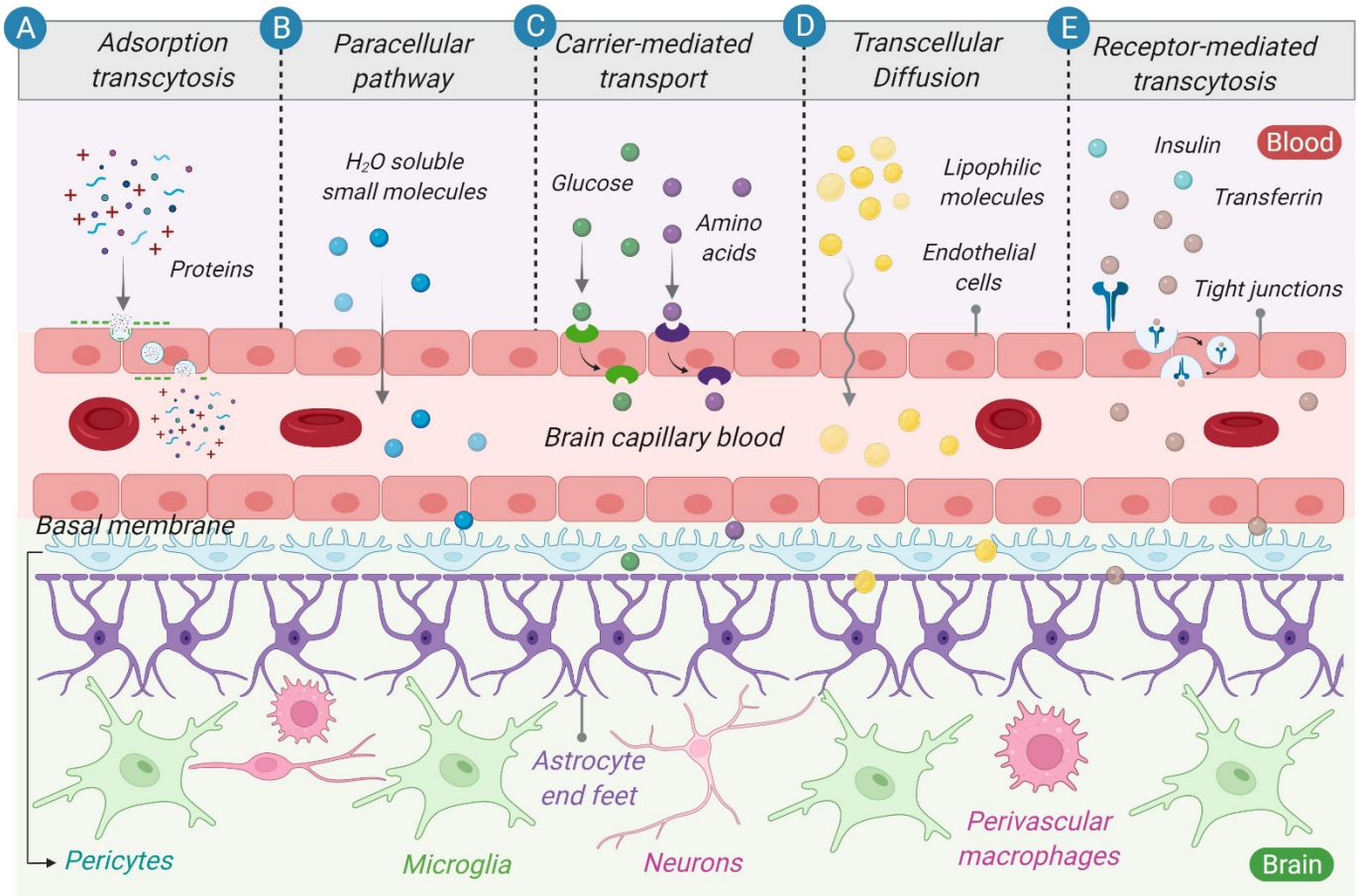

Fig 1: Transportation channels to pass the BBB. (A). Passage of cationic molecules (cationic drugs or macromolecules) across BBB via adsorptive-mediated transcytosis, (B). Passage of water-soluble agents across epithelium via paracellular route, (C). Transportation of small molecules or peptides via carrier-mediated pathway, (D). Passive diffusion of lipophilic molecules via BBB by transcelluar pathway, (E). Transportation of macromolecules or surface-modified nanoparticles via specific types of receptors expressed on BBB by receptor-mediated pathway

Therefore, BBB is the most prevalent barrier that prevents the uptake of most of the active therapeutics (large molecules) to the brain owing to epithelial-like tight junctions within the brain capillary endothelium. However, certain small molecules having molecular weight < 400 Da can cross the BBB via lipid-mediated free diffusion [17]. Furthermore, the metabolic

activity of the BBB via CYP450 enzymes is responsible to decrease the brain bioavailability of most of the CNS therapeutics by their biotransformation of drugs in a way similar to other organ systems such as the gut and liver [18]. These metabolic enzymes along with multi-drug resistance proteins expressed at BBB synergistically contribute to local brain biotransformation of drugs, thereby reducing the amount of parent drug (active moiety) by active extrusion that restricts them to reach the neuronal target [19].

Despite progress in disease pathology, a limited number of drugs are available to treat neurological diseases. The major shortcomings in the existing drug therapies are the lack of drug release at the brain site and their poor bioavailability due to BBB [13,20–22]. Therefore, to overcome the challenges of brain drug delivery, a potential therapeutic approach based on nanotechnology could be very helpful.

The amphiphilic block copolymers-based polymeric micelles have gained attention over the past few decades for various biomedical applications such as drug delivery, targeting, and imaging [23–26]. The block copolymer-based micelles are generally formed in an aqueous medium upon self-assembling of amphiphilic molecules above their critical micelle concentration into nanoscopic supramolecular configuration within the nanosize range of 1-100 nm [27,28].

Polymeric micelles have been widely explored in brain-specific delivery due to their ability to penetrate BBB and to reach the brain's parenchyma owing to their nanosize, ability to enhance membrane fluidity, and their steric stabilization property due to PEGylation [29,30]. In addition to this, surface modification with ligands and incorporation of stimuli-responsive blocks (functionalized polymeric micelles) contribute to improving the BBB permeability with

their ability to deliver the loaded cargo at the target sites of the brain via receptor-mediated endocytosis pathways [31–33].

Furthermore, the biocompatible and biodegradable properties of polymeric micelles make them less toxic and highly suitable for effective treatment of CNS-related diseases including Alzheimer's diseases, Parkinson's diseases, glioblastoma, epilepsy, cerebral ischemic injury, psychosis, etc. [34,35]. The ease of surface functionalization of polymeric micelles using several targeting moieties with multi stimuli-sensitivity makes them smart nanocarriers in targeting brain-specific sites and their diagnosis [36,37].

Polymeric micelles can also overcome the poor aqueous solubility of therapeutic molecules (e.g. certain growth factors, chemotherapeutic drugs, lamotrigine, etc.) upon oral administration by encapsulating them within the core and by protecting them against the harsh environment of the gastrointestinal tract followed by their controlled release at target sites [38–40]. Therefore, this review highlights and discusses the fundamental functions of BBB, challenges associated with drug delivery, and various strategies employed using amphiphilic block copolymers based polymeric micelles to treat CNS-related diseases along with their therapeutic and diagnostic insights. The major bottlenecks in developing the polymeric micelles for brain delivery are also highlighted.

2. Barriers to brain targeting

2.1 Blood-brain barrier

The BBB is the most critical barrier that separates brain tissues from peripheral circulations. As discussed earlier, BBB is a complex structure composed of brain capillary endothelial cells

that include astrocytes and pericytes, mural cells, basement membrane, immune cells (perivascular macrophages and microglial cells), tight and adherens junctions as major components (Fig 1) [41–43]. The endothelial cells form the walls of the blood vessels. Tight junctions hold the endothelial cells together greatly prohibiting the paracellular flux of solutes. In addition, they restrict the vesicle-mediated transcellular movement of solutes due to low rates of transcytosis [44,45]. Mural cells are the vascular smooth muscle cells that surround the pericytes. The cerebral endothelial cells and the pericytes, together contribute to the formation of vascular basement membrane (extracellular matrix) while astrocytes form parenchymal basement membrane of varying compositions [46]. These basement membranes act as an additional barrier for molecules before accessing neuronal tissue. Thus, they help in maintaining the barrier property.

The two transporters expressed by the endothelial cells i.e., efflux and nutrient facilitate the movement of substrate across BBB via carrier-mediated transcytosis. Efflux transporters such as breast cancer resistance proteins and multidrug resistance proteins utilize ATP for transporting their substrate against the concentration gradient [43,47]. However, nutrient transporters allow the movement of specific nutrients from high to low concentration regions such as GLUT1 [48].

In addition to this, endothelial cells express a variety of other receptor-mediated transport systems that mostly provide nutrients from blood to the brain. However, their overexpression is utilized for active brain targeting via receptor-mediated endocytosis to treat CNS-related diseases [43].

In several neurological disorders, disturbance in endothelial-glial interaction and BBB disruption is observed [49]. For instance, downregulation of protein claudin 1/3 in some glial tumors makes capillaries leakier than that of normal brain tissues [50,51], upregulation of GLUT1 transporter and astrocytic AQP4 expression, and loss of agrin contributes to BBB damage in AD [52]. Upregulation of P-gp on astrocyte and brain endothelium, the transient opening of BBB at epileptogenic foci, and altered ABC transporter expression are observed in epilepsy [53]. Decreased efficacy of P-gp is seen in Parkinson's disease [54]. Opening of BBB due to the release of interleukin-6 from astrocytes is observed in the brain due to traumatic conditions [51]. Therefore, BBB is a significant obstacle to the treatment of brain diseases with disrupted or leaky BBB, which pushes researchers to develop novel and effective brain drug delivery systems [12,55,56].

2.2 Blood-cerebrospinal fluid barrier

The blood-cerebrospinal fluid barrier (BCB) exists in between the systemic circulations and the cerebro spinal fluid (CSF) space. It facilitates the transfer of solutes via active transport (carrier- and receptor-mediated) and passive transport of water-soluble molecules [57]. It differs from BBB in terms of the presence of several fenestrations (gap junctions) and pinocytosis vesicles that act as a macro filter for proteins [57]. BCB is formed by the epithelial cells of choroid plexuses localized in the four ventricles and the subarachnoid structures of the brain [57,58]. Choroid plexuses are highly vascularized tissue composed of capillaries enveloped by a layer of differentiated ependymal epithelium without any tight junctions [59]. Choroid plexuses act as physical, immunological, and enzymatic barriers that regulate drug passage, metabolism, and signaling functions and impede their entrance into CSF as well [60–

62]. In addition to this, they also control the concentration of molecules in CSF and the various efflux and influx transport systems (e.g. solid-lipid carrier and ATP-binding cassette) at the epithelial cells of choroid plexuses that regulate the entry of endogenous and exogenous agents [63,64]. Therefore, the entrance of molecules into the CNS depends on the affinity with the active transport systems at the BCB. Further, secretion channels that are working at the epithelial cells of choroid plexuses, which control the CSF flow, also play an important role [65]. The diagrammatic presentation of the CNS barriers is depicted in Fig 2.

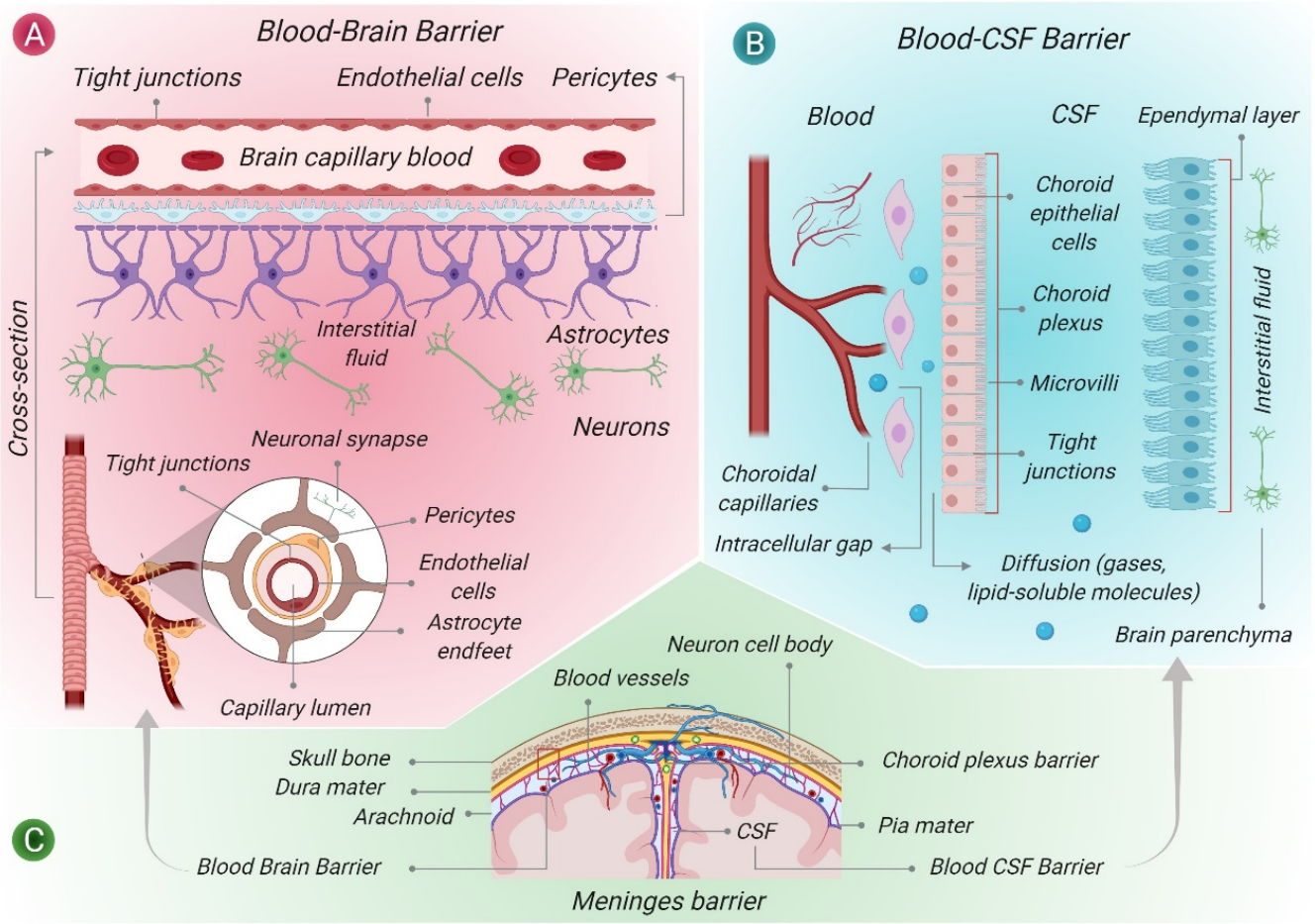

Fig 2: The three main barriers in the central nervous system

2.3. Blood-tumor barrier

The blood-tumor barrier (BTB) is characterized by aberrant pericyte distribution and loss of astrocytic endfeet. Therefore, BBB integrity is disrupted [66]. Under such conditions, BTB becomes highly permeable and heterogeneous in terms of non-uniform permeability and active efflux of molecules. This results in a suboptimal accumulation of drugs at tumor site of brain (glioma) [67]. Under such conditions, local and distal changes occur that directly compromise neuronal viability and vascular functions [68]. Further expansion in tumor, results in angiogenesis to fulfill the increased nutritional demand of proliferating cancer cells with increased blood supply as well [69,70]. This occurs due to disruption in vascular integrity because of non-uniform pericyte vessel coverage and stem cell-derived pericyte [66,71]. Overall, such events impede drug delivery at the site of brain tumor. To facilitate drug delivery, various approaches such as inhibition of efflux transporters and opening of tight junctions by using a hyperosmotic solution of mannitol and receptor-mediated drug delivery systems have been utilized [72,73]. The diagrammatic presentation of the BTB is presented in Fig 3.

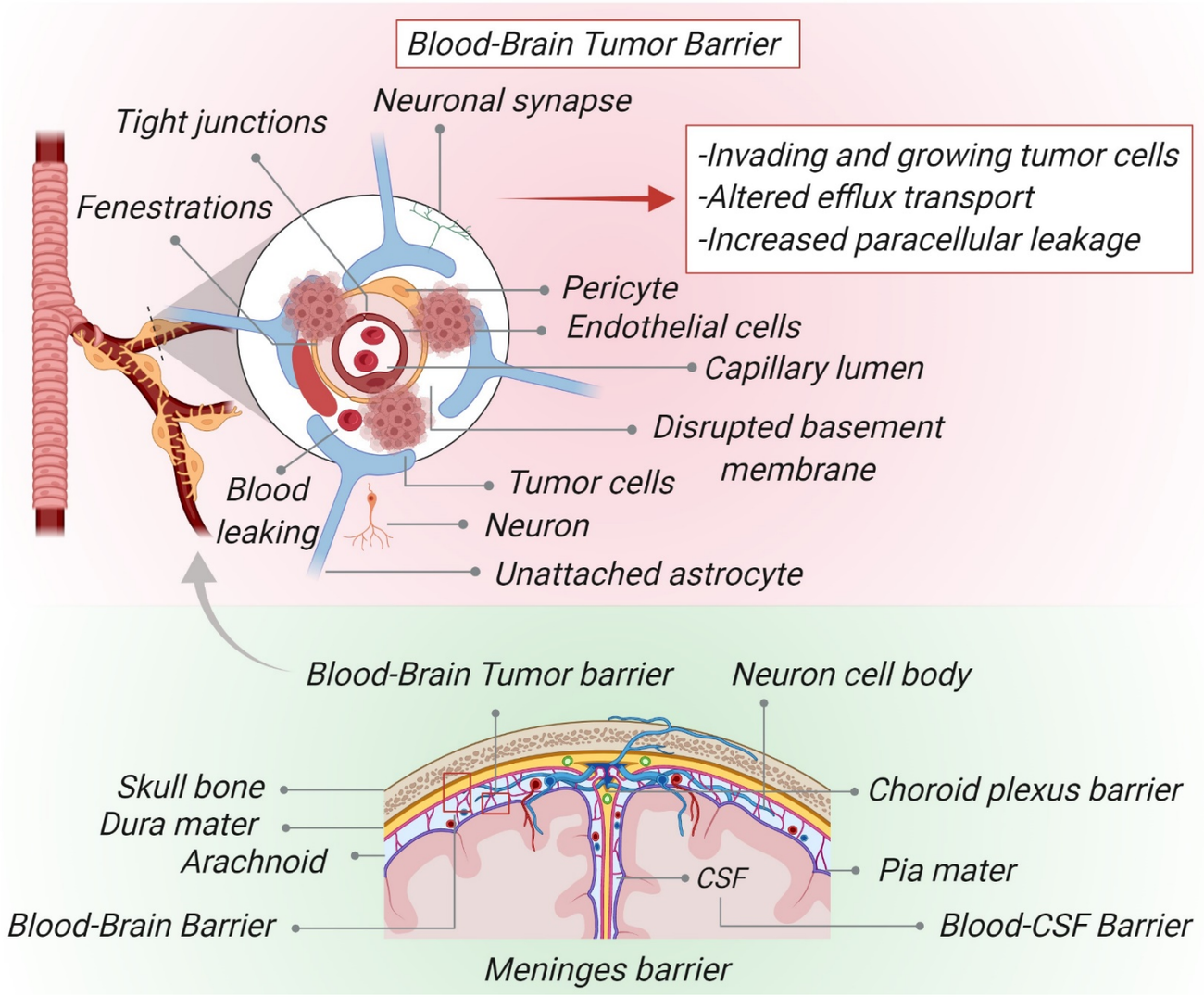

Fig 3: The brain tumor barrier involved in hindering drug delivery

3. Polymeric micelles

Amphiphillic block copolymers when added in an aqueous medium above their critical micelle concentration value-form polymeric micelles. Above this concentration, the hydrophobic inner core of the copolymer comes closer to aggregate and distances itself from water molecules to form polymeric micelles [74]. These are generally made of biocompatible, non-immunogenic, biodegradable core-forming blocks i.e., polyesters, polyethylene oxide or poly (amino acids) attached with biologically compatible corona forming blocks usually PEG (Polyethylene glycol) [34,75]. Their ease of functionalization makes them an efficient nanosystem for brain targeting (Fig 4) [36]. Various approaches used for the functionalization of polymeric micelles for brain targeting are discussed in the subsequent sections.

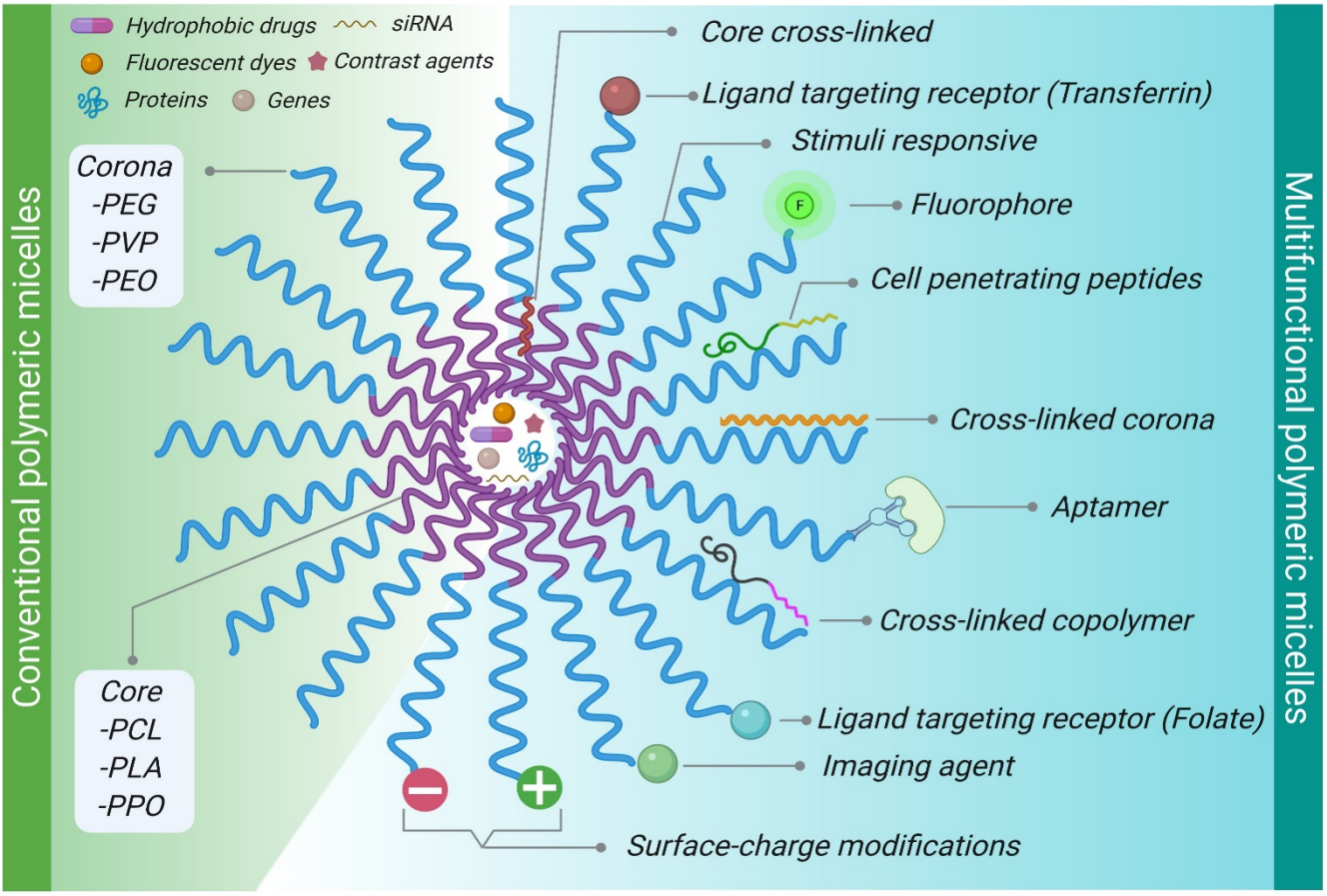

Fig 4: The diagrammatic presentation of the functionalization of polymeric micelles for brain drug delivery

4. Amphiphilic block copolymers

The functional chemistry of these block copolymers is highly utilized in the functionalization of polymeric micelles for brain targeting [76]. This is achieved by modifying the molecular features of copolymers by controlled/living radical polymerization techniques including atom transfer racial polymerization, reversible addition-fragmentation chain transfer radical polymerization, and nitroxide-mediated polymerization. In addition to this, there are click and coupling reactions used for exploiting the active functional moieties at the chain terminal [77–79].

Such approaches offer the formation of block copolymers with stimuli-sensitivity/multi stimuli-sensitivity by incorporating stimuli-responsive moieties and active targeting ability by conjugating targeting ligands with their core-forming block [80–83]. Such copolymers containing functional groups offer the possibility for post-polymerization modification by chemical means and covalent coupling methods that provide large possibilities to fine-tune the copolymer functionality at molecular and submolecular levels [75,79,84,85]. The commonly exploited functional groups of copolymers required for their chemical modification include amines, alcohol, and carboxylic group "etc." [85,86]. Furthermore, some of the copolymers, mostly Pluronics have been widely explored in the delivery of antiepileptic drugs across BBB due to their P-gp inhibition ability [87,88]. Thus, such block copolymers-based properties play important role in functionalizing the polymeric micelles to achieve better BBB permeability and targeting potential as discussed below.

4.1 Stimuli-responsiveness

Various stimuli such as intrinsic (pH, redox, reactive oxygen species, hypoxia, enzymes, etc.) and extrinsic (magnetic, temperature, light, ultrasound, etc.) are used to control the behavior of drug release from polymeric micelles and enable targeting at the area of interest [89]. There are various techniques used in the synthesis of smart block copolymers composed of stimuli-sensitive blocks or their modification for stimuli functionalization as mentioned above [90]. Such functional

properties of copolymers enable them to respond to stimuli. These polymers are used for the designing of stimuli-responsive polymeric micelles (functionalized). Moreover, the specificity of the response towards the stimuli is important for site-specific drug delivery and minimizing off-target effects [91]. The polymeric micelles based on stimuli sensitive blocks are the smart nanocarriers, that reveal characteristic alterations in their properties (charge switching, structural changes, swelling, and disassembly) when subjected to specific environmental conditions such as pH, temperature, enzymes; or externally applied triggers, such as radiation and ultrasound [91–93]. The schematic presentation of the smart copolymers used to impart stimuli-responsiveness for the functionalization of polymeric micelles in brain-specific drug delivery is presented in Fig 5.

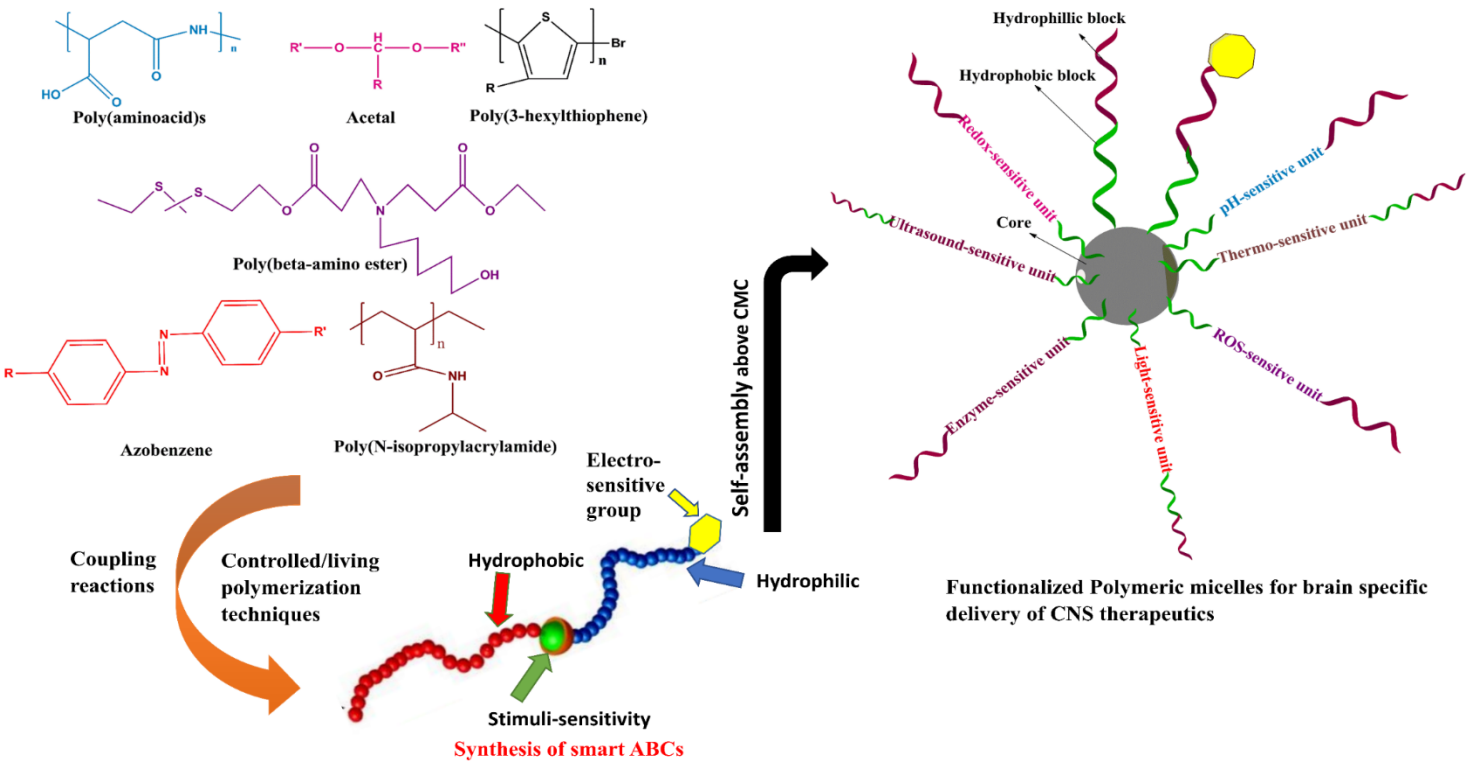

Fig 5: Functionalized polymeric micelles (stimuli-responsive) in brain-specific delivery

Such molecular features of copolymer based polymeric micelles have been extensively exploited in the treatment of various tumors including glioma. This is because of the well-studied tumor environment that provides selectivity for tumor cells over healthy tissues [29,94–96]. For instance, the incorporation of ionizable groups in the copolymers at extra/intracellular pH of tumor cells undergoes ionization that results in the delivery of loaded drugs at the endo/lysosomal compartment of tumor cells [97]. The elevated level of reduced glutathione in tumor cells (i.e., 4-times higher than normal tissues) makes tumor environment reductive and hypoxic [97,98]. For which, redox-responsive moieties, mostly disulfide bonds that are susceptible to rapid cleavage by glutathione are incorporated either with the core-forming blocks or in between the corona and core-forming blocks. This results in the delivery of anticancer drugs in the cytosol or cell nuclei of the tumor cells [99–101]. A high concentration of enzymes such as matrix metalloproteinases are responsible to control tumor growth, angiogenesis, invasion and metastasis. These are also promising biological triggers for selective drug delivery at tumor site. Incorporation of specific enzymatic linkers (e.g., lipopeptides, Gly-Pro-Leu-Gly-Val-Arg-Gly-Lys) in the copolymer structures undergo degradation in the presence of elevated matrix metalloproteinase enzymes at the extra/intracellular compartments of tumor cells [102,103]. Furthermore, the elevated levels of reactive oxygen species in the majority of the tumors including glioma are considered one of the hallmarks utilized for targeting purposes. Therefore, the incorporation of reactive oxygen species -responsive groups such as thioketal and sulfide in the main chain of the copolymer or as a responsive conjugating linker between drug and block copolymer provides higher selectivity for tumor cells [104,105]. Overall, such approaches provide spatiotemporal drug release without any exposure to healthy brain tissues. Thus, the loading of anticancer drugs into such nanocarriers can enhance the therapeutic effect of anticancer drugs and could be utilized for the imaging (imaging agents) of tumor cells as well. The studies on stimuli-responsive copolymers utilized in the functionalization of polymeric micelles and their delivery at glioma sites are presented in Table 1.

1 **Table 1:** Site-specific delivery of functionalized polymeric micelles at brain tumor site

Amphiphilic block copolymer	Approach	Stimuli sensitive functional group		Outcome	References
		pH (Acid-labile)			
PEG-b-PEYM	ATRP	Orthoester	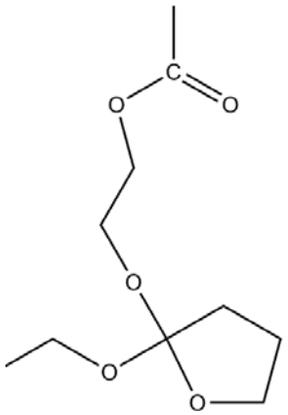	➢ Higher cellular uptake of functionalized PMs was observed in human glioma cells within 60 min via endocytosis	[106]
HA-DOX	Reaction between amine group of HA and carbonyl group of DOX	Hydrazone	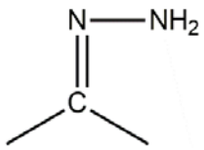	➢ 4-fold higher intracellular accumulation of functionalized PMs was observed in U87 and C6 cells than free DOX	[107]
Dex-SA and Dex-His	Steglich esterification followed by coupling reaction	Stearic acid Histidine	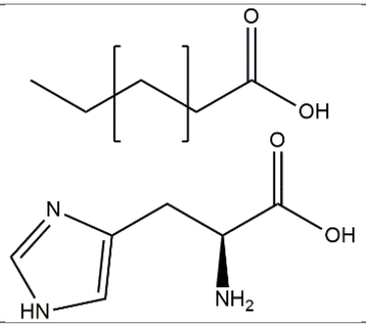	➢ Effective cellular uptake of mixed functionalized PMs in U87MG cells due to macropinocytosis as an indicated by strong fluorescence	[108]

		MMP 2/9-responsive		
PEG-co-PCL	MMCB	Protamine 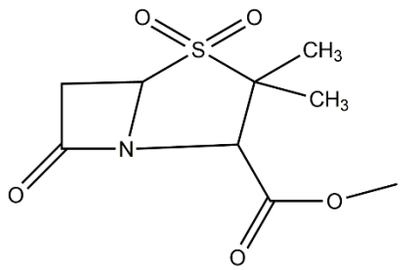	➢ 1.2-fold increase in the penetration capacity of functionalized PMs was noted into C6 glioma spheroid ➢ 3.8-fold increase in cellular uptake of functionalized PMs was observed into C6 glioma cells (MMP-dependent) via lipid raft-mediated endocytosis	[109]
		ROS-responsive		
mPEG-TK-MPH		Thioketal 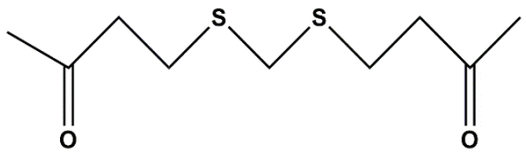	➢ 1.1-folds increase in the cytotoxic action of functionalized PMs was noted in U251MG cells with higher ROS levels	[105]
		Redox-responsive		
Cystamine modified HA-SS-CUR	Coupling reactions with grafting methods	Disulfide 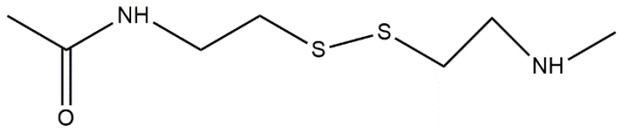	➢ 4-folds increase in the release profile of drug was observed in the presence of GSH conditions ➢ 1.8-fold increase in the cytotoxic action of functionalized PMs was noted in G422 cells with higher cellular uptake	[110]

PCL-PEI-SS-PEG	CLPT	PEI-SS 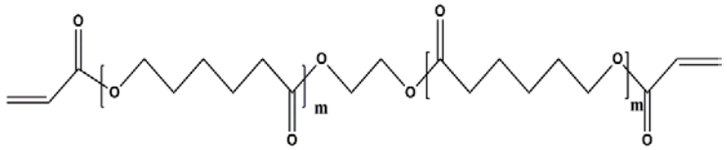	➢ GSH-dependent release of drug loaded functionalized PMs was observed in C6 glioma cells i.e. 1-folds higher in the presence of GSH	[111]

Abbreviations: CLPT, Controlled living polymerization technique; **C6-cells**; Spindle-like cells that simulate human glioblastoma multiforme **; Dex**, Dextran-stearic acid, **Dex-His**, Dextran-histidine; **DOX**, Doxorubicin; **G422 cells**; Intracerebral gliobalastoma cell line; **GSH**, Reduced glutathione; **HA-ss-CUR**, Hyaluronic acid-disulfide linkage-Curcumin; **HA-DOX**, Hyaluronic acid-Doxorubicin; **MMCB**, Maleimide-mediated covalent binding; **MMP**, Matrix metalloproteinase; **mPEG-TK-MPH**, Methoxy polyethylene glycol- thioketal-Melphalan; **PEG-co-PCL**, Polyethylene glycol-co-polycaprolactone; **PEG-b-PEYM**, poly(ethylene glycol) (PEG) block and a hydrophobic polymethacrylate block; PCL-**PEI-SS-PEG**, Polycaprolactone-Polyethylenimine-disulfide bond-polyethylene glycol; **PEI-SS**, Polyethylenimine-disulfide bond; **ROS**, Reactive oxygen species; **U251MG cells**; Glioma cell-line;; **U87MG cells**, Malignant glioblastoma cell line

In recent times, copolymers containing functional moieties responding towards extrinsic stimuli such as electrical, magnetic [112], ultrasound and light are being widely explored for brain targeting due to their invasiveness and biodegradability. The chemical structures of such functional moieties used are presented in Fig 6 [113]. For example, conjugation of electro-sensitive groups such as ferrocene (Fc) with copolymers, imparts electro-responsive functionality to micelles. This property favored brain-specific targeting of polymeric micelles with electro-responsive cargo release at the targeted site under the application of electrical stimulation [114]. The developed functionalized polymeric micelles based on electro-responsive copolymers upon exposure to electrical stimulation undergo phase transition due to oxidation of Fe^{2+} in Fc into Fe^{3+}. This changes the HLB of functionalized polymeric micelles and triggers the swelling and ultimately disassembly of micellar structure for targeted cargo release [115]. Recently, Meng et al. reported a 1.6-fold increase in cumulative drug release over 30 min in PBS pH 7.4 under electrical stimulation with 1.4-fold stronger fluorescence intensity in brain using Pluronic F127/TPGS-Fc (n-alpha tocopherol PEG1000 succinate-Fc) mixed functionalized P polymeric micelles [92].

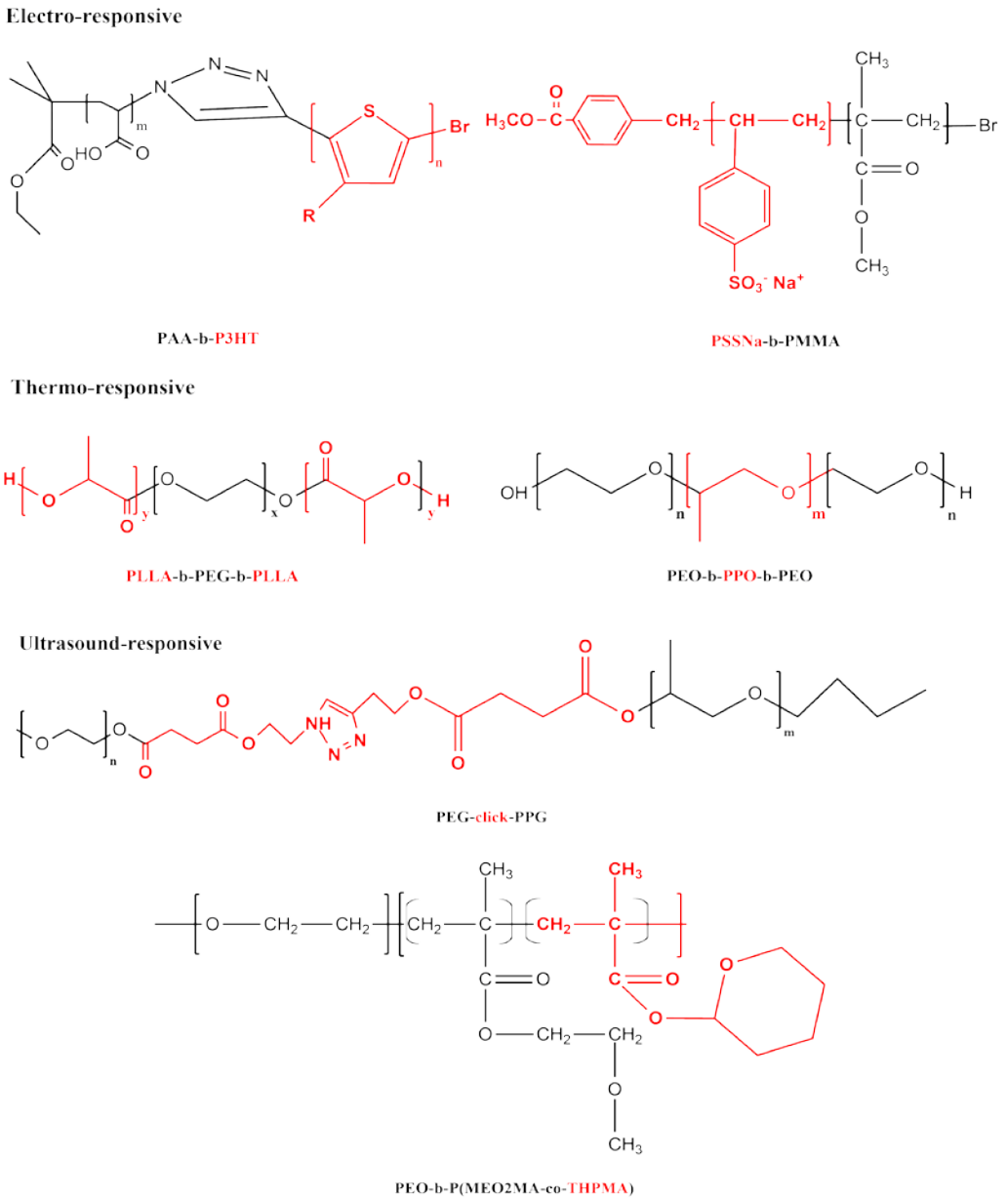

Fig 6: Smart amphiphilic block copolymers containg functional moieties for extrinsic stimuli (Red color signifies stimuli-responsiveness)

Abbreviations: PAA-b-P3HT, Polyacrylic acid-block- poly(3-hexylthiophene-2,5-diyl); **PAzoMA-b-(PELG-g-MPEG)**, Poly[6-(4-methoxy-azobenzene-4'-oxy) hexylmethacrylate-block-(poly L-glutamate-graft- methoxy polyethylene glycol); **PEG-click-PPG**, Poly (ethylene glycol)-click-Poly (propylene glycol); **PEO-b-PPO-b-PEO**, Poly (ethylene oxide)-block-Poly (propylene oxide)-block-Poly (ethylene oxide); **PEO-b-P(AzoMA-NIPAm)**, Polyethyleneoxide-block-Poly([6-(4-methoxy-azobenzene-4'-oxy)-hexylmethacrylate-(N-isopropylacrylamide); **PEO-b-P(MEO2MA-co-THPMA)**, Poly(ethylene oxide)-block-poly(2-methoxyethoxy)ethyl methacrylate-co-tetramethylpiperidinyloxy-4-yl methacrylate); **PLLA-b-PEG-b-PLLA**, Poly (L-lactic acid)-block-Poly (ethylene glycol)-Poly (L-lactic acid); **PSSNa-b-PMMA**, Poly (sodium styrene sulfonate)-block-poly (methyl methacrylate)

The use of thermoresponsive copolymers with lower critical solution temperature lower than 37 °C such as Pluronic F127 loaded with magnetic nanoparticles exhibits magnetic property in response to the applied magnetic field. Upon exposure to the magnetic field, magnetic nanoparticles loaded in polymeric micelles generate local hyperthermia that results in degradation of thermoresponsive polymer for controlled drug release at the target site with increased permeability [116]. For instance, Huang et al. reported 17-fold increase in the drug release profile in cortical and subcortical regions of brain over 30 min using Pluronics F127 based functionalized polymeric micelles loaded with SPION (superparamagnetic iron oxide nanoparticles) upon exposure to magnetic field [117]. Karami et al. reported 3.4-fold increase in the naproxen brain accumulation using functionalized polymeric micelles (magnetic) based on methoxy poly (ethyleneglycol)-poly (caprolactone) with SPION in comparison to free drug respectively upon intravenous administration [112]. Ultrasound sensitive copolymers with labile chemical bonds such as PEO-b-PTHPMA (acetal units), upon exposure to high-intensity focused ultrasound irradiation converts hydrophobic THPMA units (ultrasound sensitive unit) into hydrophilic methacrylic acid groups by initiating thermosensitive hydrolytic reaction. This increase in the hydrophilicity of the copolymer increases the LCST of the thermo-responsive polymer from 25 to 42 °C. As a result, disruption of polymeric micelles under focused ultrasound results in the release of loaded molecular cargo at the site of interest [118–120]. In addition, the incorporation of multiple ester bonds in the copolymers makes polymeric micelles sensitive to high-intensity focused ultrasound. Under such conditions, weak bonds in copolymer undergo mechano-chemical cleavage because of solvodynamic shear or short-lived and localized hot spot produced by ultrasonic cavitation that controls payload release [78,121]. Further, the co-encapsulation of ultrasound contrast agent (microbubble) and therapeutic moieties in the core of polymeric micelles could be used in the theranostic field to treat brain diseases [91].

In one of the studies, Nance et al. reported the delivery of PEG-PLGA based polymeric micelles in endothelium and interstitial space of rats' brain under the exposure of magnetic resonance-guided focused ultrasound with intravascular microbubble contrast agents (it avoids the risk of skull heating by concentrating the ultrasound energy) to improve the treatment efficacy for CNS diseases by non-invasively peremabilizing the BBB. The exposure of magnetic resonance-guided focused ultrasound permeabilized the BBB successfully which led to the delivery of biodegradable polymeric micelles into the brain parenchyma region after intravenous administration in rats once crossing the BBB.

The magnetic resonance imaging revealed 150-µm deeper penetration of the polymeric micelles into the brain tissues of rats. The exposure of higher focused ultrasound (0.6 MPa) exhibited 2.3-fold increase in the total area of brain than that of focused ultrasound at 0.4 MPa. Exposure of higher focused ultrasound (0.6 MPa) exhibited 4.6-fold increase in accumulation of nanoparticles as a measure of fluorescence enhancement in brain parenchyma than that of lower focused ultrasound of 0.4 MPa pressure. In addition, 1.4-fold increased nanoparticles fraction was observed in endothelium and interstitial space of brain by using higher pressure focused ultrasound than that of lower pressure FU [12].

However, the limited contact of the microbubbles with the vessel walls makes them less optimal for therapeutic applications [122]. Recently, acoustic cluster therapy bubbles are widely utilized in increasing the brain permeability followed by the uptake of therapeutic molecules loaded in nanoparticles upon exposure of high frequency ultrasound. This is due to their ability to cover larger area of blood vessels with higher retention time. This results in the intensified contact with the endothelium than that of conventional microbubbles [123]. The core-cross linked polymeric micelles as brain penetrating nanoparticles have shown increase in drug's penetration and accumulation in the brain's parenchyma of the mouse over small hydrophilic macromolecules post acoustic cluster therapy [122].

The conjugation of copolymers with chromophores such as azobenzene and its derivatives impart light-responsive property to polymeric micelles [124]. Ultraviolet-responsive hydrophobic blocks such as poly (4,5-dimethoxy-2- nitrobenzyl methacrylate) have been employed in photo controlled cargo release at the target site. Such copolymers based polymeric micelles undergo photoisomerization reaction and photochemical phase transition (irreversible cleavage) upon UV light exposure. As a result, it disrupts micellar structure by transforming the hydrophobic block into a hydrophilic block for cargo release at the target site [125,126]. For instance, Xiang et al. reported 3-fold increase in the drug release profile at pH 7.0 over 16 hours using poly(methoxy polyethylene glycol monomethacrylate)-poly (4,5-dimethoxy-2- nitrobenzyl methacrylate) based functionalized polymeric micelles upon exposure of ultraviolet irradiation [125].

4.2 Chemical conjugation

The stimuli-responsive biodegradable smart linkers have been utilized for the conjugation of the therapeutic molecules with the core-forming blocks consisting of functional groups amenable for linkage [75,81,127]. This approach provides good entrapment of the therapeutic molecules in the micellar core and has been well explored in the smart delivery of anticancer drugs with a controlled release profile [128]. In addition, this approach overcomes the limitation of poor drug release profile associated with covalently bound copolymer-drug conjugates by triggering the entrapped drug release in response to specific stimuli (micelle disassembly) [129,130].

From the past few decades, conjugation approaches based on hydrophilic polymers have been used for protein delivery in the brain by increasing their retention time and reducing proteolysis [131]. However, conjugation with copolymers mostly with Pluronics (L81, P85, L121, and P123) has led to an increase in BBB penetration of proteins than that of

hydrophilic polymers. This is due to their ability to interact with the hydrophobic surfaces (cell membrane) or their amphiphilic nature. Thus, these are considered more suitable for membrane transport. Despite their amphiphilic nature and ease of chemical modification by changing the number of individual chain units to optimize their hydrophobicity, these are relatively less explored [81,132,133]. Similarly, modification of proteins with poly(2-oxazoline)-based block copolymers (POx) has also attracted attention for protein delivery by increasing the internalization into the brain via lipid-raft mediated mechanism [134]. Examples of proteins that have been conjugated with such copolymers include horseradish peroxidase [81], leptin [135,136], superoxide dismutase, and many more as presented in Table 2 [137,138].

For instance, Yi et al. revealed that the horseradish peroxidase-conjugated Pluronic block copolymers with shorter PPO chains exhibited the highest cellular uptake by primary bovine brain microvessel endothelial cells. This study indicated the strong influence of hydrophobic PPO block length on the transport efficiency of Pluronic conjugates [81]. Similarly, in one of the studies, superoxide dismutase 1 modified with P(EtOx-b-BuOx) containing hydrophilic 2-ethyl-2-oxazoline (EtOx) and hydrophobic 2-butyl-2-oxazoline (BuOx) repeating units exhibited ~1.75 higher half-life in blood circulations than native superoxide dismutase 1 with good penetration efficiency via caveolae-mediated and/or clathrin and caveolae-independent endocytosis, thereby enabling it to reach brain parenchyma [137]. Several studies claimed the great versatility of POx rather than Pluronics owing to their ease of chemical modification at the chain end containing functional molecules. Furthermore, Meng et al. developed TPGS and Pluronic F127 based mixed polymeric micelles for β-galactosidase delivery across BBB. The *in vivo* studies revealed 3-fold higher accumulation of the mixed polymeric micelles in the brain than F127 based polymeric micelles upon intravenous administration. This was attributed to their small size (<200 nm) which

provided reduced uptake by the reticuloendothelial system. Therefore, prolonged half-life in blood results in passive brain targeting properties. This indicated that the small size of the polymeric micelles has the potential to effectively enhance the penetration of drugs across the BBB. Moreover, the developed mixed polymeric micelles increased the cellular uptake by the brain capillary endothelial cells via an adsorptive-mediated endocytic pathway. Further, the potential of TPGS/F127 (reversal surfactant) in inhibiting the P-gp ATPase is reported to be involved in their increased uptake across brain capillary endothelial cells. Interestingly, the developed polymeric micelles exhibited different accumulation in four different regions of the brain including the cortex, caudate, hippocampus, and substantia nigra of rat's brain [139]. In contrast, intravenous administration of free β-galactosidase exhibited no therapeutic activity in the brain [139].

Table 2: Proteins modified with Amphiphillic block copolymers for their brain delivery

Amphiphilic block copolymer	Protein conjugated	Linker	Outcome	References
Pluronic P85 and L81	HRP	Conjugation via biodegradable linker DSP	➢ 4 to 5-fold increase in the brain uptake of HRP was observed upon conjugation with P85 and L81 than that of unconjugated HRP	[81]
Pluronic P85 and L121	HRP	Conjugation via biodegradable disulfide bond	➢ 6 to 10-fold increase in transport efficiency of the HRP-conjugate in BMECs was observed using P85 and L121 than that of unconjugated-HRP ➢ 3.3-fold increase in the transport efficiency of the Pluronic conjugate than stearoyl-modified HRP in BMECs	[140]
P(EtOx-b-BuOx)	SOD1	Conjugation via biodegradable disulfide linker	➢ 7-fold higher cellular uptake of conjugate was observed in neuronal cells than P(MeOx-b-BuOx) based conjugation approach ➢ 2-fold increase in the brain parenchyma/serum ratio of the	[137]

		conjugate was noted than capillary/serum ratio

Abbreviations: BMECs, Brain microvessel endothelial cells; **DSP**, Dithiobis(succinimidyl propionate); **HRP**, Horseradish peroxidase; **P(EtOx-b-BuOx)**, Poly(2-ethyl-2-oxazoline-block-2-butyl-2- oxazoline); **P(MeOx-b-BuOx)**, Poly(2-methyl-2-oxazoline-block-2-butyl-2- oxazoline); **SOD1**, Superoxide dismutase1

In addition, based on the presence of receptors that are overexpressed at the diseased cells are responsible for selectively driving the polymeric micelles across BBB endothelium, the conjugation of active ligands with the corona-forming blocks of polymeric micelles (surface-functionalization), increases the BBB penetration and specificity [75,141]. This receptor-mediated transcytosis mechanism is a complex and multi-stage process, in which the nanocarriers actively interact with the cell membrane for the effective internalization into cells via energy-dependent endocytosis process and expulsion via exocytosis as presented in Fig 7 [142]. There is a large number of biological ligands that have been studied for this purpose. These include proteins, aptamers, peptides, cell-penetrating peptides, and small molecules for increasing the cellular uptake of nanoparticles loaded with therapeutic cargos. To achieve this, polymeric micelles are generally functionalized either by chemically conjugating the active ligands with the block copolymers or physically adsorbed on their surface [143]. For example, Quader et al. conjugated cRGD moiety with the α-end of acetal-PEG-PBLA-acetylation using one-pot acetal-deprotection and thiazolidine ring formation reaction to form the functionalized polymeric micelles. The mixture of this modified copolymer and MeO-PEG-PBLA was used for the conjugation of epirubicin via pH-sensitive hydrazone bond for the targeted delivery in brain tumors. Thus, the developed micellar system overcame the BTB via integrin (αvβ3 and αvβ5)-mediated enhanced recognition and internalization [144].

Ruan et al. conjugated stapled RAP-12 protein (receptor-associated protein-12 with higher α-helical conformation) with PEG-PLA copolymer by Michael's addition reaction to impart multi-functional targeting ability in polymeric micelles upon self-assembly. The thin-film hydration method was used for the loading of paclitaxel (PTX) in functionalized polymeric micelles. The developed functionalized polymeric micelles were able to overcome the BBB/BTB by targeting vasculogenic mimicry and glioma cells via low-density lipoprotein

receptor-related protein-1-mediated endocytosis [145]. Luo et al. synthesized AS1411-functionalized poly (L-γ-glutamyl-glutamine)-paclitaxel (PGG-PTX) conjugation system that self-assembled into nanoconjugate by o/w emulsion solvent evaporation method. The functionalization of AS1411 with the corona PGG led to increased accumulation of the polymeric micelles in glioma cells i.e., by 3-fold than that of the non-functionalized polymeric micelles. Such difference was due to the high affinity and binding specificity of functionalized polymeric micelles with nucleolin, which is a multifunctional protein overexpressed in glioma cells [146].

Furthermore, the cell-penetrating peptides containing short chains of amino acid residues (5-30 residues) also can penetrate the BBB via electrostatic interactions with the exposed plasma membrane [147,148]. These also act as transporters that mediate the transport of small macromolecules across the cell membrane [149]. These cell-penetrating peptides are divided into three categories i.e., natural (Tat-derived peptides), synthetic (polyarginine), and chimeric peptides (transportan). Furthermore, based on the physicochemical traits of these peptides, there are cationic peptides (arginine and lysine residues), hydrophobic peptides composed of hydrophobic amino acids, and amphipathic peptides containing both hydrophobic and hydrophilic amino acids [147,150–152]. These cell-penetrating peptides follows two types of cell internalization pathways. These include energy-independent (direct penetration or membrane transduction) and energy-dependent (endocytosis) pathways as presented in Fig 8 [148].

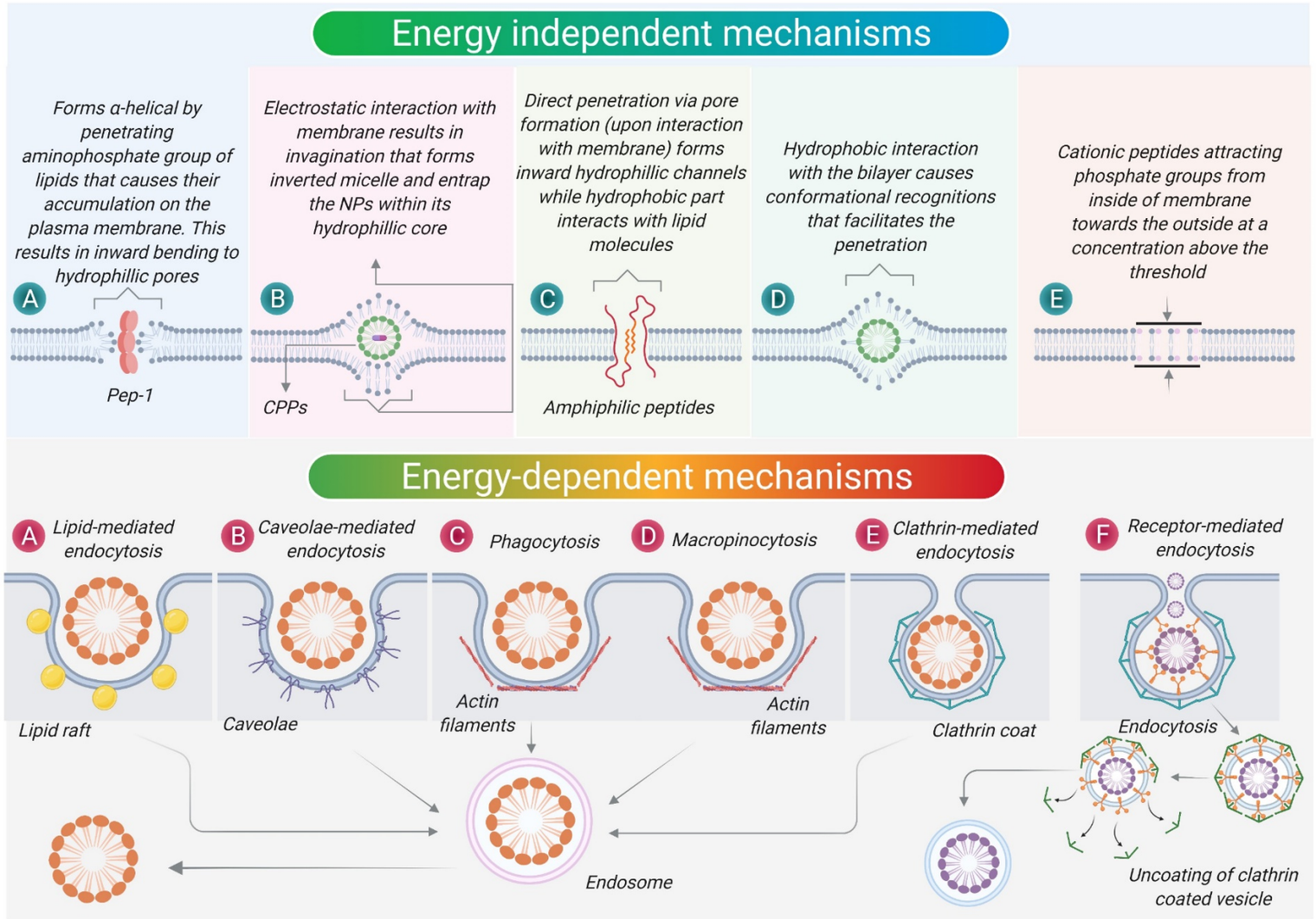

Fig 7: The various mechanisms involved in the internalization of the active ligands into the brain [148]

In one of the studies, Tanaka et al. synthesized mPEG-PCL copolymer by ring open polymerization reaction and conjugated Tat (arginine-rich peptides) with hydroxyl group of mPEG-PCL by ester bond via an esterification reaction. The modified copolymer successfully formed micelles by w/o emulsion method for the direct intranasal brain delivery. The conjugation of Tat with copolymer led to 5-fold higher brain distribution profile of functionalized polymeric micelles in comparison to non-functionalized polymeric micelles, respectively. In addition, it increased the intracellular uptake in glioma cells by 2.5-fold in comparison to non-functionalized polymeric micelles respectively via the macropinocytosis pathway [153].

However, polymeric micelles functionalized with cell-penetrating peptides offer higher drug distribution in the entire brain due to the non-specific affinity of cell-penetrating peptides with different cells. As a result, it could lead to unwanted toxicities in healthy brain cells [154]. Therefore, to overcome this issue, polymeric micelles can be designed as a “dual-stage” targeted drug delivery nanocarrier. For instance, Kanazawa et al. modified mPEG-PCL-Tat by designing stearic acid conjugated Bom for the formation of mixed functionalized polymeric micelles to target gastrin-releasing peptide receptors overexpressed in intracerebral gliomas. The use of Bom led to selective and higher cellular uptake of functionalized polymeric micelles in C6 glioma cells by 4.4- and 1.7-fold in comparison to non-functionalized and functionalized polymeric micelles without Bom respectively. Such difference was attributed to gastrin-releasing peptide receptor-mediated Bom-specific mechanism. Thus, this nanocarrier system showed potential for targeting brain tumors with the potential to overcome BTB [155]. Further, the case studies regarding the functionalization of polymeric micelles with targeting ligands are presented in Table 3.

Table 3: Functionalized polymeric micelles composed of chemically conjugated amphiphilic block copolymer with targeting ligands for brain targeting

Amphiphilic block copolymer	Conjugation approach	Stimuli-responsiveness	Method of crossing BBB	Indication	Outcome	Reference
			CPPs			
PE-PEG	Mal groups of PEG were reacted with the thiol moiety of angiopep-2	-	Angiopep-2 ligand based transcytosis via LDL receptors on BBB	Targeted delivery of amphotericin B to treat fungal infections of CNS	➢ 2.8-fold increase in the uptake of functionalized PMs in brain was observed than that of non-functionalized PMs	[156]
Dex-PTX	The ligand was conjugated via amide linkage after incorporating carboxylic group to dex	pH-triggered release	RVG29 mediated transport across BBB via nAchR receptor	Delivery of PTX to intracranial glioma cells	➢ Functionalized PMs exhibited strong fluorescence for 48h than that of non-functionalized PMs ➢ 3-fold decrease in the brain tumor volume by functionalized PMs was noted than that of non-functionalized PMs	[157]
CHO-POESO	The ligand was conjugated with POESO block of the copolymer in the presence of EDC/DMAP	pH-sensitive masking sequence $(HE)_5$ for charge shielding to avoid non-specific binding	Arginine rich peptide $(RG)_5$ mediated transcytosis via LDL receptors on BBB	Targeted delivery of PTX to the glioma cells	➢ 1.1-fold increase in the release of drug at acidic pH was noted than non-functionalized PMs within 2h ➢ 4.2-fold increase in the uptake of the functionalized PMs into brain was observed at pH 6.5 than that of physiological pH 7.4	[158]

mPEG-SS-g-P(ae-Asp)	The ligand was incorporated during ring open reaction in the presence of EDC	pH/redox-triggered release	TAT mediated cellular uptake via LDL-receptors	Targeted delivery of DOX to tumor cells	➢ Shedding of corona under tumor-redox condition, exposed TAT for internalization of the functionalized PMs in tumor cells ➢ Core-cross linking approach based on catechol and Fe^{3+} incorporation maintained the stability of functionalized PMs at physiological pH and facilitated the drug release at lysosomal pH	[159]
			Peptides			
PEG-PHA	The ligand was conjugated via thiazole-5-carboxamide linkage with PEG Hydrazide functionalization via ester-amide exchange reaction	pH-triggered release	cRGD peptide based cellular uptake via integrins ($\alpha_v\beta_3/\alpha_v\beta_5$) – mediated endocytosis	Targeted delivery of epirubicin against GBM	➢ 1.4-fold increase in the internalization of the functionalized PMs was observed in brain than that of non-functionalized PMs ➢ 2-fold increase in the penetration capacity of functionalized PMs was noted in U87MG glioma spheroids than that of non-functionalized PMs ➢ 12-fold higher antitumor efficacy of functionalized PMs was observed than that of non-functionalized PMs	[144]

Pluronic P105	The ligands was conjugated by modifying the amino-terminated Pluronic P105 using DCC	-	Glucose and folic acid mediated cellular uptake by caveolae- and clathrin-mediated endocytosis	Delivery of DOX in glioma cells using "dual-targeting" strategy	➢ The functionalized PMs increased the bioavailability of DOX by 4.6-fold ➢ The formulation increased the distribution of loaded DOX in brain ($p<0.05$) than that of free DOX solution ➢ Improved the percentage survival of mice bearing glioma by 1.5-fold than that of PMs functionalized with glucose and folic acid alone	[160]
PEG-P(Glu)	The ligand was conjugated via C-6 into the α-end of PEG by ether linkage	-	Glucose ligand mediated tumor accumulation via GLUT1-transporter pathway	Targeted delivery of cisplatin in brain tumor cells	➢ The functionalized PMs decreased the tumor growth more effectively ($p<0.05$) than that of non-functionalized PMs despite low GLUT1 expression by glioma cells	[161]
CPT-SS-PEG-COOH	The ligand was conjugated via amide linkage to the carboxylic group of the PEG	Redox-responsive release	iRGD peptide based transportation via $\alpha_v\beta$ integrin and neuropilin-1 pathways	Combined chemotherapy with photodynamic therapy to target glioma cells	➢ 3.3-fold increase in the penetration capacity of the functionalized PMs was observed across BTB than that of non-functionalized PMs ➢ 1.1-fold increase in the cytotoxic action of functionalized PMs was noted against glioma cells than non-functionalized PMs ➢ Increased the survival rate of mice bearing glioma ($p<0.01$) than non-functionalized PMs	[96]

					➢ The co-loading of photosensitizer IR780 and CPT in functionalized PMs exhibited excellent cytotoxic potential than that of individual therapies	
PEG-PLA	Copolymer activation by EDC/NHS with addition of peptide in DMSO	-	Tfr-T12 mediated endocytosis via Tfr expressed on BBB and glioma cells	Targeted delivery of PTX at glioma site	➢ The functionalized PMs showed highest intracellular fluorescence in glioma cells than that of non-functionalized PMs by overcoming BBB/BTB ➢ 1.6-fold increase in the cytotoxic action of the functionalized PMs was observed than that of non-functionalized PMs	[162]
PLGA-PLL-PEG	Conjugated via the reaction of the N-terminal cysteine on ligands with the maleimide-PEG-SCM	-	Fusion peptide TPL (K-s-A) and Tet1 mediated BBB penetration and neuronal targeting via GT1b ganglioside receptor or by binding with BCECs	Delivery of neuroprotective peptide NAP to the AD lesions	➢ 3.1-fold increase in the uptake of functionalized PMs was observed in bEnd cells than that of free NAP ➢ 4-fold increase in the brain intracellular accumulation of functionalized PMs was observed in mice bearing brain metastasis than non-functionalized PMs	[163]

PEG-PLA	The ligand was conjugated by Michael addition reaction	-	Stapled RAP12 mediated LDL receptor related protein-1 transportation across BBB	Delivery of PTX to glioma cells	➢ 1.5- and 1.3-fold increase in the cellular uptake of functionalized PMs was observed in bEnd cells and U87 cells than non-functionalized PMs ➢ 2.7-fold higher penetration capacity of functionalized PMs was noted across BBB than non-functionalized PMs ➢ The functionalized PMs increased the anti-glioma efficacy by 2.3-fold than that of non-functionalized PMs	[145]
			Aptamers			
mPEG-PCL	Carboxyl group of the mPEG conjugated with 10 OD of GMT89	-	GMT8 ligand based higher affinity and specificity to bind with glioma cells	Intracellular delivery of DTX at glioblastoma cells	➢ 1.8-fold stronger fluorescence intensity of functionalized PMs was observed at the glioma site than non-functionalized PMs ➢ 1.1-fold increase in cell apoptosis rate was noted by the functionalized PMs than that of non-functionalized PMs	[164]
PEG-PLA	NHS-induced activation of terminal carboxyl group of copolymer and conjugated with 5'-	-	FB4 aptamers mediated active transport via Tfr expressed on BBB	Intracellular delivery of flurbiprofen to treat AD	➢ 2.2-fold higher cellular binding/uptake efficacy of functionalized PMs was observed in bEnd cells than non-functionalized PMs	[165]

	NH_2-modified FB4 aptamer	➢ 1.4-fold higher intracellular accumulation of functionalized PMs was noted in bEnd cells than non-functionalized PMs

Abbreviations: AD, Alzheimer's disease; **bEnd cells,** Microvascular brain endothelial cells derived from mouse brain; **BBB,** Blood brain barrier; **BTB,** Blood brain tumor barrier; **BCECs,** Brain capillary endothelial cells; **CHO-POESO**, Cholesterol-polyoxyethylene sorbitol oleate; **CPT-SS-PEG-COOH**, Camptothecin-disulfide bond-polyethylene glycol containing carboxylic group; **Dex-PTX**, Dextran-paclitaxel; **DMAP,** Dimethyl aminopyridine; **DMSO,** Dimethyl sulfoxide; **DTX,** Docetaxel; **EDC**, 1-Ethyl-3-(3-dimethylaminopropyl)carbodiimide; **GBM,** Glioblastoma multiform; **GLUT1,** Glucose transporter-1; **$(HE)_5$**, Polyanionic masking peptide (histidine-glutamic acid repeats); **K-s-A**, HER2-targeting KAAYSL (K) with MMP1(matrix metalloproteinase 1)-sensitive VPMS-MRGG (s) and LRP1-targeting angiopep2 (A); **LDL**, Low density lipoprotein; Mal, Maleimide; **mPEG-PCL**, Methoxy polyethylene glycol-polycaprolactone**;** mPEG-SS-g-P(ae-Asp), Methoxypolyethylene glycol-disulfide bond-graft- poly(N-(2-aminoethyl)-l-aspartamide); **nAchR**, Nicotinic acetylcholine receptors; **NHS**, N-hydroxysuccinimide; **PEG-P(Glu),** Poly (ethylene glycol)-poly(L-glutamic acid); **PEG-PHA**, Poly(ethylene glycol)-b-poly(hidrazinyl-aspartamide); **PEG-PLA**, Polyethylene glycol-polylactic acid; **PEG-SCM**, Polyethylene glycol-succinimidyl carboxymethyl ester; **PE-PEG**, 1,2-Distearoyl-sn-glycero-3-phosphoethanolamine-N-[methoxy(polyethylene glycol)-2000; **PLGA-PLL-PEG**, Poly(lactic-*co*-glycolic acid)- poly(*ε*-carbobenzoxy-L-lysine)-polyethylene glycol; **PTX**, Paclitaxel; **$(RG)_5$**, Arginine rich peptide; **Tfr**, Transferrin receptor; **U87 cells**, Malignant glioblastoma cells

4.3 Inhibition of P-gp efflux transporter

P-gp (Permeability-glycoprotein) is prototypic energy- and Na^+-dependent transporter or multidrug resistance which is encoded by multidrug resistance protein1/ATP-binding cassette subfamily B member 1 belonging to the family ATP-binding cassette transporters [166,167]. This multidrug resistance protein is also expressed by the reactive astrocytes via TNF-α and nuclear factor (NF)-κB signaling [168]. Its fundamental function is to impede the entry of harmful substances into the brain parenchyma from systemic circulations. Its overexpression is found in multiple neurological disorders and brain tumors. In brain tumors, P-gp is overexpressed at the BTB and in the cell membrane of tumor cells [169]. In addition, its overexpression is associated with multi-drug resistance against several anticancer and antiepileptic drugs [170]. However, temporary disruption of BBB upon exposure to higher focused ultrasound along with ultrasound contrast agents (microbubble) results in down-regulation of P-gp on the blood vessels [171]. This non-invasive approach is widely used to enhance the drug permeability into the brain tissues [172].

In addition, progressive dysfunction of P-gp with aging at the BBB is a contributing factor in increasing the risk of neurodegenerative diseases due to the increased risk of brain exposure to different xenobiotics and their possible toxicity [166,167,173]. For instance, its dysfunction reduces the clearance of the amyloid-β protein from the brain to the blood. Its regional up-regulation in the midbrain and frontal regions is found in *de novo* Parkinson's disease [174]. Therefore, it plays important role in reducing the brain bioavailability and efficacy of various CNS therapeutics via the efflux mechanism. Thus, it is considered a promising obstacle in drug delivery to the brain. Moreover, most of the direct P-gp transporter inhibitors under clinical trials have failed due to their potential in disrupting the basal transporter function throughout the body owing to the wide distribution of P-gp [175,176]. Therefore, modulation of the P-gp

activity without disrupting the barrier function may require more elegant strategies to deliver the therapeutic molecules across BBB [87].

Polymer-based nanotechnology is one of the most attractive and rapidly growing areas of nanomedicine-based technology. Examples of such materials are low molecular weight polymeric P-gp inhibitors. These include PEG300, TPGS (Vitamin E derivatives), polyethoxylated derivatives, thiomers, tween 80, and chitosan-4-thiobutylamidine [177–180]. Such polymers have been explored in increasing the oral bioavailability and penetration of therapeutic agents across the intestinal membrane using Caco-2 cell monolayer and its related *in-vivo* models by inhibiting P-gp activity. Therefore, such polymers carry the immense potential to be utilized in the designing of polymeric micelles for the effective delivery of therapeutic agents across BBB with enhanced retention effect [181–183].

Among these polymers, a polyethoxylated polymer such as polyethylene oxide (PEO) has been used as a hydrophilic block in the development of Pluronic block copolymers consisting polypropylene oxide (PPO) as a hydrophobic block of varying chemical compositions to modulate the P-gp efflux transporter activity on BBB [176]. Their self-assembling property in micellar structure with higher P-gp inhibition activity has been extensively utilized in brain-specific drug delivery [184,185].

The P-gp modulating mechanisms of Pluronics include influence on mitochondrial function, energy conservation (ATP-depletion), and fluidization of BBB membrane in cells expressing P-gp, which leads to its inhibition [49]. The presence of cholesterol content in the membrane is responsible to alter the basal ATPase activity of cells-expressing P-gp. Moreover, the interaction of single-chain units of Pluronics (chelation) with the exposed cell membrane causes an increase in membrane fluidity. As a result, contributes to disrupted P-gp transport

activity. However, the PPO chain length (hydrophobic) has a strong influence on membrane microviscosity [81,186,187]. The schematic illustration of both the pathways is presented in Fig 8.

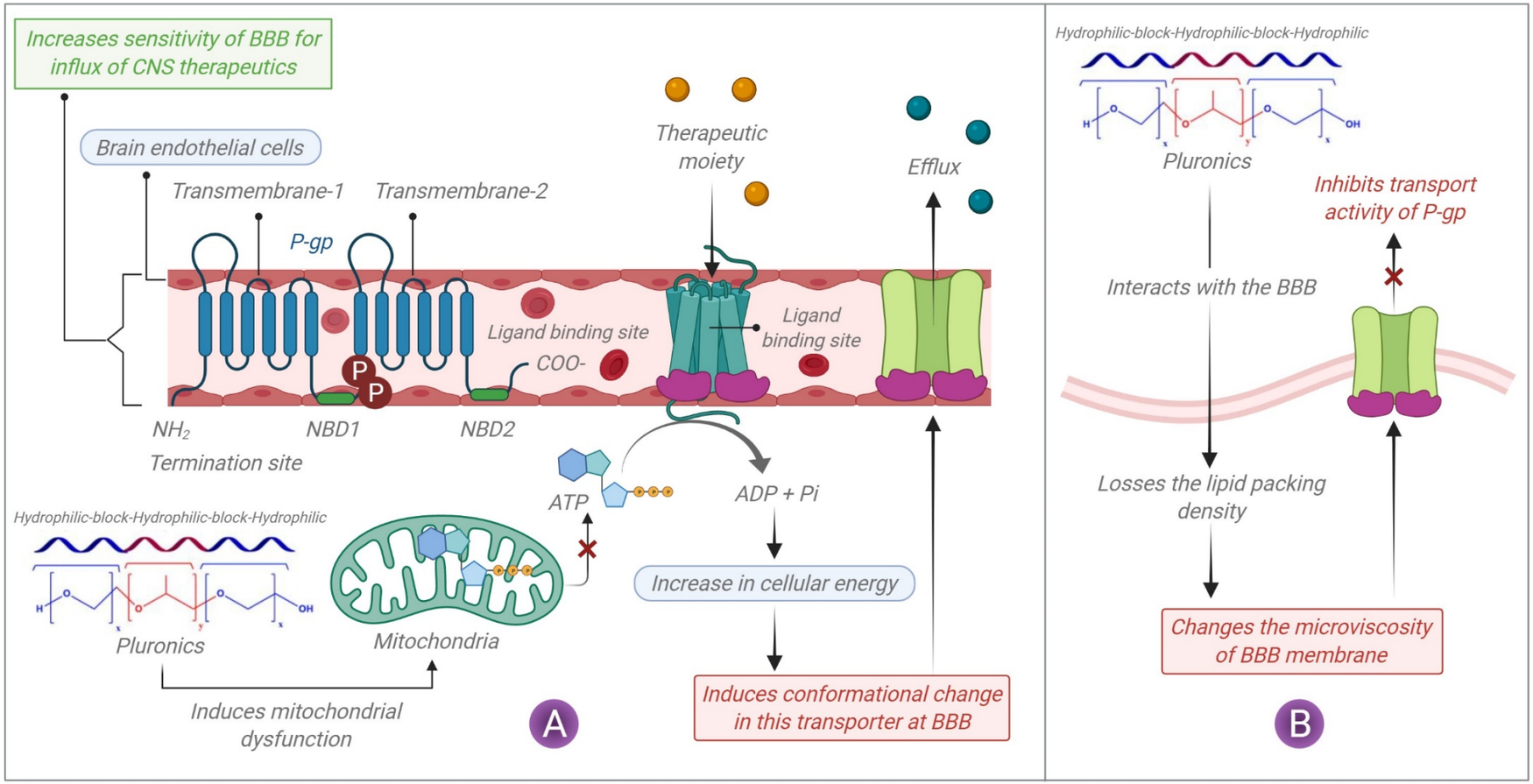

Fig 8: Mechanism of Pluronics in inhibiting P-gp-mediated efflux transport (A) Inhibition of ATP (B) Membrane fluidization

Abbreviations: ADP, Adenosine di phosphate; **ATP**, Adenosine triphosphate; **BBB**, Blood brain barrier; **NBD1/2**, Nucleotide binding domain 1 and 2; **P-gp**, P-glycoprotein

Several studies claimed the role of Pluronics as P-gp inhibitor. For instance, Muller et al. reported the first study regarding the effect of Pluronics on P-gp activity in BBB. This study revealed that the concentration of Pluronic P85 has a strong influence on the accumulation of rhodamine 123 in brain microvascular endothelial cells monolayers. The block copolymer P85 at a concentration below critical micelle concentration enhanced the accumulation of the rhodamine 123 in brain microvascular endothelial cells through inhibition of P-gp-mediated drug efflux. In addition, at a concentration above critical micelle concentration, P85 block copolymer increased the vesicular transport of the drug into brain microvessels. Such effect of the P85 block copolymer was found in cells/membranes overexpressing P-gp rather than the normal cells [188].

Batrakova et al. reported that the Pluronic block copolymers with differing HLB values and block lengths have a strong influence in inhibiting P-gp activity. The Pluronics with intermediate PPO block length (from 30 to 60 units) with HLB < 20 are reported to be the most effective ones in inhibiting P-gp efflux in brain microvascular endothelial cells than the Pluronics with HLB of 20–29 and PPO block length > 60 units respectively. Therefore, optimization of the Pluronic block copolymer composition is critically important for effective P-gp inhibition on BBB [182]. The studies on the inherent property of such block copolymer of varying composition in brain-specific delivery is presented in Table 4.

Table 4: Types of Pluronics with varied composition in brain specific delivery

Pluronic block copolymers	Average no of PPO units	Average no of PEO units	HLB value	Outcome	Reference
F127	65.2	200.4	22	➢ F127 based PMs increased the uptake of Rho123 (P-gp substrate) in RBECs of BBB (enhanced fluorescence) than free Rho 123 ➢ F127 based PMs increased the drug release in CSF by 1.1-fold than that of PBS within 24 h	[139,187,189]
P85	39.6	52.2	16	➢ P85 based PMs increased the drug release in CSF by 1.2-fold than that of PBS within 72h	[187,189]
F68	29.0	152.0	29	➢ F68 based PMs increased the drug release in CSF by 1.0-folds than that of PBS within 24 h	[189]
L121 and P123	68.2 70.0	10.0 40.0	1 8	➢ The L121 and P123 based mixed PMs exhibited higher brain/blood ratio ($p<0.05$) than free drug	[87,190,191]

				➢ The formulation decreased the blood concentration of drug with 15-fold increase in the brain concentration of drug via inhibition of P-gp mediated efflux mechanism	
P123	70.0	40.0	8	➢ P123 increased the brain uptake of PMs by 2-fold than free drug	[87,190,191]

Abbreviations: CSF, Cerebrospinal fluid; **PBS**, Phosphate buffer saline; **PMs**, Polymeric micelles; **RBECs**, Rat brain endothelial cells; **TPGS**, D-α-tocopheryl polyethylene glycol succinate

5. Application in neurotherapeutics

In this section, we described the challenges associated with the treatment of various CNS diseases and the applications of polymeric micelles as an alternative therapeutic option.

5.1. Alzheimer's disease

Alzheimer's disease is an acquired complex cognitive disorder that is associated with behavioral impairments/non-cognitive symptoms as the disease progresses [192,193]. This disease predominantly affects the memory-related regions of the brain with an accumulation of neurofibrillary tangles and extracellular amyloid plaques as a distinctive feature [194]. In addition, impaired hypothalamic function, metabolic derangement, disturbances in monoamine signaling and mood, and inflammation are also associated with Alzheimer's disease [195–197]. Despite the extensive investigation in understanding the pathophysiology of Alzheimer's disease over the past three decades, limited success has been achieved in terms of effective treatment to cure it. As the existing drugs have failed to provide a good therapeutic response in patients with Alzheimer's disease due to the following problems related to their inability to cross BBB. This includes hydrophilicity, extensive metabolism, poor solubility, and bioavailability via oral route [193,198]. Therefore, the effectiveness of the treatment can be increased by utilizing the principle of site-specific targeting and delivering strategies of polymeric micelles. For instance, Agwa et al. functionalized the polymeric micelles for targeted delivery of conjugated linoleic acid to the brain via an oral route to treat Alzheimer's disease. For the effective targeting of brain, linoleic acid was covalently attached with lactoferrin (Lf) via carbodiimide coupling reaction that formed the amide bond between the carboxylic groups of conjugated linoleic acid and primary amines of Lf. The developed polymeric micelles offered sustained-release profile and resulted in 2.8-fold increase in the concentration of drug in brain tissue than other organs without any toxic effects. This increased concentration of Lf was

attributed to Lf binding sites in brain endothelial capillary cells (receptor-mediated endocytosis). Its *in-vivo* study revealed 3-fold decrease in the hippocampus acetylcholinesterase activity, 3-fold increase in total antioxidant capacity with 2.2-fold decrease in the amyloid-β peptide 1-42 levels upon oral administration than diseased rats respectively [199].

The limited availability of anti- Alzheimer's disease drugs with potential to provide symptomatic relief by acetylcholinesterase inhibition and NMDA glutamate antagonism without any effect on disease progression has shifted the attention of researchers onto the other effective alternative approaches [200]. This includes peptide and siRNA (more potent and selective) based therapies with efficiency to regulate epigenetic changes and reduce the amyloid plaque area of brain by binding with amyloid-β, which is one of the hallmarks of Alzheimer's disease. However, their poor *in-vivo* stability, inefficient cell entry, lack of oral bioavailability, degradation by endopeptidases, and poor pharmacokinetic profile, are significant challenges in the clinical administration of the aforementioned therapeutics [76,164,201–203]. Therefore, the unique functional properties and prolonged retention effect of polymeric micelles have been utilized in the delivery of the aforementioned therapeutics for the effective management of Alzheimer's disease. PEGylation is one of the approaches used for augmenting their metabolic stability and reducing immunogenicity. For the effective amyloid-β targeting, functionalized cross-linked and hybrid micellar systems have been utilized to deliver the therapeutics by overcoming the transport barriers [76,164,204].

Further, the phytoconstituent-based therapies with efficiency to regulate hippocampal expression have also gained attention as an effective strategy to treat Alzheimer's disease. This is because of the reported pharmacological activities of phytoconstituents in *in-vivo* Alzheimer's disease models in regulating the hippocampal expression and progression at post-transcriptional levels. However, their poor penetration across BBB is also a major challenge. For instance Yang et al.

co-functionalized PEG-PLA based polymeric micelles with neural cell adhesion molecule mimetic peptide C3 and triphenylphosphonium via thiol-maleimide coupling reaction for neuronal-mitochondria targeting of resveratrol. The co-functionalized micelles showed 3.9-fold higher fluorescence in brain than non-functionalized polymeric micelles. *In vivo* studies revealed, higher localization of the co-functionalized polymeric micelles in brain neurons of transgenic mice than in the hippocampus and cortex regions of brain upon intravenous administration. The co-functionalized polymeric micelles delivered 2.6-fold higher concentration of resveratrol in brain mitochondria with 1.2-fold prolonged retention in blood than drug-loaded in non-functionalized polymeric micelles respectively. Further in animal model, the co-functionalization enhanced the therapeutic response of the resveratrol by reducing mitochondrial reactive oxygen species generation ($p<0.05$), higher SIRT-1 and synaptophysin expression ($p<0.05$), reducing hyperphosphorylation of tau-protein ($p<0.05$) and markedly reducing plaque burden in hippocampus and cortex regions than free drug respectively. The immunofluorescent images revealed reduced levels of microglial marker Iba-1 by functionalized polymeric micelles in hippocampal region of transgenic mice with Alzheimer's disease than free drug [205]. Further, the case studies on the polymeric micelles and its functionalization for the delivery of drugs, peptides, siRNA, and phytoconstituents across BBB for the effective treatment of Alzheimer's disease are presented in Table 5.

Table 5: Polymeric micelles based drug delivery systems and its functionalization to treat Alzheimer's disease

ABC	Targeting ligands/Stimuli	Size	Therapeutics	Biological model/route of administration	Outcome	References
				Synthetic drug therapy		
Polysorbate attached α,β-poly(N-2-hydroxyethyl)-d,l-aspartamide-squalenyl-C17	-	34 nm	Rivastigmine	➢ Neuro2A cells	➢ 2-fold increase in the drug concentration loaded in PMs was observed in Neuro2A cells than free drug ➢ 1-folds increase in the stability of drug loaded in PMs in human plasma than free drug (prolonged retention effect) ➢ Good cellular uptake potential	[206]
PCL-PMPC-PGMA	Asparagine endopeptidase-responsive	105 nm	Donepezil, PTX, insulin	➢ SAMP8 mice/ intranasal	➢ 1.2-fold higher number of NeuN in mice hippocampus than non-functionalized PMs (rescued memory deficits) ➢ 18.3-fold higher brain retention of donepezil than non-functionalized PMs	[207]
PEG-PLGA	-	Below 200 nm	Memantine	➢ bEnd cells ➢ APPswe/PS1dE9 mice/oral	➢ *In vitro* studies revealed 40% retention of the PMs in bEnd cells ➢ 2.3-folds decrease in the amyloid plaques was observed by the drug loaded PMs in cortex region of mice brain than free drug ($p<0.01$) respectively	[208]
DSPE-PEG2000	-	58.6 nm	Galantamine	➢ Wistar rats (β-Amyloid-induced)/oral	➢ 5.4-fold increase in brain concentration of drug loaded PMs was observed in 8h with 4.3-fold increase in AUC_{24} (brain levels) than free drug ➢ Enhanced pharmacological activity with higher reductions in MDA and nitrile levels ($p<0.001$) was observed upon treatment with drug loaded PMs than free drug ➢ The formulation increased the levels of GSH ($p<0.01$) than free drug	[209]
mPEG-PCL	-	84 nm	Metformin romidepsin	➢ Swiss albino mice (STZ-induced)/intravenous	➢ 1.0-folds and 1.1-fold decrease in the AchE activity/ histone H3 acetylation levels and CREB mRNA expression levels was observed by drug loaded PMs in mice brain than physical mixture of both the drugs respectively ➢ 1.3-fold reduction in the inflammatory markers was observed by drug loaded PMs than physical mixture of both the drugs	[210]

				Peptide therapy		
PEG-PLA	Wheat germ agglutinin	120 nm	VIP (neuroprotective peptide)	➢ Kunming mice SD rats (ethylcholine aziridium)/intranasal	➢ 5.6-, 6.6- and 7.7-fold increase in $AUC_{0\text{-}12h}$ of functionalized PMs was observed in olfactory bulb, cerebrum and cerebellum than non-functionalized PMs ➢ 2.1-fold increase in the cholinergic activity was noted than non-functionalized PMs	[211]
PEG-co-PCL	Lactoferrin	88 nm	NAP peptide	➢ ICR mice (amyloid $_{1\text{-}40}$ and IBO-induced)/intranasal	➢ Higher $AUC_{0\text{-}8h}$ ratio of brain/blood of functionalized PMs was observed than ($p<0.001$) non-functionalized PMs ➢ The functionalized PMs reduced the AchE activity by 1-folds than ($p<0.05$) non-functionalized PMs ➢ 1.1-fold increase in cholinesterase activity with decreased number of neuronal loss was noted in hippocampus CA1 region upon treatment with functionalized PMs ($p<0.05$) than non-functionalized PMs	[212]
				siRNA based therapy		
LPEI-g-PEG	Disulfide cross-linking	Below 100	siRNA for BACE1 (N/P ratio of 5)	➢ N2a cells ➢ C57BL/6J mice/intraventricular	➢ The functionalized PMs successfully targeted BACE1 and APP in cytoplasm of N2a cells ➢ 1.5- and 1.3-fold reduction was observed in BACE1 and APP levels with greater than 95% cell viability than nontransfected control respectively ➢ 1.8-fold higher *in-vivo* BACE1 knockdown efficiency of the PMs was observed in cortex and hippocampus region of mice brain than non-transfected control	[213]
PEG-PDMAEMA	CGN and QSH peptide	70 nm	siRNA for BACE1 (N/P ratio of 10)	➢ ICR mice (amyloid-β_{42}-induced)/intravenous	➢ Higher BACE1 inhibition efficiency ($p<0.05$) by functionalized PMs was observed in hippocampus region than sham control ➢ 2.5-fold increase in hippocampus/cerebellum ratio of functionalized PMs was noted than non-functionalized PMs	[204]

PEG-PDMAEMA	CGN and QSH peptide	70 nm	siRNA for BACE1 (N/P ratio of 10)	➢ APP/PS1 mice/intravenous	➢ 1.9- and 3.9-fold higher concentration of functionalized PMs was observed in brain region than non-functionalized PMs ➢ The functionalized PMs inhibited amyloid-β production by silencing BACE1 gene expression and its downstream proteins ($p<0.05$) than non-functionalized PMs ➢ The functionalized PMs reduced the *in-vivo* amyloid plaque burden to a greater extent in hippocampus region of mice than non-functionalized PMs	[214]
				Phytoconstituents		
mPEG-PCL	-	70 nm	Resveratrol	➢ PC12 cells (amyloid-β treated)	➢ Higher cellular uptake of PMs was noted in the cytoplasm of PC12 cells ➢ 1.4-fold increase in the cell viability of PMs was observed than free drug ➢ 1.9-fold higher reduction in caspase-3 activation by PMs than free drug	[215]
PEG-PLA	-	80 nm	Curcumin	➢ Tg2576 mice/oral	➢ 6-fold higher AUC and mean residence time of PMs was noted in brain than free curcumin ➢ Reduced the plaque area of brain ($p=0.046$) than free curcumin respectively and indicated potential for AD therapy	[216]
PEG-Lys-PCL	-	91 nm	Baicalein	➢ Wistar rats (scopolamine-induced)/intraperitoneal	➢ 5.0- and 2.2-fold increase in the BDNF gene expression by PMs was observed than scopolamine control and memantine treated group respectively ➢ 15.0-fold increase in SIRT6 gene expression by PMs was observed than scopolamine control without any significant difference with memantine treated group ➢ 27.0-and 3.1-fold increase in SELADIN gene expression by PMs was noted than scopolamine control and memantine treated group	[217]

Abbreviations: AchE, Acetylcholinesterase; **AD,** Alzheimer's diseases; **APP,** Amyloid precursor protein; **AUC,** Area under curve; **bEnd cells,** Brian endothelial cells; **BACE1**, β-site amyloid precursor protein-cleaving enzyme 1; **BDNF,** Brain derived neuronal factor; **bFGF**, basic fibroblast growth factor; **CA1,** Hippocampal cornu ammonis; **CGN,** Human synthetic cingulin peptide; **CREB,** Cyclic AMP-response element binding protein; **DSPE-PEG2000**, 1, 2-Distearoyl-sn-glycero-3-phosphoethanolamine-polyethylene glycol 2000; **GSH**, Reduced glutathione; **LPEI-g-PEG**, Linear polyethyleneimine-graft-polyethylene glycol**; MDA**, Malondialdehyde; **mPEG-PCL**, methoxypolyethylene glycol-polycaprolactone; **NAP**, Neuroactive peptide**; NeuN**, Neuronal specific nuclear protein; **Neuro2A/N2a cells**, Mouse neuroblastoma cell line; **PC12 cells,** Pheochromocytoma of the rat adrenal medulla; **PMs,** Polymeric micelles; **PCL-PMPC-PGMA**, Polycaprolactone-Poly (2-methacryloyloxyethyl phosphoryl choline) - poly (glycidyl meth- acrylate); **PEG-co-PCL**, Polyethylene glycol-co-polycaprolactone; **PEG-Lys-PCL**, Poly Ethylene Glycol-Lysine-(Poly Caprolactone); **PEG-PDMAEMA**, Polyethylene glycol- Poly(2-dimethylamino)ethyl methacrylate);; **PEG-PLA**, Polyethylene glycol-polylactic acid; **PEG-PLGA**, Polyethylene glycol-Polylactic-co-glycolic acid; **QSH,** D-enantiomeric peptide, QSHYRHISPAQV; **SD**, Spragy-dawley; **siRNA**, Small interfering ribonucleic acid; **SIRT6,** Sirtuin 6; **STZ,** Streptozotocin; **VIP**, Vasoactive intestinal peptide

5.2 Parkinson's disease

This disease is the second most commonly occurring neurodegenerative disease that is characterized by movement disorder with additional non-motor symptoms [218]. The movement disorder occurs mainly because the dopaminergic neurodegeneration of substantia nigra pars compacta region in the midbrain results in striatal dopamine depletion [219]. While the non-motor symptoms appear due to widespread neurodegeneration involving cortex and brainstem regions [220]. Mitochondrial dysfunction, oxidative stress, and impairment of microglia are also associated with the disease as observed in the case of neurodegenerative disorders [221]. The presence of α-synuclein (α-syn) aggregates (Lewy bodies) contributes to the pathogenesis of Parkinson's disease [222].

Mostly the available anti- Parkinson's disease drugs restore the dopaminergic activity in striatum by acting on dopaminergic pathways including dopaminergic neurons, receptors (agonists and antagonists), and its associated metabolic pathways by acting on monoamine oxidase-B and catechol-O-methyltransferase [223]. However, their poor pharmacokinetic profile and undesirable side effects at higher doses such as dyskinesia, anxiety, depression, and motor complications limit their therapeutic efficacy [224]. The encapsulation of anti-Parkinson's disease drugs in micelles has been reported to increase the therapeutic effect of drugs by improving consistency, brain penetration, metabolic stability, controlled release, and bio-distribution of drugs [225]. For instance, Bi et al. developed PEG-PLA based polymeric micelles surface-functionalized with LF for the intranasal delivery of rotigotine to brain for the treatment of Parkinson's disease. The functionalization led to higher cellular uptake of PMs in 16HBE and SH-SY5Y cells ($p<0.05$) than non-functionalized polymeric micelles via LF-mediated enhanced penetration with higher intracellular localization around nuclei. The *in vivo* study revealed enhanced fluorescence signals of functionalized polymeric micelles in mice brain (higher brain accumulation) post 6h incubation than non-functionalized polymeric

micelles upon intranasal administration in a concentration-dependent manner respectively. Further, an increase in AUC_{0-8h} of rotigotine by 1.2-, 1.3-, 1.9-, and 1.2- fold in olfactory bulb, striatum, cerebrum with removed striatum, and cerebellum was observed in case of functionalized PMs compared to non-functionalized PMs respectively [226].

Vong et al. developed poly(L-DOPA)-based self-assembled nanodrug based on poly(L-DOPA $(OAc)_2$) as hydrophobic segment and PEG as hydrophilic segment by dialysis method to improve the Parkinson's disease symptoms of L-DOPA. The cleavage of peptide bonds and acetyl groups in copolymer in the presence of physiological enzymes (protease and esterase) provided a prolonged supply of drug into the systemic circulation with improved dopamine conversion in brain upon intraperitoneal administration of L-DOPA loaded polymeric micelles. Its *in vivo* studies revealed 7.9-fold increase in AUC of plasma in mice treated with the polydopamine nanoparticles than free drug upon intraperitoneal administration respectively. The therapeutic effect of the polydopamine nanoparticles was increased by 1.2- and 1.4-fold ($p<0.05$) than the free drug as a measure of reduced foot slips and resting tremor score in grid/beam walk test without any potential toxicity. In addition, the polydopamine nanoparticles inhibited the L-DOPA-induced dyskinesia in mice by reducing the abnormal involuntary muscle score ($p<0.01$) and increasing the latency time ($p<0.05$) than free drug respectively. Therefore, polymeric micelles can be used to enhance the clinical utility of anti-Parkinson's disease drugs [227].

In one of the studies, Wang et al. developed polymeric micelles-based thermosensitive gel composed of mPEG-PLGA to enhance the solubility and brain delivery of rotigotione. *In vivo* study revealed 1.2-fold higher mean residence time of drug-loaded polymeric micelles based thermosensitive gel upon intranasal administration than drug-loaded polymeric micelles. In addition, the formulation revealed 1.79-fold higher mean residence time of drug-loaded polymeric micelles based thermosensitive gel in comparison with intravenous administration.

Polymeric micelles based thermosensitive gel enhanced the distribution of drug in olfactory bulb, cerebrum, cerebellum, and striatum by 2.7-, 1.7-, 1.6-, and 1.8-fold upon intranasal administration without damaging nasal mucosa of rats in comparison to intravenous administration of free drug solution [228]. Brynskikh et al. developed polyion complex micelles composed of PEG-PEI for the packaging of catalase for brain delivery. Further, to enhance the BBB penetration and to overcome the breakdown of the catalase, the packed nanoenzyme was loaded into bone marrow macrophage to treat Parkinson's disease. The *in vivo* study performed on C57Bl/6 mice revealed higher localization of functionalized polymeric micelles in brain than non-functionalized PMs respectively. The functionalized polymeric micelles with bone marrow macrophage exhibited a good biodistribution profile of the loaded enzyme in the brain of MPTP (1-methyl-4-phenyl-1,2,3,6-tetrahydropyridine)-intoxicated mice than enzyme loaded polymeric micelles without bone marrow macrophage. Further, it exhibited 2-fold reduction in the micro- gliosis (CD11b expression) and 2-fold increase in the tyrosine-hydroxylase expressing dopaminergic neurons in mice than non-functionalized polymeric micelles and control upon intravenous administration, respectively [229].

Amongst phytoconstituents, acteoside and Epigallocatechin-3-gallate are capable of ameliorating oxidative stress-induced nuceli/DNA fragmentation and in regulating tyrosine hydroxylase /α-syn expression in substantial nigra region of brain [230]. These have been loaded in PMs to enhance their therapeutic efficacy and brain delivery. For instance, Xue et al. developed chitosan-coated mPEG-PLA based polymeric micelles conjugated with nerve growth factor, acteoside and pDNA to treat Parkinson's disease. The schematic illustration of conjugation and its treatment process. The *in vivo* study performed on MPTP-intoxicated C57 mice revealed higher fluorescent intensity of functionalized polymeric micelles in substantia nigra region of brain by nerve growth factor receptor-mediated endocytosis than control upon

intraperitoneal administration. The functionalized polymeric micelles released acteoside and pDNA into the neurons via entry by nerve growth factor receptor expressed on neurons and repaired damaged dopaminergic neurons by reducing tyrosine hydroxylase /α-syn expression ratio in mice ($p<0.01$) than disease-induced group respectively [231]. The case studies regarding brain-specific delivery of therapeutics for the treatment of Parkinson's disease using polymeric micelles are presented in Table 6.

Table 6: Polymeric micelles based drug delivery systems and its functionalization to treat PD

ABC	Targeting ligands	Size	Therapeutics	Biological model/route of administration	Outcome	Reference
				Proteins		
PEG-PLGA	Lactoferrin	Less than 150 nm	Urocortin	➢ bEnd.3 cells ➢ BALB/c mice (6-OHDA-induced)/intravenous	➢ 3-fold increase in brain accumulation of functionalized PMs was observed than non-functionalized PMs via endocytosis mechanism involving lactoferrin ➢ 2.4- and 2.3-fold increase in AUC and C_{max} of coumarin-6 in brain by functionalized PMs was noted than non-functionalized PMs ➢ The functionalized PMs reduced the striatum lesion of mice with higher contents of dopamine, DOPAC, and HVA than PBS group respectively	[232]
PEG-PLGA	Odorranalectin	114 nm	Urocortin	➢ Hemiparkinsonian rats (6-OHDA-induced)/intranasal	➢ Stronger fluorescence intensity of functionalized PMs was noted in brain for up to 8h ($p<0.05$) than non-functionalized PMs ➢ 3.4-fold decrease in rotation number of rats by functionalized PMs was observed in rotation behavior test than non-functionalized PMs ➢ 2.2-fold increase in dopamine levels was noted by functionalized PMs in lesioned striatum of rats than non-functionalized PMs	[233]

			Genes			
PEG-PAMAM	Lactoferrin	-	hGDNF	➢ SD rats (Rotenone-induced)/intravenous	➢ 1.7-fold higher GDNF expression levels by lactoferrin functionalized PMs was noted than transferrin functionalized PMs ➢ 6.2-fold higher GDNF expression levels by lactoferrin functionalized PMs post five injections in rats than its single injection respectively ➢ 8-fold higher dopamine levels was noted in rats treated with lactoferrin functionalized PMs than that of functionalized PMs without GDNF	[234]
DGL-PEG	Angiopep	119 nm	hGDNF	➢ SD rats (Rotenone-induced)/intravenous	➢ Higher cellular uptake of functionalized PMs was observed than non-functionalized PMs in BCECs ➢ The functionalized PMs reduced the loss of dopaminergic neurons in nigrostriatal system of rat's brain than non-functionalized PMs after 45 days of treatment	[235]
PEG-PEI	-	129 nm	siSNCA	➢ PC12 cells	➢ The PMs exhibited better transfection efficiency of 72.4% in PC12 cells than lipofectamine/siSNCA ➢ The formulation showed higher intracellular distribution in PC12 cells by escaping the lyososme ➢ 1.0-folds decrease in mRNA SNCA expression levels was observed by functionalized PMs than	[236]

						lipofectamine/siSNCA respectively with higher cell viability	
Phytoconstituents							
Pluronic® F127 and sodium dodecyl sulfate	-	35 nm	EGCG	➢ NLCs ➢ Knockdown parkin transgenic *Drosophila Melanogaster*		➢ The developed PMs ameliorated the generation of reactive oxygen species in NLCs and maintained mitochondrial membrane potential ($p<0.01$) than free EGCG respectively ➢ 2.5-fold decrease in MDA levels was noted by PMs than free EGCG in flies ➢ The formulation increased the survival proportion and climbing performance of transgenic parkin flies ($p<0.05$) than that of free EGCG	[237]

Abbreviations: BCECs, Brain capillary endothelial cells; **DGL-PEG**, Dendrigraft poly-L-lysine-polyethylene glycol; **DOPAC**, 3, 4-Dihydroxyphenyl acetic acid; **EGCG**, Epigallocatechin-3-gallate; **GFP**, Green fluorescent protein; **hGDNF**, Human glial cell line-derived neurotrophic factor; **HVA**, Homovanillic acid; **MDA**, Malondialdehyde; **NLCs**, Nerve like cells; **6-OHDA**, 6-hydroxydopamine; **PBS**, Phosphate buffer saline; **PC12 cells**, Pheochromocytoma cell line; **PEG-PAMAM**, Polyethylene glycol-poly(amidoamine); **PEG-PEI**, Polyethyleneglycol- polyethyleneimine; **PEG-PLGA**, Polyethylene glycol-poly(lactic-co-glycolic acid); **SD rats**, Spraguy-dawley rats; **siSNCA**, α-synuclein siRNA

5.3 Gliomas

Gliomas are the most commonly occurring primary brain tumors (intra-axial) found in adults with high heterogeneity [238]. These are of mostly neuroepithelial origin and differ in mutation status in diverse patients [239,240]. These possess similarities with the glial cells of the brain and are composed of astrocytomas, oligodendrogliomas, and ependymomas depending upon the type of glial cell involved in tumor [241]. Amongst these, the high-grade astrocytomas i.e., “glioblastoma multiforme”, is the most aggressive and malignant form of all brain tumors. They are mostly found in cerebrum and cerebellum region of brain [242]. The glioma cells consist of glioblastoma stem cells, which are highly infiltrative, invasive, aggressive and resistant to therapy. This results in incomplete cytoreductive surgeries and reoccurrence of tumor within 2 cm of the original lesion [238]. Thus, these are characterized by invasive phenotype with high migration ability [243]. Furthermore, the side effects of radiotherapy and poor efficacy of the usual chemotherapy increase the mortality risk i.e., the median survival time of 14.6 months in glioma patients [244]. Therefore, the encapsulation of various CNS therapeutics into the polymeric micelles is reported to offer higher drug delivery across the BBB/BTB. The case studies on polymeric micelles used in the treatment of gliomas are presented in Table 7.

Table 7: Polymeric micelles based drug delivery systems and its functionalization to treat gliomas

ABC	Targeting ligands/stimuli	Size	Therapeutics	Biological model/route of administration	Outcome	Reference
				Chemotherapeutic drugs		
PEG-PLA	-	30 nm	Cyclopamine and temozolomide	➢ U87MG cells	➢ 3.7-fold increase in inhibition of GBM cells by cyclopamine loaded PMs than free drug ➢ 1.3-fold decrease in clonogenicity of GBM cells by cyclopamine loaded PMs than free drug by attenuating Gli1 expression ➢ Combination of cyclopamine loaded PMs with temozolomide exhibited combination index between 0.1 and 0.3 and indicated synergism	[245]
PEtOz-SS-PCL	Reduction responsive	88.4 nm	Doxorubicin	➢ Orthotopic C6-Luci cells-bearing mice/intravenous	➢ 2.4-fold increase in doxorubicin concentration by functionalized PMs in mices' brain than free drug via EPR effect ➢ 1.1-fold decrease in the tumor growth rate of drug loaded functionalized PMs in mice than free drug ➢ 1.4-fold increase in median survival time of mice than free drug	[246]
DSPE-PEG2000	Borneol	14.9 nm	Doxorubicin	➢ C6-glioblastoma cells ➢ C6 cells bearing ICR mice/intravenous	➢ 0.9-folds higher drug penetration across BBB by functionalized PMs than non-functionalized PMs ➢ Functionalized PMs reduced the tumor volume in histopathological brain samples of mice than non-functionalized PMs	[247]
PEG-PCL	Tat-cell penetrating peptide/bombesin (GRPR ligand)	79.6 nm	Camptothecin	➢ C6-glioma cells ➢ C6 glioma rat model/intranasal	➢ 1.8-fold decrease in the cell-viability of glioma C6 cells by drug loaded fusnctionalized PMs than non-functionalized PMs via	[155]

					receptor mediated endocytosis due to GRPR binding on glioma cells ➢ 2.0- and 1.3-fold increase in the mean survival time of rats by functionalized PMs than free drug and functionalized PMs without bombesin	
PEG-PLA	Cyclic RGD	35 nm	Paclitaxel	➢ U87MG cells ➢ U87MG cells bearing mice/intravenous	➢ 2.5-fold increase in the cytotoxic effect of drug loaded functionalized PMs than non-functionalized PMs due to higher binding of targeting ligand with glioma cells ➢ 2.3-fold decrease in the tumor volume of mice by drug loaded functionalized PMs than non-functionalized PMs with higher intracranial tumor accumulation	[248]
PEG-PLA	RI-VAP	25 nm	Paclitaxel	➢ U87MG cells bearing nude mice/intravenous	➢ Higher transcytosis efficiency and cellular uptake than non-functionalized PMs due to higher affinity to bind with GRP78 overexpressed on glioma cells ➢ Higher targeting ability ($p<0.001$) than non-functionalized PMs ➢ Higher reduction in tumor volume than ($p<0.001$) non-functionalized PMs	[249]
PEG-PLA	Stapled RAP12	35 nm	Paclitaxel	➢ U87MG cells bearing ➢ BALB/c nude mice/intravenous	➢ 3.0-fold increase in the penetration capacity of functionalized PMs in brain than non-functionalized PMs ➢ 2.1-fold higher accumulation of functionalized PMs in mice brain than non-functionalized PMs ➢ 1.3-fold increase in anti-glioma efficacy in mice than non-functionalized PMs and functionalized PMs without stapled RAP12	[145]
Proteins/peptides						

PEG-PLA	Cyclic RGD peptide	22.4 nm	sPMI	➢ U87MG cells ➢ U87MG cells implanted BALB/c nude mice/intravenous	➢ 1.9-fold decrease in the cell viability of glioma cells by peptide loaded functionalized PMs than sPMI alone respectively by increasing the protein levels of p53 and MDM2 ➢ 2.4-fold increase in the apoptotic effect by peptide loaded functionalized PMs in glioma cells than sPMI alone by arresting cells in G1 and G2 phase ➢ 3.6-fold decrease in the tumor volume of mice by peptide loaded functionalized PMs with temozolomide than that of functionalized PMs without temozolomide respectively	[250]
				Nucleic acid		
CDX–PEG–b-PLA and PEG-PEI	Cyclic RGD	-	TRIAL gene and paclitaxel	➢ U87 cells bearing nude mice/intravenous	➢ 2.1-fold increase in the transfection efficiency of functionalized mixed PMs was observed upon co-loading of drug and gene ➢ The co-loaded functionalized mixed PMs resulted in prolonged survival time in mice bearing glioblastoma cells ($p<0.0001$) than individual functionalized mixed PMs because of synergistic anti-glioblastoma effect	[251]
PLA-b-PDMAEMA	-	65 nm	miR-21 inhibitor and doxorubicin	➢ LN229 glioma cells bearing BALB/c-A nude mice/intratumoral	➢ 2.5-fold higher transfection efficiency of PMs than PEI due to higher surface charge density and improved endosomal escaping ability ➢ 9-fold decrease in the tumor volume by PMs was observed than that of negative control after 22 days of treatment	[252]

R7L10 amphiphilic peptide	-	-	Glioblastoma-specific thymidine kinase gene and bevacizumab	➢ Glioblastoma bearing BALB/c-A nude mice/intratumoral	➢ 100-fold lower *in vitro* transfection efficiency of peptide PMs was observed than PEI ➢ 2.1-fold decrease in cell viability by peptide PMs was observed than PEI ➢ 1.2- and 1.5-fold decrease in the tumor volume by peptide PMs was noted than drug alone and blank PMs	[253]
PEG-PEI-PCL	Folic acid	54 nm	Anti-BCL-2 siRNA and temozolomide	➢ Rat bearing orthotropic glioma/intracranial	➢ The co-loaded functionalized PMs reduced the tumor volume ($p < 0.05$) in rats in comparison to functionalized PMs containing individual therapy ➢ The co-loaded functionalized PMs reduced the expression level of BCL-2 in glioma cells ($p<0.05$) than that of functionalized PMs containing individual therapy ➢ 2.2- and 2.5-fold decrease in tumor volume by co-loaded functionalized PMs was noted than that of individual functionalized PMs containing drug/siRNA respectively	[254]
				Phytoconstituents		
pNP-PEG$_{3400}$-DOPE	scFv (GLUT1 antibody)	14.8 nm	Curcumin and doxorubicin	➢ U87MG cells	➢ 2.9-fold increase in doxorubicin concentration in the nuclei was observed by functionalized PMs than free drug ➢ The co-loaded functionalized PMs exhibited increased cytotoxic effect than ($p<0.05$) that of non-functionalized PMs. ➢ Therefore, indicated synergism with improved combination index ➢ 1.9-fold decrease in cell viability of U87MG spheroids was noted by co-loaded functionalized PMs than ($p<0.005$) that of free curcumin/doxorubicin respectively	[255]

Chitosan-Pluronic	-	51 nm	Myricetin	➢ DBTRG-05MG cells ➢ Nu/nu mice/intragastric	➢ Higher permeability across BBB of myricetin PMs was observed than ($p<0.05$) free myricetin ➢ 2.1-fold increase in the content of myricetin PMs was observed in brain than free myricetin within 40 minutes of intragastric administration ➢ 1.3-fold decrease in tumor volume of mice by myricetin PMs was noted than that of blank PMs	[256]
mPEG-PCL	-	34 nm	Honokiol and doxorubicin	➢ C6 cells bearing nude BALB/c mice	➢ 1.4- and 3.1-fold increase in cell apoptosis by co-loaded PMs was noted than individual PMs (containg both drugs alone) ➢ 2.3-and 3.6-fold decrease in the tumor volume by the co-loaded PMs was observed than that of individual PMs ➢ 1.8- and 3.4-fold decrease in the tumor weight by co-loaded PMs was noted than individual PMs	[257]

Abbreviations: BBB, Blood brain barrier; **BCL-2,** B-cell lymphoma 2; **C6-cells**, Spindle-like cells that simulate human glioblastoma; **CDX-PEG-b-PLA**, Cyclodextrin-polyethylene glycol-block-poly lactic acid; **DSPE-PEG2000**, Distearoyl phosphatidyl ethanolamine-polyethylene glycol; **DBTRG-05MG cells**, Denver Brain Tumor Research Group 05; **EPR**, Enhanced permeation effect; **GBM**, Glioblastoma multiforme; **GLUT1**, Glucose transporter antibody single chain fragment variable; **GRP-78**, Glucose-regulated protein-78; **GRPR**, Gastrin releasing peptide receptor; **LN229 cells**, Mutated p53 malignant glioblastoma cell line; **MDM2**, Murine double minute 2; **mPEG-PCL**, Methoxy polyethylene glycol –polycaprolactone; **PEG-PCL**, Polyethylene glycol-polycaprolactone; **PEG-PEI**, Polyethylene glycol-polyethylenimine; **PEG-PEI-PCL**, Polyethylene glycol-polyethylenimine-polycaprolactone; **PEG-PLA**, Poly(ethylene glycol)-co-poly(lactic acid); **PLA-b-PDMAEMA**, Poly(lactic acid)-block-polydimethylaminoethyl methacrylate; **PEtOz-SS-PCL**, Poly (2-ethyl-2-oxazoline)-b-poly (epsilon-caprolactone); **pNP-PEG$_{3400}$-DOPE**, Nitrophenylcarbonyl-polyethylene glycol3400- 1,2-dioleoyl-sn-glycero-3- phosphoethanolamine; **R7L10**, Arginine stretch and a 10-leucine stretch**; siRNA,** Small interfering ribonucleic acid; **sPMI**, Stapled peptide antagonist; **U87MG cells**, Malignant glioblastoma cell line

For instance, Li et al. developed docetaxel conjugated polylactic acid-polyethylene glycol functionalized with cyclic Arginine-Glycine-Aspartic acid-D-Tyrosine-Lysine c(RGDyK) ligand for targeting integrin $\alpha_v\beta_3$ receptors overexpressed in glioblastoma. These showed higher cellular uptake by U87MG and 9L cancer cells ($p<0.05$) in comparison to free drug and non-functionalized polymeric micelles respectively because of higher binding affinity of targeting ligand with integrin receptors. The functionalized PMs exhibited 1.5- and 2.2-fold increase in G2/M phase arrest of cancer cells in comparison to non-functionalized PMs and free drug with 4-fold higher area under curve than free drug respectively. *In vivo* study revealed about 1.9- and 2.9-fold decrease in relative tumor volume than non-functionalized polymeric micelles and free drug upon intravenous administration in tumor-bearing mice [258]. Nguyen et al. developed cationizable and non-ionizable polymeric micelles composed of DSPE-mPEG(2000) (1,2-distearoyl-sn-glycero-3-phosphoethanolamine-methylpolyethyleneglycol-2000) (cationizable) and DSPE-PEG(2000)-amine (non-ionizable) copolymer to study their impact on *in vivo* intra-arterial treatment of glioma in rats. The *in vivo* study revealed 1.6-fold increase in the concentration of cationizable polymeric micelles in hemisphere of healthy rats ($p<0.01$) in comparison to non-ionizable polymeric micelles respectively upon intra-arterial delivery. On the other hand, intra-arterial delivery of both the polymeric micelles in glioma-bearing rats revealed higher fluorescence in tumor (higher deposition) targeted by cationizable polymeric micelles than non-ionizable polymeric micelles along with heterogeneous distribution in lesion present in non-sectioned brains. Such variability in micellar deposition within tumor was demonstrated due to structural variability within lesion and subtle difference in arterial blood supply and pH. Thus, this study indicated that the optimization of polymeric micelles as a nanocarrier for site

specific drug delivery could offer significant impact on intra-arterial treatment of glioma [259].

In another study, Guo et al. developed carmustine loaded polymeric micelles based on DSPE-PEG and bifunctionalized it using Pep-1 and borneol to penetrate across BBB and to target interleukin-13 receptor overexpressed on glioma cells. These showed higher cellular uptake by human brain microvascular endothelial cells ($p<0.01$) than non-functionalized polymeric micelles respectively without producing any cytotoxic effect on endothelial cells. The developed bifunctionalized polymeric micelles exhibited good penetration efficiency across brain endothelial cells than non-functionalized micelles. However, no significant difference was observed between borneol functionalized polymeric micelles and bi-functionalized micelles, which indicated that borneol modification contributed in increasing the BBB penetration and Pep-1 in recognizing the tumor cells. The *in vivo* study revealed the highest accumulation and the longest retention of the bifunctionalized micelles at the brain sites (higher fluorescence) upon intravenous administration. Thus, exhibited higher biodistribution profile owing to better permeability and brain targeting efficiency ($p<0.01$) than non-functionalized polymeric micelles. The dual functionalized polymeric micelles exhibited greater reduction in tumor growth of orthotopic Luc-BT325 glioma tumor bearing nude mice than free drug and functionalized polymeric micelles without Pep-1. These also prolonged the survival time by 1.0- folds and 1.1-fold than non-functionalized polymeric micelles and free drug respectively [260].

Zhang et al. developed polyoxazoline-polyurethane (PMeOxPU(SS)-PMeOx) based polymeric micelles by incorporating disulfide bonds (reduction-responsive) into polyurethane backbone along with pH-sensitivity (PMeOx) for the efficient delivery of doxorubicin to glioma cells. The *in vitro* study revealed 1.2-fold increase in drug release

by dual responsive functionalized polymeric micelles at pH 5.0 in comparison to drug release at pH 7.4 buffer in the presence of redox reagent dithiothreitol. Furthermore, about 1.1-fold higher release of drug was observed at pH 5.0 in case of dual-responsive polymeric micelles as compared to redox-responsive micelles (single-responsive) after second and fourth hour. The developed dual-responsive polymeric micelles reduced the IC_{50} value of loaded drug by 6.3-fold than redox-responsive polymeric micelles because of the presence of disulfide bonds in polymer's backbone that triggered more release of drug, which markedly reduced the tumor growth of C6-glioma cells. The prepared dual-responsive blank polymeric micelles were found non-toxic to C6-glioma cells, which makes them a suitable nanocarrier for *in vivo* drug delivery [261].

5.4 Huntington's disease

Huntington's disease is rarely occurring form of chronic neurodegenerative disease with four to ten cases per 100, 000 in populations of Western European origin [262]. This disease is caused by the repetition of CAG-trinucleotide in the gene that encodes for Huntingtin protein or by the expansion polyglutamine tract in Huntingtin protein with complex and unclear etiology [262,263]. It is characterized by neurodegeneration in striatum (caudate nucleus and putamen) with specific loss of efferent medium spiny neurons. This ultimately leads to shrinkage of brain [264]. The clinical manifestations of the huntington's disease include movement disorder (chorea, loss of coordination, and psychiatric symptoms) and cognitive impairments [262].

Amongst the recent treatment strategies, lithium salts have been widely explored as effective drugs to treat chronic neurodegenerative diseases including Huntington's disease due to their multifold actions i.e., neuroprotective, anti-inflammatory and enzyme inhibitory effects [265,266]. Therefore, larger doses of lithium salts are considered to be

an effective treatment strategy to treat Huntington's disease [267,268]. However, lithium salt therapy requires optimization due to its toxicity in other organs owing to slow BBB penetration [269]. Therefore, the encapsulation of lithium salts or any neuroprotective therapeutic molecule in polymeric micelles could be a prominent strategy to target them at the brain site via endocytosis.

For instance, Xue et al. developed ethylene oxide containing self-fluorescent amphiphile i.e. tetraphenylethelene that self-assembled in micellar structure consisting ethylene oxide as corona and tetraphenylethelene as core to encapsulate lithium ion (tetraphenylethelene -$(EO)_4$-L_2). These showed strong blue fluorescence due to presence of TPE upon incubation with HeLa cells for 12h without any cytotoxicity. The obtained results indicated that the lithium based polymeric micelles should be explored in the clinical treatment of Huntington's disease. In addition, they paved the way for the new generation of lithium based drugs [267].

Recently, Pepe et al. developed amphiphilic hyaluronic acid-fatty acid conjugates loaded with curcumin owing to its anti-apoptotic action for the treatment of Huntington's disease. The developed nanoparticles increased the curcumin's brain bioavailability (green fluorescence) as compared to pure curcumin upon incubation with striatal-derived immortalized cell line expressing mutant Huntingtin ($STHdh^{111/111}$). *In vitro* cell line study under apoptotic conditions revealed higher reduction in the $STHdh^{111/111}$ cells susceptibility to apoptosis upon pre-treatment with curcumin nanoparticles ($p<0.0001$) than pure curcumin. Thus, the developed nanoparticle system indicated its potential for further *in vivo* study in rodents [270].

5.5 Amyotrophic lateral sclerosis

Amyotrophic lateral sclerosis is also a rarely occurring form of neurodegenerative disease associated with the dysfunction of motor neurons [271]. In addition to this, it affects the brain stem and spinal cord with a life span ranging from 24-48 months [272]. Biologically, this disease involves destructed motor neurons with loss of muscle tissues. As a result, it induces hemiplegia conditions in patients with amyotrophic lateral sclerosis and ultimately demise due to shutting of the respiratory system [273–275]. Amyotrophic lateral sclerosis is divided into two categories i.e. familial and sporadic among them, familial accounts for 5-20% of all the cases. There are only two drugs named riluzole and edaravone that are currently available and being used to overcome the lethal impacts of this deadly disease [276]. These drugs are able to slow down the progression of this disease however, these are but are unable to revert manifested symptoms of amyotrophic lateral sclerosis [2,277]. Looking at these challenges, Tripodo et al. developed a carrier-in-carrier system using inulin-d-α-tocopherol succinate based curcumin polymeric micelles loaded in mesenchymal stromal cells for targeting damaged brain tissues in ALS. The *in vitro* study revealed complete and persistent intracellular internalization of the developed micelles in the cytosol of mesenchymal stromal cells in a concentration-dependent manner than free curcumin. The uptake of these micelles by the stromal cells was increased by 1.2-fold (higher fluorescence intensity) than free curcumin. In addition, the viability of stromal cells was increased upon treatment with the developed micelles ($p<0.0001$) than free curcumin [278].

Jin et al. developed methoxypoly (ethylene glycol)-b-poly (D,L-lactic acid) based polymeric micelles and functionalized it by conjugating adenosine 2A receptor agonist (purine nucleotide derivative CGS21680) for the delivery of edaravone in brain by

triggering tight junction opening of the BBB. The *in vitro* study revealed 1.3-fold increase in the transendothelial cell electrical resistance by the functionalized polymeric micelles in endothelial bEnd.3 cells than non-functionalized polymeric micelles, which indicated enhanced permeability across the monolayer with reduced oxygen-glucose deprivation-induced reactive oxygen species levels. Further, the functionalized polymeric micelles significantly ($p<0.05$) quenched the effect of reactive oxygen species by lowering their levels in live RAW264.7 microphages than free drug and non-functionalized micelles [279].

A brief description about the applications of polymeric micelles as an effective nanocarrier in the delivery of antiepileptic, antipsychotic and antischizophrenic drugs is presented in Table 8.

Table 8: Polymeric micelles in the delivery of antiepileptic, antipsychotic and antischizophrenic drugs

ABC	Targeting ligands/stimuli	Size	Therapeutics	Biological model/route of administration	Outcome	Reference
				Antiepileptic		
Pluronic 407 and TPGS	-	12 nm	Diazepam	-	➢ Incorporation of P407 increased the physicochemical stability of TPGS based lyophilized PMs upon storage for 3 months at 4°C ➢ 1.1-fold slower release of drug was observed from optimized PMs (10%w/v TPGS and 1%w/v P407) at pH 7.4 for 24 h than free drug	[280]
Pluronic P123	-	18.7 nm	Lamotrigine	BCECs Sprague Dawley rats/intravenous	➢ 2.7-fold increase in the solubility of drug in PMs than free drug ➢ 2-fold increase in brain uptake of drug loaded PMs ($p<0.01$) than free drug and was not affected by P-gp inhibitor verapamil	[87]
Pluronic P123/F127	Tryptophan derivative (substrate of LAT1)	28.6 nm	Lamotrigine	BCECs Sprague Dawley rats (pilocarpine-induced)/intravenous	➢ Conjugation with tryptophan increased the transportation of PMs into brain with good epileptogenic focus targeting effect ➢ 1.9-fold increase in the levels of functionalized PMs was observed in hippocampus than non-functionalized PMs after 60 min of injection in status epilepticus rats	[281]

mPEG-PLA/TPGS	-	183.5 nm	Lamotrigine	Sprague Dawley rats/intranasal	➢ 4.6- and 1.5-fold increase in $AUC_{(0-t)}$ of drug loaded mixed PMs was noted than free drug and drug loaded PMs in hippocampus ➢ Enhanced penetration efficiency of mixed PMs was observed than free drug due to P-gp inhibition	[282]
Pluronic L121 and Pluronic P123	-	83.4 nm	Clonazepam	Swiss albino mice (PTZ-induced)/intranasal	➢ Higher concentration of drug loaded in ^{99m}Tc-mixed PMs was observed in brain ($p<0.05$) after intranasal administration than ^{99m}Tc-clonazepam and intravenous ^{99m}Tc- mixed PMs ➢ Higher brain/blood ratios ($p<0.05$) of drug loaded ^{99m}Tc-mixed PMs was observed than ^{99m}Tc-clonazepam and intravenous ^{99m}Tc- mixed PMs ➢ 68-fold increase in the relative bioavailability of the drug loaded in mixed PMs was observed in brain than blood ➢ The developed mixed PMs ($p<0.05$) enhanced the anti-convulsant efficacy of loaded drug than free drug	[190]
Pluronic L64/P84 and L64/F127	-	25-30 nm	Clozapine and oxcarbazepine	-	➢ Higher antioxidant capacity of clozapine PMs was observed in DPPH assay ($p<0.01$) than oxcarbazepine PMs, which is attributed to increased particle distribution and smaller size ➢ 14- and 6.4-fold increase in nitric oxide scavenging activity was observed by co-loaded PMs than free drugs	[283]
Antipsychotic/Antischizophrenic						

Vitamin E TPGS	-	26.5 nm	Paliperidone palmitate	Swiss albino mice (apomorphine-induced)/intramuscular	➢ 1.6- and 77.0-fold decrease in catalepsy in mice was observed by drug loaded PMs than free drug and negative control respectively ➢ 1.2- and 1.1-fold decrease in climbing and sniffing by drug loaded PMs was noted than free drugs and negative control	[284]
Pluronic F127	-	170.3 nm	Aripiprazole	-	➢ Sustained drug release from PMs i.e. 97.3% in 20 h while only 32.8% of free drug was released in 12 h in pH 1.2 buffer ➢ The optimized lyophilized PMs was stable after 3 months of storage	[285]
Pluronic F127 and Gelucire 44/14	-	175 nm	Lurasidone	Wistar rats and sheep nasal mucosa/intranasal	➢ 1.3-fold increase in penetration of drug loaded mixed PMs across nasal mucosa was observed than free drug ➢ Higher C_{max} of drug loaded in mixed PMs was attained in brain upon intranasal administration than mixed PMs administered intravenously	[286]

Abbreviations: AUC, Area under curve; **BCECs**, Brain capillary endothelial cells; **C_{max}**, Maximum concentration; **DPPH,** 2,2-diphenyl-1-picrylhydrazyl; **LAT1**, L-type amino acid transporter 1; **mPEG-PLA**, Methoxy poly(ethylene glycol)-poly(lactide); **P-gp**, P-glycoprotein; **PTZ**, Pentylenetetrazole; **TPGS**, D-alpha-tocopheryl polyethylene glycol 1000 succinate

6. Diagnostic applications

Contrast agents have been widely utilized in the diagnosis of diseases as they provide high-resolution image by accumulating in tissues without any side effects. There are imaging agents with high relaxivity and durability that are used to identify the pathological condition in cells and tissue. However, both of these lacks specificity for cellular receptors that limits their distribution at the site of interest [93,287].

Polymeric micelles could be suitable nanocarrier in delivering such diagnostic agents at the site of interest by limiting their distribution at the site of diagnosis. Therefore, these can provide high quality images and can improve the diagnosis of a brain related diseases by simplifying the task of detection, monitoring and visual inspection [288,289]. For this purpose, surface-functionalization property of polymeric micelles enables them to be utilized as diagnostic nanocarriers by incorporating imaging/ diagnostic moieties covalently or non-covalently into copolymer network [93,287]. This imparts magnetic resonance as well as certain, fluorescent and optical properties to the polymeric micelles that has led to their role in the clinical diagnosis of brain diseases [290,291]. Further, the surface functionalization of polymeric micelles makes them a potent nanocarrier for mapping transport of loaded therapeutic agents along with contrast/imaging agents at the target site [292].

For instance, Xiao et al. developed H40-poly(L-glutamate-hydrazone)-b-poly(ethylene glycol) based polymeric micelles and conjugated DOX with core forming block via hydrazone linkage for the site specific delivery of drug in brain. Further, they functionalized the polymeric micelles by conjugating cRGD peptide for targeting glioma cells and 1,4,7-

triazacyclononane-N, N', N''-triacetic acid (NOTA) for positron emission tomography imaging of glioma (multifunctional micelles). These showed higher tumor fluorescence signal of DOX in comparison to non-functionalized polymeric micelles (without peptide) after 24h of PET scans in U87MG glioma cells as presented in the images of *ex-vivo* fluorescence study. The positron emission tomography/computed tomography images of a U87MG tumor-bearing mouse at 4h post-injection of the multifunctional polymeric micelles. The image confirmed higher accumulation of multifunctional polymeric micelles in glioma cells in comparison to non-functionalized polymeric micelles [293].

Chen et al. developed Boltron®H40-biodegradable photo-luminescent polymer-poly (ethylene glycol) based se2-fluorescent polymeric micelles and functionalized them by conjugating cRGD peptide for targeting $\alpha_v\beta_3$ integrin for the imaging of glioma cells. The functionalized polymeric micelles exhibited higher accumulation in glioma cells as indicated by the blue fluorescent color by targeting $\alpha_v\beta_3$ integrin receptors expressed on glioma cells via receptor-mediated endocytosis upon incubation for 6h at concentration 0.5 mg/ml and 1.0 mg/ml than non-functionalized polymeric micelles respectively [294]. This bioimaging probe could be used in a variety of microscopic techniques including fluorescent microscopy, conofocal laser scanning microscopy, and two-photon microscopy [294].

Zhou et al. developed polyethylene glycol-block-polycaprolactone based polymeric micelles encapsulated with SPIONs for optical/magnetic resonance dual-mode imaging of glioma cells. For targeting glioma cells, polymeric micelles functionalized with Lf as targeting ligand. *In vitro* study revealed increase in fluorescent signals with increase in the concentration of iron upon incubation of glioma cells with functionalized polymeric micelles.

In vivo results revealed higher accumulation of functionalized polymeric micelles in glioma cells with extended duration of hypointensity at the tumor site over 48 hours in the MR image in comparison to non-functionalized polymeric micelles. Further, the modification of functionalized polymeric micelles with near-infrared fluorescent probe, Cy5.5, led to 4-fold increase in the average fluorescence intensity of the tumor than the normal brain tissue [295].

Garello et al. developed the paramagnetic polymeric micelles as magnetic resonance imaging detectable agent with specificity for vascular cell adhesion molecule-1. Polymeric micelles maintained higher binding to the target and exhibited higher T1-signal enhancement with well-detectable imaging contrast for the visualization of neuroinflammation. Moreover, these can be used in the early detection of neurodegenerative diseases [296]. Shiraishi et al. developed poly(ethylene glycol)-b-poly(L-lysine-DOTA-gadolinium) based magnetic resonance imaging polymeric micelles for the diagnosis of cerebral ischemia-reperfusion injury in rat transient middle cerebral artery occlusion-reperfusion model. These showed clear and higher contrast images of axial slice of brain than classic contrast agent DOTA-gadolinium. The developed magnetic resonance imaging polymeric micelles provided very clear/stark contrast images in 15.5 ± 10.3% of the ischemic hemisphere after reperfusion within 30 min of post intravenous injection in rats than classic gadolinium chelate contrast agents followed by T1-hyperintense area of the devleoped polymeric micelles in striatum and cerebral cortex. This was attributed to prolonged circulation of polymeric micelles in blood (11h) and large area under curve than classic contrast agents T_1W and DWI images revealed slow distribution of polymeric micelles in ischemic hemisphere while T_2W images revealed no hemorrhage in the ischemic hemisphere [297]. Wu et al. developed reduction-responsive polymeric micelles composed of monomethoxy-poly(ethylene glycol)-S-S-hexadecyl and

SPIONs for the differential diagnosis of neuroglioma in mice (xenograft model) by reduction-triggered magnetic resonance imaging enhancement. The *in vivo* study revealed shorter T2 relaxation time with increased contrasting of tumor and 1.83-fold higher transverse relaxivity by reduction-sensitive (glutathione) aggregation of polymeric micelles in C6 tumor-bearing mice upon intravenous administration than non-responsive polymeric micelles. The reduction-responsive polymeric micelles showed more robust T2 enhancement in tumor region at 3h post-injection. In addition, these exhibited easy differentiation of inflammatory mass and malignant glioma in mice than non-sensitive polymeric micelles [298].

7. Patents

Looking at the commercial aspects of polymeric micelles, number of patents have been filed regarding brain drug delivery/brain targeting based on composition of polymeric micelles, method of delivering polymeric micelles to brain, method of targeting polymeric micelles in a particular region of brain, polymeric micelles as theragnostic carrier, and active targeting and positioning of polymeric micelles in brain. Patents of polymeric micelles filed on aforementioned strategies are presented in Table 9.

Table 9: Patents published on polymeric micelles for the treatment of brain diseases

Patent number	Year of publication	Title of patent	Key claims	References
CA2319057C	1999	Composition comprising poly(oxyethylene)-poly(oxypropylene) block copolymer and their use	➢ Oral delivery of peptides, proteins, or biological agents for the treatment of brain diseases or diseases with multidrug resistance	[299]
WOO2006/048773A1	2006	Reverse micelle composition for delivery of metal cations comprising a diglyceride and a phytosterol and method of preparation	➢ Preparation of PMs containing lithium for protecting brain in Huntington's disease	[300]
CA2756581A1	2010	Ascorbate-linked nanosystems for brain delivery	➢ Method for delivering PMs to brain cell by interacting with sodium-dependent vitamin C transporter on brain cell	[301]
CN102614105A	2012	Brain targeted amphotericin B polymeric micelle administration system	➢ Brain targeting potential was achieved by surface functionalization of PMs using angiopep-2	[302]

			➢ Enhancement in the accumulation of lipophillic drugs with low brain entrance efficiencies in the brain	
CN102212116B	2013	Acetylcholine receptor mediated brain targeted polypeptide and application thereof	➢ Diagnosis and treatment of glioma using acetylcholine receptor-mediated brain-targeted polypeptide CDX modified with PEG-PLA based PMs loaded with paclitaxel	[303]
CN103182087B	2015	Trimethyl chitosan-graft-polyethylene glycol/nucleic acid brain-targeting micellar and preparation method thereof	➢ Surface functionalization of PMs using brain targeting peptide RVG for active brain targeting ➢ Resolving of the issue related to nucleic acid medicine defects such as easy *in-vivo* degradation, poor stability, and low transfection efficiency	[304]
CN104586765A	2015	Brain tumor targeted drug delivery system and preparation method thereof	➢ Glucose and amphipathic chitosan derivative based micelles was developed to encapsulate antitumor drugs ➢ Efficient brain entry of PMs without any toxicity on normal tissues	[305]
US9393308B2	2015	Micelle structure of nano preparation for diagnosis or treatment of cancer disease and preparation method thereof	➢ Formation of hypericin (photosensitizer) loaded DSPE-mPEG has been claimed to cross blood tumor barrier to treat glioma	[306]

			➢ 2.5-fold higher light-induced cytotoxicity efficiency than hypericin alone	
US10758484B2	2016	CED of SN-38-loaded PMs against brain tumor	➢ Delivery of PMs into target region of brain via convection-enhanced delivery system using infusion pump	[307]
CN108339124B	2020	Preparation method and application of two-stage brain targeted PMs for drug delivery system	➢ Micellar core has been claimed for encapsulating lipophillic anti-tumor drugs for targeting glioblastoma by endocytosis mediated by surface targeting peptides (Ang-2 and cRGD) with reduced side-effects	[308]

8. Future direction and conclusion

The incidence of ND diseases all across the world is rapidly increasing day by day because of ageing, genetic and environmental factors. Therefore, their treatment has become the most devastating challenge all over the world due to the unique physiology of the brain that impedes the bioavailability of drugs. This issue is one of the most promising and critical ones in the treatment of ND diseases.

Thus, the design of brain-targeted nanocarrier is selectively very important. As they offer interaction of the surface decorated nanoparticles with cells at the pathological site. However, the single-molecule based targeting faces the challenge of off-target effects that impedes their use in highly complex clinical situations. Therefore, the single-targeting strategy cannot assure the retention of nanoparticles into the pathological cells. To tackle this limitation, dual or multi-functionality nanoparticles can be developed by integrating stimuli-specific moieties and two or more targeting moieties. In agreement to this, polymeric micelles have huge potential to overcome the barriers involved in the delivery of drugs into targeting brain cells without any side effects on the other organs. The biocompatible polymeric corona of the polymeric micelles offers improved therapeutic efficacy of the micellar delivery systems without undesired toxicity. The optimization of their structural design for the entrapment of the drugs into its core and its multifunctionality adds to the efficacy and potential of polymeric micelles to reach CNS. The incorporation of BBB targeting moiety and pathological stimuli-specific moiety, ensure the accessibility of the polymeric micelles into the brain and spatiotemporal drug release at the pathological site of brain. Their magnetic resonance and fluorescence properties also makes them an efficient nanocarrier in the diagnosis of brain diseases and further reinforce their theranostic effects.

In the present, review various targeting strategies utilized in the designing of functionalized polymeric micelles and their biomedical applications for the treatment and diagnosis of CNS diseases have been discussed in detail. It was clearly understood from the searched literature that various functionalized polymeric micelles have been tailored to target the brain to treat various brain-related diseases and showed success in preclinical studies. This tremendous effort done on a preclinical scale has provided the scientists to initiate clinical trials for the functionalized polymeric micelles for treating brain diseases. Many patents on polymeric micelles for brain delivery have been filed. However, their clinical translation to market is still elusive as none of the polymeric micelles based products is available in the market. This could be because of the increased ligand density at the corona that causes steric hindrance. Therefore, impair targeting. Thus, further approaches are required to optimize the ligand density. However, polymeric micelles are capable enough to escape the setback of steric hindrance by incorporating stimuli-responsive moieties (bioresponsive) along with a single ligand. The reason of their less exploration could also be due to the limited synthesis of novel targeting ligands required for active targeting of brain diseases with varying pathophysiologies.

In terms of their commercialization potential, USFDA have approved Genexol- polymeric micelles for lung as well as metastatic breast cancer [309], Nanoxel® [310] and Paclical-polymeric micelles for ovarian cancer [311], and oral-Lyn™ for the management of diabetes mellitus [312]. In addition to this, estrasorb- polymeric micelles have been reported for treating menopause [313]. The data indicates that most of the commercially available polymeric micelles are used for treating cancer and many are under various clinical phases as well. Despite this, the clinical studies on polymeric micelles in treating brain diseases including glioma are extremely limited. This highlights the major bottlenecks related to clinical translation of polymeric micelles for treating brain disease.

The overall CNS barriers are the major factors that impede the delivery of polymeric micelles-loaded cargos to brain. Therefore, the better understanding of each barrier function is pre-requisite to design the various strategies to overcome such barriers with site-specificity. In addition, the safety and stability aspect of polymeric micelles are also important as per the regulatory perspective. In terms of their thermodynamic stability, critical micelle concentration value of block copolymer is important. As the dilution of polymeric micelles in systemic circulations upon intravenous injection lowers the copolymer concentration below their critical micelle concentration value. In agreement to this, number of studies claimed enhancement in the stability profile of polymeric micelles using covalent and non-covalent crosslinking strategies [314]. Therefore, the stability aspects of polymeric micelles are speculative and warrants further study. Similarly, clinical toxicity of polymeric micelles is also an important factor for drug delivery applications that completely relies on to the concentration of block copolymer used and their number of monomers. In addition, it also depends on to the material type, shape, size and coating of polymeric micelles. Therefore, it is important to optimize the block copolymer-based parameters to make them less toxic pertaining to brain delivery. In addition to this, the site-specificity of polymeric micelles is elusive and requires tremendous efforts in identifying percentage of loaded cargos released in the brain.

Therefore, the focus should be towards the development of flexible and scalable polymeric micelles to reach clinical translation. Consideration of flexibility, scalability and toxicity aspects related to block copolymers or, polymeric micelles developed for brain delivery will definitely help in developing bench-to-bedside translation of polymeric micelles for treating diseases at their specific site and brain in particular.

Conflict of interest: Declared none

List of abbreviations

ACT, Acteoside; **ADP**, Adenosine di phosphate; **ASF**, Actinomyosin stress fibers; **α-syn**, α-synuclein; **APP,** Amyloid precursor protein; **APPDN**, mPEG-PCL-ACT-CTS-pDNA-NGF; **ATP**, Adenosine triphosphate; **AUC,** Area under curve; **BACE1**, β-site amyloid precursor protein-cleaving enzyme 1; **BBB,** Blood brain barrier; **BCB,** Brain cerebro-spinal fluid; **DNF,** Brain derived neuronal factor; **bEnd cells,** Microvascular brain endothelial cells derived from mouse brain; **bFGF**, basic fibroblast growth factor; **BMECs,** Brain microvessel endothelial cells; **Bor/CMS-M**, Carmustine loaded PMs functionalized with borneol; **BTB,** Blood brain tumor barrier; **C6-cells**; Spindle-like cells that simulate human glioblastoma multiforme; **C_{max},** Maximum concentration; **CA1,** Hippocampal cornu ammonis; **CGN,** Human synthetic cingulin peptide; **CHO-POESO**, Cholesterol-polyoxyethylene sorbitol oleate; **CLPT**, Controlled living polymerization technique; **CMS-M**, Carmustine PMs; **CNS**, Central nervous system; **CPPs,** Cell penetrating peptides; **CREB,** Cyclic AMP-response element binding protein; **CSF**, Cerebrospinal fluid; **CT-NM/Res**, Neuronal mitochondria-targeted micelles functionalized with mimetic peptide C3 and NCAM for resveratrol delivery; **CTS**, Chitosan; **CUR**, Curcumin; **Cy5.5**, Fluorescent dye; **DAPI**, 4′,6-diamidino-2-phenylindole; **DBTRG-05MG cells**, Denver Brain Tumor Research Group 05; **Dex-PTX**, Dextran-paclitaxel; **DGL-PEG**, Dendrigraft poly-L-lysine-polyethylene glycol; **DiD**, 1,1′-dioctadecyl-3,3,3′,3′- tetramethylindodicarbocyanine; **DiR**, 1,1′-dioctadecyl-3,3,3′,3′-tetramethylindotricarbocyanine iodide (fluorescent dye); **DiR-NPs**, Non-functionalized PMs with fluorescent dye; **DMAP,** Dimethyl aminopyridine; **DMSO,** Dimethyl sulfoxide; **DSPE-PEG2000**, 1, 2-Distearoyl-sn-glycero-3-phosphoethanolamine-polyethylene glycol 2000; **DOPAC**, 3, 4-Dihydroxyphenyl acetic acid; **DOX**, Doxorubicin; **DSP**, Dithiobis(succinimidyl propionate); **DTX,** Docetaxel; **DWI**, Diffusion-weighted imaging; **EDC**, 1-Ethyl-3-(3-dimethylaminopropyl)carbodiimide; **EDV-AM**, Edaravone functionalized PMs; **FITC-TH**, Fluorescein isothiocyanate tyrosine hydroxylase; **G422 cells**; Intracerebral glioblastoma cell line; **GBM,** Glioblastoma multiform; **Gd-DTPA**, Gadolinium-diethylenetriamine-pentaacetic acid; **GFP**, Green fluorescent protein; **GLUT1**, Glucose transporter antibody single chain fragment

variable; **GRPR**, Gastrin releasing peptide receptor; **GSH**, Reduced glutathione; **HA-ss-CUR**, Hyaluronic acid-disulfide linkage-Curcumin; **16HBE cells**, Human bronchial epidermal cells; **HA-DOX**, Hyaluronic acid-Doxorubicin; **H40-DOX-cRGD**, Doxorubicin loaded PMs with NOTA and cRGD; **$(HE)_5$**, polyanionic masking peptide (histidine-glutamic acid repeats); **hGDNF**, Human glial cell line-derived neurotrophic factor; **HIFU,** High intensity focused ultrasound; **HLB,** Hydrophilic-lipophilic balance; **HRP**, Horseradish peroxidase; **HVA**, Homovanillic acid; **K-s-A**, HER2-targeting KAAYSL (K) with MMP1-sensitive VPMS-MRGG (s) and LRP1-targeting angiopep2 (A); **LAT1**, L-type amino acid transporter 1; **LDL**, Low density lipoprotein; **Lf**, Lactoferrin; **Lf-NPs**, Lactoferrin functionalized PMs; **LN229 cells**, Mutated p53 malignant glioblastoma cell line; **LPEI-g-PEG**, Linear polyethyleneimine-graft-polyethylene glycol; **MMCB**, Maleimide-mediated covalent binding; **MMP**, Matrix metalloproteinase; **mPEG-PCL**, Methoxy polyethylene glycol-polycaprolactone**;** Mal, Maleimide; **MDA**, Malondialdehyde; **mPEG-PLA**, Methoxy poly(ethylene glycol)-poly(lactide); **mPEG-TK-MPH**, Methoxy polyethylene glycol- thioketal-Melphalan; **nAchR**, Nicotinic acetylcholine receptors; **Nano**, Plain nanoparticles; **Nano-CUR**, Curcumin loaded nanoparticles; **NAP**, Neuroactive peptide; **NBD1/2**, Nucleotide binding domain 1 and 2; **NCAM**, Neuronal cell adhesion molecule; **NeuN**, Neuronal specific nuclear protein; **Neuro2A/N2a cells**, Mouse neuroblastoma cell line; **NGF**, Nerve growth factor; **NGFR**, Nerve growth factor receptor; **NHS**, N-hydroxysuccinimide; **NLCs**, Nerve like cells; **NOTA**, 1,4,7-Triazacyclononane-1,4,7-triacetic acid; **OGD**, Oxygen-glucose deprivation; **6-OHDA**, 6-hydroxydopamine; **PBS**, Phosphate buffer saline; **pDNA**, plasmid DNA; **PTZ**, Pentylenetetrazole; **PI**, Propidium iodide; **PC12 cells,** Pheochromocytoma of the rat adrenal medulla; **Pep-1/Bor/CMS-M**, Carmustine loaded PMs functionalized with Borneol and Pep-1, 4-chlorobenzenesulfonate salt (fluorescent dye); **pNP-PEG_{3400}-DOPE**, Nitrophenylcarbonyl-polyethylene glycol3400- 1,2-dioleoyl-sn-glycero-3- phosphoethanolamine; **PEG-b-PEYM**, poly(ethylene glycol) (PEG) block and a hydrophobic polymethacrylate block; **PEI-SS**, Polyethylenimine with disulfide linkage; **PAA-b-P3HT**, Polyacrylic acid-block- poly(3-hexylthiophene-2,5-diyl); **PAzoMA-b-(PELG-g-MPEG)**, Poly[6-(4-methoxy-azobenzene-4'-oxy) hexylmethacrylate-block-(poly L-glutamate-graft- methoxy polyethylene glycol); **PEG-click-**

PPG, Poly (ethylene glycol)-click-Poly (propylene glycol); **PEO-b-PPO-b-PEO**, Poly (ethylene oxide)-block-Poly (propylene oxide)-block-Poly (ethylene oxide); **PEO-b-P(AzoMA-NIPAm)**, Polyethyleneoxide-block-Poly([6-(4-methoxy-azobenzene-4'-oxy)- hexylmethacrylate-(N-isopropylacrylamide); **PEO-b-P(MEO2MA-co-THPMA)**, Poly(ethylene oxide)-block-poly(2-methoxyethoxy)ethyl methacrylate-co-tetramethylpiperidinyloxy-4-yl methacrylate); **PEO-b-PTHPMA;** Polyethyleneoxide-block-tetramethylpiperidinyloxy-4-yl methacrylate; **PLLA-b-PEG-b-PLLA**, Poly (L-lactic acid)-block-Poly (ethylene glycol)-Poly (L-lactic acid); **PSSNa-b-PMMA**, Poly (sodium styrene sulfonate)-block-poly (methyl methacrylate); **P(EtOx-b-BuOx)**, Poly(2-ethyl-2-oxazoline-block-2-butyl-2- oxazoline); **P(MeOx-b-BuOx)**, Poly(2-methyl-2-oxazoline-block-2-butyl-2- oxazoline); **PEG-P(Glu),** Poly (ethylene glycol)-poly(L-glutamic acid); **PEG-PHA**, Poly(ethylene glycol)-b-poly(hidrazinyl-aspartamide); **PEG-SCM**, Polyethylene glycol-succinimidyl carboxymethyl ester; **PE-PEG**, 1,2-Distearoyl-sn-glycero-3-phosphoethanolamine-N-[methoxy(polyethylene glycol)-2000; **PLGA-PLL-PEG**, Poly(lactic-*co*-glycolic acid)- poly(*ε*-carbobenzoxy-L-lysine)-polyethylene glycol; **PCL-PMPC-PGMA**, Polycaprolactone-Poly (2-methacryloyloxyethyl phosphoryl choline) - poly (glycidyl meth-acrylate); **PEG-Lys-PCL**, Poly Ethylene Glycol-Lysine-(Poly Caprolactone); **PEG-PDMAEMA**, Polyethylene glycol- Poly(2-dimethylamino)ethyl methacrylate); **PEG-PLA**, Polyethylene glycol-polylactic acid; **PEG-PLGA**, Polyethylene glycol-Polylactic-co-glycolic acid; **PEG-b-P(L-DOPA(OAc)2),** Poly(ethylene glycol)- block -poly(O,O'-diacetyl- L-DOPA); **PEG-PAMAM**, Polyethylene glycol-poly(amidoamine); **PEG-PEI**, Polyethyleneglycol- polyethyleneimine; **PEG-PLGA**, Polyethylene glycol-poly(lactic-co-glycolic acid); **PEG-PLA**, Poly(ethylene glycol)-co-poly(lactic acid); **PLA-b-PDMAEMA**, Poly(lactic acid)-block-polydimethylaminoethyl methacrylate; **PEtOz-SS-PCL**, Poly (2-ethyl-2-oxazoline)-b-poly (epsilon-caprolactone); **QSH,** D-enantiomeric peptide, QSHYRHISPAQV; **RBECs**, Rat brain endothelial cells; **Res**, Resveratrol; **(RG)$_5$**, Arginine rich peptide; **RISC**, Dysregulated RNA-induced silencing complex; **SD rats**, Spraguy-dawley rats; **shRNA**, Short hairpin-RNA; **SH-SY5Y**, Neuroblastoma cell line; **siSNCA**, α-synuclein siRNA; **SIRT1**, Sirtuin-1; **SIRT6,** Sirtuin 6; **SPIO**, Superparamagnetic ironoxide; **sPMI**, Stapled peptide antagonist; **STZ,** Streptozotocin; **Tfr**, Transferrin receptor; **T-NM/Res**,

NCAM functionalized PMs loaded with resveratrol; **(TPE-(EO)$_4$-L$_2$)**, Tetraphenylethelene-ethylene oxide with lithium ion (Li^+);**TPGS**, D-α-tocopheryl polyethylene glycol succinate; **TPP**, Triphenylphosphonium; **T_2W**, T_2 weighted imaging; **U251MG cells**; Glioma cell-line; **U87MG cells**, Malignant glioblastoma cell line; **U87 cells**, Malignant glioblastoma cells; **Untr**, Untreated; **VIP**, Vasoactive intestinal peptide; **ZO-1**, Zonula occluden-1

References

[1] N.J. Abbott, M.E. Pizzo, J.E. Preston, D. Janigro, R.G. Thorne, The role of brain barriers in fluid movement in the CNS : is there a ‘ glymphatic ’ system ?, Acta Neuropathol. 135 (2018) 387-407. https://doi:10.1007/s00401-018-1812-4.

[2] A. Akhtar, A. Andleeb, T.S. Waris, M. Bazzar, A.R. Moradi, N.R. Awan, M. Yar, Neurodegenerative diseases and effective drug delivery: A review of challenges and novel therapeutics, J. Control. Rel. 330 (2021) 1152–1167. https://doi:10.1016/j.jconrel.2020.11.021.

[3] M. Agrawal, S. Saraf, S.G. Antimisiaris, Nose-to-brain drug delivery : An update on clinical challenges and progress towards approval of anti-Alzheimer drugs, J. Control. Rel. 281 (2018) 139–177. https://doi:10.1016/j.jconrel.2018.05.011.

[4] M. Agrawal, S.Saraf, S. Saraf, S.G. Antimisiaris, N. Hamano, S. Li, M. Chougule, S.A. Shoyele, U. Gupta, Ajazuddin, A. Alexander, Recent advancements in the field of nanotechnology for the delivery of anti-Alzheimer drug in the brain region, Expert Opin Drug Deliv. 15 (2018) 589-617. https://doi:10.1080/17425247.2018.1471058.

[5] Silberberg, D.; Anand, N.P.; Michels, K.; Kalaria, R.N. Brain and other nervous system disorders across the lifespan — global challenges and opportunities, *Nature*. 2015, *527*, 151–154.

[6] Kumar, R. Prevalence and risk factors for neurological disorders in children aged 6 months to 2 years in northern India, *Dev. Med. Child. Neurol*. 2013, *55*, 348-56.

[7] Kanwar, J.R.; Sriramoju, B.; Kanwar, R.K. Neurological disorders and therapeutics targeted to surmount the blood-brain barrier, *Int. J. Nanomed.* 2012,*7*, 3259–3278.

[8] Dubey, S.K.; Lakshmi, K.K.; Krishna, K.V.; Agrawal, M.; Singhvi, G.; Narayana, R.; Saraf, S.; Saraf, S.; Shukla, R.; Alexander, A. Insulin mediated novel therapies for the treatment of Alzheimer ’ s disease, *Life Sci.* 2020, *249*, 117540.

[9] Pathan, S.A.; Iqbal, Z.; Zaidi, S.M.A.; Talegaonkar, S.; Vohra, D.; Jain, K.; Azeem, A.; Jain, N.; Lalani, J.R.; Khar, R.K.; Ahmad, F.J. CNS Drug Delivery Systems : Novel Approaches, *Recent. Pat. Drug. Deliv. Formul.* 2009, *3*, 71–89.

[10] Sweeney, M.D.; Sagare, A.P.; Zlokovic, B.V. Blood–brain barrier breakdown in Alzheimer disease and other neurodegenerative disorders, *Nat. Rev Neurol.* 2018, *14*, 133–150.

[11]Oller-Salvia, B.; Sánchez-Navarro, M.; Giralt, E.; Teixidó, M. Blood-brain barrier shuttle peptides: An emerging paradigm for brain delivery, *Chem. Soc. Rev*. 2016, *45*, 4690–4707.

[12] Nance, E.; Timbie, K; Miller, G.W.; Song, J.; Louttit, C.; Klibanov, A.L.; Shih, T.Y.; Swaminathan, G.; Tamargo, R.J.; Woodworth, G.F.; Hanes, J.; Price, R.J. Non-invasive delivery of stealth, brain-penetrating nanoparticles across the blood - Brain barrier using MRI-guided focused ultrasound, *J. Control. Rel.* 2014, *189*, 123–132.

[13] Dong, X. Current strategies for brain drug delivery, *Theranostics*. 2018, *8*, 1481–1493.

.[14]Abbott, N.J.; Rönnbäck, L.; Hansson, E. Astrocyte-endothelial interactions at the blood-brain barrier, *Nat. Rev. Neurosci*. 2006, *7*, 41–53.

[15] Zhang, T.T.; Li, W.; Meng, G.; Wang, P.; Liao, W. Strategies for transporting nanoparticles across the blood-brain barrier, *Biomater. Sci.* 2016, 4, 219–229.

[16] Vieira, D.B.; Gamarra, L.F. Getting into the brain: Liposome-based strategies for effective drug delivery across the blood–brain barrier, *Int. J. Nanomed.* 2016, *11*, 5381–5414.

[17] Pardridge, W.M. Drug transport across the blood-brain barrier, *J. Cereb. Blood Flow Metab.* 2012, 32, 1959–1972.

[18] Ghosh, C. Blood-Brain Barrier P450 Enzymes and Multidrug Transporters in Drug Resistance: A Synergistic Role in Neurological Diseases, *Curr. Drug Metab*. 2011, *999*, 1–10.

[19] Agúndez, J.A.G.; Jiménez-Jiménez, F.J.; Alonso-Navarro, H.; García-Martín, E. Drug and xenobiotic biotransformation in the blood–brain barrier: A neglected issue, *Front. Cell. Neurosci.* 2014, *8*, 8–11.

[20] Agrawal, M.; Tripathi, D.K.; Saraf, S.; Saraf, S.; Antimisiaris, S.G.; Mourtas, S.; Hammarlund-udenaes, M.; Alexander, A. Recent advancements in liposomes targeting strategies to cross blood-brain barrier (BBB) for the treatment of Alzheimer ’ s disease, *J. Control. Rel.* 2017, *260*, 61–77.

[21] Upadhyay, R.K. Drug Delivery Systems , CNS Protection , and the blood brain barrier, *BioMed.*

Res. Int. 2014, *2014*, 869296.

[22] Mignani, S.; Shi, X.; Karpus, A.; Majoral, J.P. Non-invasive intranasal administration route directly to the brain using dendrimer nanoplatforms: An opportunity to develop new CNS drugs, *Eur. J. Med. Chem*. 2020, *209*, 112905.

[23] Sawant, R.R.; Sawant, R.M.; Torchilin, V.P. Mixed PEG – PE / vitamin E tumor-targeted immunomicelles as carriers for poorly soluble anti-cancer drugs : Improved drug solubilization and enhanced in vitro cytotoxicity, *Eur. J. Pharm. Biopharm.* 2008, 70, 51–57.

[24] Torchilin, V. Tumor delivery of macromolecular drugs based on the EPR effect, *Adv. Drug Deliv. Rev.* 2011, *63*, 131–135.

[25] Sawant, R.R.; Torchilin, V.P. Multifunctionality of lipid-core micelles for drug delivery and tumour targeting, *Mol. Memb. Biol.* 2010, *27*, 232–246.

[26] Lee, Y.J.; Kang, H.C.; Hu, J.; Nichols, J.W.; Jeon, Y.S.; Bae, Y.H. pH-Sensitive Polymeric Micelle-Based pH Probe for Detecting and Imaging Acidic Biological Environments, *Biomacromol.* 2012, *13*, 2945-2951.

[27] Shin, H.C.; Alani, A.W.G.; Rao, D.A.; Rockich, N.C.; Kwon, G.S. Multi-drug loaded polymeric micelles for simultaneous delivery of poorly soluble anticancer drugs, *J. Control. Rel.* 2009, *140*, 294–300.

[28] Nishiyama, N.; Kataoka, K. Current state, achievements, and future prospects of polymeric micelles as nanocarriers for drug and gene delivery, *Pharmacol. Ther.* 2006, *112*, 630–648.

[29] Curcio, M.; Cirillo, G.; Rouaen, J.R.C.; Saletta, F.; Nicoletta, F.P.; Vittorio, O.; Iemma, F. Natural polysaccharide carriers in brain delivery: Challenge and perspective, *Pharmaceutics*. 2020, *12*, 1–26.

[30] Batrakova, E.V.; Bronich, T.K.; Vetro, J.A.; Kabanov, A.V. Polymer micelles as drug carriers, *Adv. Drug. Deliv. Rev.* 2006, *21*, 57–93.

[31] Ghosh, B.; Biswas, S. Polymeric micelles in cancer therapy : State of the art, *J. Control. Rel.* 2021, *332*, 127–147.

[32] Kaur, J.; Mishra, V.; Singh, S.K.; Gulati, M.; Kapoor, B.; Chellappan, D.K.; Gupta, G.; Dureja, H.; Anand, K.; Dua, K.; Khatik, G.L.; Gowthamarajan, K. Harnessing amphiphilic polymeric

micelles for diagnostic and therapeutic applications: Breakthroughs and bottlenecks, *J. Control. Rel*. 2021, *334*, 64–95.

[33] Abourehab, M.A.S.; O.A.A. Ahmed, Balata, G.F.; Almalki, W.H. Self-assembled biodegradable polymeric micelles to improve dapoxetine delivery across the blood–brain barrier, *Int. J. Nanomed.* 2018, *13*, 3679–3687.

[34] Letchford, K.; Burt, H. A review of the formation and classification of amphiphilic block copolymer nanoparticulate structures: micelles, nanospheres, nanocapsules and polymersomes. *Eur. J. Pharm. Biopharm*. 2007, *65*, 259–69.

[35] Famta, P.; Famta, M.; Kaur, J.; Khursheed, R.; Kaur, A.; Khatik, G.L, Rahman, S.N.R.;Shunmugaperumal, T. Protecting the Normal Physiological Functions of Articular and Periarticular Structures by Aurum Nanoparticle-Based Formulations: an Up-to-Date Insight. AAPS. Pharm. Sci. Tech. 2020, *21*, 95.

[36] Panzhinskiy, E.; Hua, Y.; Lapchak, P.A.; Topchiy, T.E.; Lehmann, J.; Ren, S. Nair, Novel Curcumin Derivative CNB-001 Mitigates Obesity-Associated Insulin Resistance, *J. Pharmacol. Exp. Thera.* 2014, 349, 248–257.

[37] Movassaghian, S.; Merkel, O.M.; Torchilin, V.P. Applications of polymer micelles for imaging and drug delivery, *Nanomed. Nanobiotechnol*. 2015, *7*, 691–707.

[38] Zhang, T.; Luo, J.; Fu, Y.; Li, H.; Ding, R.; Gong, T.; Zhang, Z. Novel oral administrated paclitaxel micelles with enhanced bioavailability and antitumor efficacy for resistant breast cancer, *Colloids. Surf. B. Biointerf.* 2017, *150*, 89–97.

[39] Zhang, Y.; Huang, Y.; Li, S. Polymeric micelles: Nanocarriers for cancer-targeted drug delivery, *AAPS. Pharm. Sci. Tech*. 2014, *15*, 862–871.

[40] Koteswari, P.; Nithya, P.; Srinivasababu, P.; Sunium, S.; Babu, G. Formulation Development and evaluation of fast disintegrating tablets of Lamotrigine using liqui-solid technique, *Int. J. Pharm. Invest*. 2014, *4*, 207-14.

[41] Ransohoff, R.M. How neuroinflammation contributes to neurodegeneration, *Science*. 2016, *353*, 777–783.

[42] Saunders, N.R.; Ek, C.J.; Habgood, M.D.; Dziegielewska, K.M. Barriers in the brain: a

renaissance?, *Trends. Neurosci*. 2008, *31*, 279–286.

[43] Dingezweni S. The blood–brain barrier. *South. Afr. J. Anaesth. Anal.* 2020, *26*, S32–4.

[44]Coomber, B.L.; Stewart, P.A. Morphometric Analysis of CNS Microvascular Endothelium, *Microvasc. Res.* 1985, 30, 99-115.

[45] Moura, R.P.; Almeida, A.; Sarmento, B. The role of non-endothelial cells on the penetration of nanoparticles through the blood brain barrier, *Prog. Neurobiol*. 2017, *159*, 39–49.

[46]Sorokin, L. The impact of the extracellular matrix on inflammation, *Nat. Rev. Immunol.* 2010, *10*, 712–723.

[47] Ha, S.N.; Hochman, J.; Sheridan, R.P. Mini Review on Molecular Modeling of P-Glycoprotein (Pgp), *Curr. Top. Med. Chem*. 2007, *7*, 1525–1529.

[48] Cornford, E.M.; Hyman, S.; Swartz, B.E. The Human Brain GLUTl Glucose Transporter : Ultrastructural Localization to the Blood-Brain Barrier Endothelia, *J. Cereb. Blood. Flow. Metab.* 1994, *14*, 106–112.

[49] Ahn Y, Jun Y. Measurement of pain-like response to various NICU stimulants for high-risk infants. *Early. Hum. Dev*. 2007, *83*, 55–62.

[50]Liebner, S.; Fischmann, A.; Rascher, G.; Duffner, F.; Grote, E.H.; Wolburg, H. Claudin-1 and claudin-5 expression and tight junction morphology are altered in blood vessels of human glioblastoma multiforme, *Acta. Neuropathol*. 2000, *100*, 323–331.

[51] Wolburg, H.; Jörg, K.W.; Gesa, K.; Liebner, R.S.; Hamm, S.; Duffner, F.; Werner, E.G.; Britta, R. Localization of claudin-3 in tight junctions of the blood-brain barrier is selectively lost during experimental autoimmune encephalomyelitis and human glioblastoma multiforme, *Acta Neuropathologica*. 2003, *105*, 586–592.

[52] Berzin, T.M.; Zipser, B.D.; Rafii, M.S.; Kuo, V.; Yancopouloš, G.D.; Glass, D.J.; Fallon, J.R.; Stopa, E.G. Agrin and microvascular damage in Alzheimer's disease, *Neurobiol. Aging.* 2000, *21*, 349–355.

[53] Marroni, M.; Marchi, N.; Cucullo, L.; Abbott, N.J.; Signorelli, K.; Janigro, D. Vascular and Parenchymal Mechanisms in Multiple Drug Resistance : a Lesson from Human Epilepsy, *Curr. Drug. Targets*. 2003, *4*, 297–304.

[54] Kortekaas, R.; Leenders, K.L.; Van Oostrom, J.C.H.; Vaalburg, W.; Bart, J.; Willemsen, A.T.M.; Hendrikse, N.H. Blood – Brain Barrier Dysfunction in Parkinsonian Midbrain In Vivo, *Ann. Neurol*. 2005, *57*, 176–179.

[55] Pardridge, W.M. The blood-brain barrier: Bottleneck in brain drug development, *Neurotherapeutics*. 2005, *2*, 3–14.

[56] Kumar, M.; Sharma, P.; Maheshwari, R.; Tekade, M.; Shrivastava, S.K.; Tekade, R.K. Beyond the blood-brain barrier: Facing New Challenges and Prospects of Nanotechnology-Mediated Targeted Delivery to the Brain, In *Nanotechnology-based targeted drug delivery systems for brain tumors*, Kesharwani, P.; Gupta, U., Eds.;, Elsevier Inc., United States, 2018; pp 397-437.

[57] Tumani, H.; Huss, A.; Bachhuber, F. The cerebrospinal fluid and barriers – anatomic and physiologic considerations, *Handb. Clin. Neurol*. 2018, *146*, 21-32.

[58] Pardridge, W.M. CSF, blood-brain barrier, and brain drug delivery, *Expert. Opin Drug Deliv*. 2016, *13*, 963–975.

[59] Lun, M.P.; Monuki, E.S.; Lehtinen, M.K. Development and functions of the choroid plexus – cerebrospinal fluid system, *Nat. Rev. Neurosci*. 2015, *16*, 445-457.

[60] Ueno, M.; Chiba, Y.; Murakami, R.; Matsumoto, K. Blood – brain barrier and blood – cerebrospinal fluid barrier in normal and pathological conditions, *Brain Tumor Pathol.* 2016, *33*, 89-96.

[61] Solár, P.; Zamani, A.; Kubíčková, L.; Dubový, P.; Joukal, M. Choroid plexus and the blood – cerebrospinal fluid barrier in disease, *Fluids Barriers CNS*. 2020, *35*, 1–29.

[62] Engelhardt, B.; Sorokin, L. The blood – brain and the blood – cerebrospinal fluid barriers : function and dysfunction, *Semin. Immunopathol*. 2009, *31*, 497–511.

[63] François, J,; Egea, G.; Strazielle, N.; Catala, M.; Silva, V.; Fiona, V.; Engelhardt, B. Molecular anatomy and functions of the choroidal blood - cerebrospinal fluid barrier in health and disease, *Acta Neuropathol.* 2018, *135*, 337-361.

[64] Bryniarski, M.A.; Ren, T.; Rizvi, A.R.; Snyder, A.M.; Morris, M.E. Targeting the choroid plexuses for protein drug delivery, *Pharmaceutics*. 2020, *12*, 1–34.

[65] Nau, R.; Sörgel, F.; Eiffert, H. Penetration of drugs through the blood-cerebrospinal fluid/blood-brain barrier for treatment of central nervous system infections, *Clin. Microbiol. Rev.* 2010, *23*, 858–

883.

[66]Dubois, L.G.; Campanati, L.; Righy, C.; Andrea-meira, I.D.; Cristina, T.; De Sampaio,L.; Porto-carreiro, I.; Pereira, C.M.; Kahn, S.A.; Dossantos, M.F.; De Almeida, M.; Oliveira, R.; Ximenes-da-silva, A.; Lopes, M.C.; Faveret, E.; Gasparetto, E.L.; Moura-neto, V. Gliomas and the vascular fragility of the blood brain barrier, *Front. Cell. Neurosci.* 2014, *12*, 1–13.

[67] Arvanitis, C.D.; Ferraro, G.B.; Jain, R.K. The blood–brain barrier and blood–tumour barrier in brain tumours and metastases, *Nat. Rev. Cancer*. 2020, *20*, 26–41.

[68] Seano, G.; Nia, H.T.; Emblem, K.E.; Datta, M.; Ren, J.; Krishnan, S.; Kloepper, J.; Pinho, M.C.; Ho, W.W.; Ghosh, M.; Askoxylakis, V.; Ferraro, G.B.; Riedemann, L.; Gerstner, E.R.; Batchelor, T.T.; Wen, P.Y.; Lin, N.U.; Grodzinsky, A.J.; Fukumura, D.; Huang, P.; Baish, J.W.; Padera, T.P.; Munn, L.L.; Jain, R.K. Solid stress in brain tumours causes neuronal loss and neurological dysfunction and can be reversed by lithium, *Nat. Biomed. Eng*. 2019, *3*, 230-245.

[69] Voutouri, C.; Kirkpatrick, N.D.; Chung, E.; Mpekris, F.; Baish, J.W. Experimental and computational analyses reveal dynamics of tumor vessel cooption and optimal treatment strategies, *PNAS*. 2018, *116*, 2662-2671.

[70] Carmeliet, P.; Jain, R.K. Molecular mechanisms and clinical applications of angiogenesis, *Nature*. 2011, *473*, 298-307.

[71] Cheng, L.; Huang, Z.; Zhou, W.; Wu, Q.; Donnola, S.; Liu, J.K.; Fang, X.; Sloan, A.E.; Mao, Y.; Lathia, J.D.; Min, W.; Mclendon, R.E.; Rich, J.N.; Bao, S. Glioblastoma Stem Cells Generate Vascular Pericytes to Support Vessel Function and Tumor Growth, *Cell.* 2013, *153*, 139–152.

[72] Schinkel, A.H. Disruption of the Mouse m & la P-Glycoprotein Gene Leads to a Deficiency in the Blood-Brain Barrier and to Increased Sensitivity to Drugs, *Cell*. 1994, *77*, 491–502.

[73] Robey, R.W.; Pluchino, K.M.; Hall, M.D.; Fojo, A.T.; Bates, S.E.; Gottesman, M.M. Revisiting the role of ABC transporters in multidrug-resistant cancer, *Nat. Rev. Cancer*. 2018, *18*, 452-464.

[74] Gaucher, G.; Dufresne, M.H.; Sant, V.P.; Kang, N.; Maysinger, D.; Leroux, J.C. Block copolymer micelles : preparation , characterization and application in drug delivery, *J. Control. Rel.* 2005, *109*, 169–188.

[75] Adams, M.L.; Lavasanifar, A.; Kwon, G.S. Amphiphilic block copolymers for drug delivery, *J. Pharm. Sci*. 2003, 92,1343–1355.

[76] Cabral, H.; Miyata, K.; Osada, K.; Kataoka, K. Block Copolymer Micelles in Nanomedicine Applications, *Chem. Rev*. 2018, 118, 6844–6892.

[77] Gao, G.H.; Li, Y.; Lee, D.S. Environmental pH-sensitive polymeric micelles for cancer diagnosis and targeted therapy, *J. Control. Rel.* 2013, *169*, 180–184.

[78] Li, F.; Xie, C.; Cheng, Z.; Xia, H. Ultrasound responsive block copolymer micelle of poly(ethylene glycol)-poly(propylene glycol) obtained through click reaction, *Ultrason. Sonochem*. 2016, *30*, 9–17.

[79] Feng, H.; Lu, X.; Wang, W.; Kang, N.G.; Mays, J.W. Block copolymers: Synthesis, self-assembly, and applications, *Polymers*. 2017, *9*, 494.

[80] Braunová, A.; Kaňa, M.; Kudláčová, J.; Kostka, L.; Bouček, J.; Betka, J.; Šírová, M.; Etrych, T. Micelle-forming block copolymers tailored for inhibition of P-gp-mediated multidrug resistance: structure to activity relationship, *Pharmaceutics.* 2019, *11*, 579.

[81] Yi, X.; Batrakova, E.; Banks, W.A.; Vinogradov, S.; Kabanov, A.V. Protein conjugation with amphiphilic block copolymers for enhanced cellular delivery, *Bioconjug. Chem*. 2008, *19*, 1071–1077.

[82] Klaikherd, A.; Nagamani, C.; Thayumanavan, S. Multi-stimuli sensitive amphiphilic block copolymer assemblies, *J. Am. Chem. Soc*. 2009, *131*, 4830–4838.

[83] Yin, J.; Chen, Y.; Zhang, Z.H.; Han, X. Stimuli-responsive block copolymer-based assemblies for cargo delivery and theranostic applications, *Polymers*. 2016, *8*, 268.

[84] Egli, S.; Schlaad, H.; Bruns, N.; Meier, W. Functionalization of Block Copolymer Vesicle Surfaces, *Polymers*. 2011, *3*, 252–280.

[85] Kaditi, E.; Mountrichas, G.; Pispas, S. Amphiphilic block copolymers by a combination of anionic polymerization and selective post-polymerization functionalization, *Eur. Polym. J.* 2011, *47*, 415–434.

[86] Loureiro, J.A.; Gomes, B.; Coelho, M.A.N.; Do Carmo Pereira, M.; Rocha, S. Targeting nanoparticles across the blood-brain barrier with monoclonal antibodies, *Nanomed*. 2014, *9*, 709–722.

[87] Liu, J.S.; Wang, J.H.; Zhou, J.; Tang, X.H.; Lan, X.; Shen, T.; Wu, X.Y.; Hong, Z. Enhanced

brain delivery of lamotrigine with Pluronic® P123-based nanocarrier, *Int. J. Nanomed*. 2014, *9*, 3923–3935.

[88] Sezgin-bayindir, Z.; Ergin, A.D.; Parmaksiz, M.; Elcin, A.E.; Elcin, Y.M.; Yuksel, N. Evaluation of various block copolymers for micelle formation and brain drug delivery: In vitro characterization and cellular uptake studies, *J. Drug Deliv. Sci. Technol.* 2016, *36*, 120–129.

[89] Jhaveri, A.M.; Torchilin, V.P. Multifunctional polymeric micelles for delivery of drugs and siRNA, *Front. Pharmacol.* 2014, *5*, 1–26.

[90] Hu, X.; Oh, J.K. Direct Polymerization Approach to Synthesize Acid-Degradable Block Copolymers Bearing Imine Pendants for Tunable pH-Sensitivity and Enhanced Release, *Macromol. Rapid Commun*. 2021, *41*, e2000394.

[91] Johnson, R.P.; Preman, N.K. In *Exogenous stimuli-responsive drug-release systems*, Makhlouf, A,S.H, Abu-thabit, N.Y., Eds., Stimuli responsive block copolymers for drug delivery applications.Elsevier Ltd., 2018, pp 221-246

[92] Meng, X.Y.; Jia, L.J.; Junhong, N.T.; Xiao-tong, L.; He, T.; Ze-ning, M.; Liu, J.S.; Shen, T. Electro-responsive brain-targeting mixed micelles based on Pluronic F127 and D-α-tocopherol polyethylene glycol succinate–ferrocene, *Colloids Surf, A Physicochem Eng. Asp.* 2020, *601*, 124986.

[93] Nair, H.A.; Rajawat, G.S.; Nagarsenker, M.S. Stimuli-responsive micelles: A nanoplatform for therapeutic and diagnostic applications, In *Drug targeting and stimuli sensitive drug delivery systems*, Grumezescu, A.M., Eds., Elsevier Inc., Romania, 2018, pp. 303-342.

[94] Zhang, M.; Song, C.C.; Su, S.; Du, F.S.; Li, Z.C. ROS-Activated Ratiometric Fluorescent Polymeric Nanoparticles for Self-Reporting Drug Delivery, *ACS Appl. Mater. Interf.* 2018, *10*, 7798–7810.

[95] Mollazadeh, S.; Mackiewicz, M.; Yazdimamaghani, M. Recent advances in the redox-responsive drug delivery nanoplatforms: A chemical structure and physical property perspective, *Mater. Sci. Eng C*. 2021, *118*, 111536.

[96] Lu, L.; Zhao, X.; Fu, T.; Li, K.; He,Y.; Luo, Z.; Dai, L.; Zeng, R.; Cai, K. An iRGD-conjugated prodrug micelle with blood-brain-barrier penetrability for anti-glioma therapy, *Biomaterials.* 2019, *230*, 119666.

[97] Zhou, Q.; Zhang, L.; Yang, T.H.; Wu, H. Stimuli-responsive polymeric micelles for drug delivery and cancer therapy, *Int. J. Nanomed*. 2018, *13*, 2921–2942.

[98] Bansal, A.; Simon, M.C. Glutathione metabolism in cancer progression and treatment resistance, *J. Cell. Biol*. 2018, *217*, 2291–2298.

[99] Li, J.; Huo, M.; Wang, J.; Zhou, J.; Mohammad, J.M.; Zhang, Y.; Zhu, Q.; Waddad,A.Y.; Zhang, Q. Redox-sensitive micelles self-assembled from amphiphilic hyaluronic acid- deoxycholic acid conjugates for targeted intracellular delivery of paclitaxel, *Biomaterials*. 2012, *33*, 2310–2320.

[100]Sun, Y.; Yan, X.; Yuan, T.; Liang, J.; Fan, Y.; Gu, Z.; Zhang, X. Disassemblable micelles based on reduction-degradable amphiphilic graft copolymers for intracellular delivery of doxorubicin, *Biomaterials*. 2010, *31*, 7124–7131.

[101]Wang, Y.; Wang, F.; Sun, T.; Wang, J. Redox-Responsive Nanoparticles from the Single Disulfide Bond-Bridged Block Copolymer as Drug Carriers for Overcoming Multidrug Resistance in Cancer Cells, *Biconjug. Chem*. 2011, *22*, 1939–1945.

[102]Egeblad, M.; Werb, Z. New Functions for the matrix metalloproteinase in cancer progression, *Nat. Rev. Cancer*. 2002, *2*, 161-174.

[103]Kessenbrock, K.; Plaks, V.; Werb, Z. Matrix Metalloproteinases : Regulators of the Tumor Microenvironment, *Cell*. 2010, *141*, 52-67.

[104]Yu, L.Y.; Shen, Y.A.; Chen, M.H.; Wen, Y.H.; Hsieh, P.I.; Lo, C.L. The feasibility of ROS- and GSH-responsive micelles for treating tumor-initiating and metastatic cancer stem cells, *J. Mater. Chem B*. 2019, *7*, 3109–3118.

[105]Oddone, N.; Boury, F.; Garcion, E.; Grabrucker, A.M.; Martinez, M.C.; Da Ros, F.; Janaszewska, A.; Forni, F.; Vandelli, M.A.; Tosi, G.; Ruozi, B.; Duskey, J.T. Synthesis, Characterization, and In Vitro Studies of an Reactive Oxygen Species (ROS)-Responsive Methoxy Polyethylene Glycol-Thioketal-Melphalan Prodrug for Glioblastoma Treatment, *Front. Pharmacol*. 2020, *11*, 1–15.

[106]Tang, R.; Ji, W.; Panus, D.; Palumbo, R.N.; Wang, C. Block copolymer micelles with acid-labile ortho ester side-chains: Synthesis, characterization, and enhanced drug delivery to human glioma cells, *J. Control. Rel.* 2011, *151*, 18–27.

[107]Yin, Y.; Fu, C.; Li, M.; Li, X.; Wang, M.; He, L.; Zhang, L.; Peng, Y. A pH-sensitive hyaluronic acid prodrug modi fi ed with lactoferrin for glioma dual-targeted treatment, *Mater. Sci.*

Eng C. 2016, *67*, 159–169.

[108]Jafarzadeh-Holagh, S.; Hashemi-Najafabadi, S.; Shaki, H.; Vasheghani-Farahani, E. Self-assembled and pH-sensitive mixed micelles as an intracellular doxorubicin delivery system, *J. Colloid. Interf. Sci*. 2018, *523*, 179–190.

[109]Gu, G.; Xia, H.; Hu, Q.; Liu, Z.; Jiang, M.; Kang, T.; Miao, D.; Tu, Y.; Pang, Z.; Song, Q.; Yao, L.; Chen, H.; Gao, X.; Chen, J. PEG-co-PCL nanoparticles modified with MMP-2/9 activatable low molecular weight protamine for enhanced targeted glioblastoma therapy, *Biomaterials.* 2013, *34*, 196–208.

[110]Tian, C.; Asghar, S.; Xu, Y.; Chen, Z.; Zhang, M.; Huang, L.; Ye, J.; Ping, Q.; Xiao, Y. The effect of the molecular weight of hyaluronic acid on the physicochemical characterization of hyaluronic acid-curcumin conjugates and in vitro evaluation in glioma cells, *Colloids. Surf B. Biointerfaces*. 2018, *165*, 45–55.

[111] Xiang, Y.; Duan, X.; Feng, L.; Jiang, S.; Deng, L.; Shen, J. tLyp-1-conjugated GSH-sensitive biodegradable micelles mediate enhanced pUNO1-hTRAILa / curcumin co-delivery to gliomas, *Chem. Eng*. J. 2019, *374*, 392–404.

[112]Karami, Z.; Sadighian, S.; Rostamizadeh, K.; Hosseini, S.H.; Rezaee, S.; Hamidi, M. Magnetic brain targeting of naproxen-loaded polymeric micelles: pharmacokinetics and biodistribution study, *Mater. Sci. Eng C.* 2019, *100*, 771–780.

[113]Wu, P.; Jia, Y.; Qu, F.; Sun, Y.; Wang, P.; Zhang, K.; Xu, C.; Liu, Q.; Wang, X. Ultrasound-Responsive Polymeric Micelles for Sonoporation- Assisted Site-Specific Therapeutic Action, *ACS. Appl. Mater. Interfaces*. 2017, *9*, 25706-25716.

[114]Gu, H.; Mu, S.; Qiu, G.; Liu, X.; Zhang, L.; Yuan, Y.; Astruc, D. Redox-stimuli-responsive drug delivery systems with supramolecular ferrocenyl-containing polymers for controlled release, *Coord. Chem. Rev*. 2018, *364*, 51–85.

[115]Khan, A.; Wang, L.; Yu, H.; Haroon, M.; Ullah, R.S.; Nazir, A.; Elshaarani, T.; Usman, M.; Fahad, S.; Haq, F. Research advances in the synthesis and applications of ferrocene-based electro and photo responsive materials, *Appl. Organomet. Chem.* 2018, *32*, 1–28.

[116]Sahle, F.F.; Gulfam, M.; Lowe, T.L. Design Strategies for Physical Stimuli-Responsive Programmable Nanotherapeutics, *Drug. Discov. Today.* 2018, *23*, 992–1006.

[117]Huang, H.Y.; Hu, S.H.; Chian, C.S.; Chen, S.Y.; Lai, H.Y.; Chen, Y.Y. Self-assembling PVA-

F127 thermosensitive nanocarriers with highly sensitive magnetically-triggered drug release for epilepsy therapy in vivo, *J. Mater. Chem*. 2012, *22*, 8566–8573.

[118]Wang, J.; Pelletier, M.; Zhang, H.; Xia, H.; Zhao, Y. High-frequency ultrasound-responsive block copolymer micelle, *Langmuir.* 2009, *25*, 13201–13205.

[119]Xuan, J.; Boissière, O.; Zhao, Y.; Yan, B.; Tremblay, L.; Lacelle, S.; Xia, H.; Zhao, Y. Ultrasound-responsive block copolymer micelles based on a new amplification mechanism, *Langmuir*. 2012, *28*, 16463–16468.

[120]Wei, P.; Cornel, E.J.; Du, J. Ultrasound-responsive polymer-based drug delivery systems, *Drug Deliv. Transl. Res*. 2021, *11*, 1323–1339.

[121]Tong, R.; Lu, X.; Xia, H. A facile mechanophore functionalization of an amphiphilic block copolymer towards remote ultrasound and redox dual stimulus responsiveness, *Chem. Commun*. 2014, *50*, 3575–3578.

[122]Olsman, M.; Mühlenpfordt, M.; Olsen, E.B.; Torp, S.H.; Kotopoulis, S.; Rijcken, C.J.F.; Hu, Q.; Thewissen, M.; Snipstad, S.; De Lange Davies, C. Acoustic Cluster Therapy (ACT®) enhances accumulation of polymeric micelles in the murine brain, J. *Control. Rel.* 2021, *337*, 285–295.

[123]Sontum, P.; Kvåle, S.; Healey, A.J.; Skurtveit, R.; Watanabe, R.; Matsumura, M.; Ostensen, J. Acoustic Cluster Therapy (ACT) – a novel concept for ultrasound mediated, targeted drug delivery, *Int. J. Pharm*. 2015, *495*,1019-1027.

[124]Zhao, Y.; He, J. Azobenzene-containing block copolymers: The interplay of light and morphology enables new functions, *Soft Matter*. 2009, *5*, 2686–2693.

[125]Xinag, J.; Tong, X.; Shi, F.; Yan, Q.; Yu, B. Near-infrared light-triggered drug release from UV-responsive diblock copolymer-coated upconversion nanoparticles with high monodispersity, *Mater. Chem B.* 2018, *6*, 3531-3540.

[126]Zhou, Y.; Zhang, L.; Gao, H.; Zhu, F.; Ge, M.; Liang, G. Rapid detection of aromatic pollutants in water using swellable micelles of fluorescent polymers, S*ens. Actuators B Chem.* 2019, *283*, 415–425.

[127]Alven, S.; Nqoro, X.; Buyana, B.; Aderibigbe, B.A. Polymer-drug conjugate, a potential therapeutic to combat breast and lung cancer, *Pharmaceutics.* 2020, *12*, 406.

[128]Hanafy, N.A.N.; El-Kemary, M.; Leporatti, S. Micelles structure development as a strategy to

improve smart cancer therapy, *Cancers*. 2018, *10*, 1–14.

[129]Zhang, S.; Chan, K.H.; Prud, R.K.; Link, A.J. Synthesis and Evaluation of Clickable Block Copolymers for Targeted Nanoparticle Drug Delivery, *Mol. Pharm*. 2012, *9*, 2228-36.

[130]Larson, N.; Ghandehari, H. Polymeric Conjugates for Drug Delivery, *Chem. Mater*. 2012, *84*, 840-853.

[131]Veronese, F.M.; Mero, A. The impact of PEGylation on biological therapies. *Biodrugs*. 2008, *22*, 315–329.

[132]Islam, Y.; Leach, A.G.; Smith, J.; Pluchino, S.; Coxonl, C.R.; Sivakumaran, M.; Downing, J.; Fatokun, A.A.; Teixidò, M.; Ehtezazi, T. Peptide based drug delivery systems to the brain, *Nano Express*. 2020, *1*, 012002.

[133]Pitto-barry, A.; Barry, N.P.E. Pluronic® block-copolymers in medicine: from chemical and biological versatility to rationalisation and clinical advances, *Polym. Chem*. 2014, *5*, 3291-3297.

[134]Luxenhofer, R.; Schulz, A.; Roques, C.; Li, S.; Bronich, T.K.; Batrakova, E.V.; Jordan, R.; Kabanov, A.V. Biomaterials Doubly amphiphilic poly (2-oxazoline) s as high-capacity delivery systems for hydrophobic drugs, *Biomaterials.* 2010, *31*, 4972–4979.

[135]Price, T.O.; Farr, S.A.; Yi, X.; Vinogradov, S.; Batrakova, E.; Banks, W.A.; Kabanov, A.V. Transport across the Blood-Brain Barrier of Pluronic Leptin, *J. Pharmacol. Exp. Ther*. 2010, *333*, 253–263.

[136]Yi, X.; Yuan, D.; Farr, S.A.; Banks, W.A.; Poon, C.; Kabanov, A.V. Pluronic modified leptin with increased systemic circulation, brain uptake and efficacy for treatment of obesity, *J. Control. Rel*. 2014, *191*, 34-46.

[137]Tong, J.; Yi, X.; Luxenhofer, R.; Banks, W.A.; Jordan, R.; Zimmerman, M.C.; Kabanov, A.V. Conjugates of superoxide dismutase 1 with amphiphilic poly(2-oxazoline) block copolymers for enhanced brain delivery: Synthesis, characterization and evaluation in vitro and in vivo, *Mol. Pharm*. 2013, *10*, 360–377.

[138]Yi, X.; Zimmerman, M.C.; Yang, R.; Tong, J.; Vinogradov, S.; Kabanov, A.V. Pluronic-modified superoxide dismutase 1 attenuates angiotensin II-induced increase in intracellular superoxide in neurons, *Free Radic. Biol. Med*. 2010, *49*, 548–558.

[139]Meng, X.; Liu, J.; Yu, X.; Li, J.; Lu, X.; Shen, T. Pluronic F127 and D-α-Tocopheryl Polyethylene Glycol Succinate (TPGS) Mixed Micelles for Targeting Drug Delivery across The Blood Brain Barrier, *Sci. Rep.* 2017, *7*, 1–12.

[140]Batrakova, E.V.; Vinogradov, S.V.; Robinson, S.M.; Niehoff, M.L.; Banks, W.A.; Kabanov, A.V. Polypeptide point modifications with fatty acid and amphiphilic block copolymers for enhanced brain delivery, *Bioconjug. Chem*. 2005, *16*, 1334.

[141]Re, F.; Gregori, M.; Masserini, M. Nanotechnology for neurodegenerative disorders, *Maturitas.* 2012, *73*, 45–51.

[142]Deng, H.; Dutta, P.; Liu, J. Stochastic modeling of nanoparticle internalization and expulsion through receptor-mediated transcytosis, *Nanoscale.* 2019, *11*, 11227–11235.

[143]Yoo, J.; Park, C.; Yi, G; Lee, D.; Koo, H. Active targeting strategies using biological ligands for nanoparticle drug delivery systems, *Cancers.* 2019, *11*, 640.

[144]Quader, S.; Liu, X.; Chen, Y.; Mi, P.; Chida, T.; Ishii, T.; Miura, Y.; Nishiyama, N.; Cabral, H.; Kataoka, K. cRGD peptide-installed epirubicin-loaded polymeric micelles for effective targeted therapy against brain tumors, *J. Control. Rel*. 2017, *258*, 56–66.

[145]Ruan, H.; Yao, S.; Wang, S.; Wang, R.; Xie, C.; Guo, H.; Lu, W. Stapled RAP12 peptide ligand of LRP1 for micelles-based multifunctional glioma-targeted drug delivery, *Chem. Eng. J.* 2021, *403*, 126296.

[146]Luo, Z.; Yan, Z.; Jin, K.; Pang, Q.; Jiang, T.; Lu, H.; Liu, X.; Pang, Z.; Yu, L.; Jiang, X. Precise glioblastoma targeting by AS1411 aptamer-functionalized poly (L-γ-glutamylglutamine)–paclitaxel nanoconjugates, *J Colloid Interf Sci.* 2017, *490*, 783–796.

[147]Sharma, G.; Lakkadwala, S.; Modgil, A.; Singh, J. The role of cell-penetrating peptide and transferrin on enhanced delivery of drug to brain, *Int. J. Mol. Sci.* 2016, *17*, 806.

[148] Desale, K.; Kuche, K.; Jain, S. Cell-penetrating peptides (CPPs): An overview of applications for improving the potential of nanotherapeutics, *Biomater. Sci.* 2021, *9*, 1153–1188.

[149]Deshayes, S.; Morris, M.C.; Divita, G.; Heitz, F. Cellular and Molecular Life Sciences Cell-penetrating peptides : tools for intracellular delivery of therapeutics, 2005, *62*, 1839–1849.

[150]Gagat, M.; Zielińska, W.; Grzanka, A. Cell-penetrating peptides and their utility in genome function modifications, *Int. J. Mol. Med*. 2017, *40*, 1615–1623.

[151]Hervé, F.; Ghinea, N.; Scherrmann, J.M. CNS delivery via adsorptive transcytosis, *AAPS*. 2008, *10*, 455–472.

[152]Zou, L.L.; Ma, J.L.; Wang, T.; Yang, T.B.; Liu, C.B. Cell-Penetrating Peptide-Mediated Therapeutic Molecule Delivery into the Central Nervous System, *Curr. Neuropharmacol.* 2013, *11*, 197–208.

[153]Tanaka, K.; Kanazawa, T.; Shibata, Y.; Suda, Y.; Fukuda, T.; Takashima, Y.; Okada, H. Development of cell-penetrating peptide-modified MPEG-PCL diblock copolymeric nanoparticles for systemic gene delivery, *Int. J. Pharm*. 2010, *369*, 229–238.

[154]Asil, S.M.; Ahlawat, J.; Barroso, G.G.; Narayan, M. Nanomaterial based drug delivery systems for the treatment of neurodegenerative diseases, *Biomater. Sci*. 2020, *8*, 4088–4107.

[155]Kanazawa, T.; Taki, H.; Okada, H. Nose-to-brain drug delivery system with ligand/cell-penetrating peptide-modified polymeric nano-micelles for intracerebral gliomas, *Eur. J. Pharm. Biopharm.* 2020, *152*, 85–94.

[156]Shao, K.; Huang, R.; Li, J.; Han, L.; Ye, L.; Lou, J.; Jiang, C. Angiopep-2 modified PE-PEG based polymeric micelles for amphotericin B delivery targeted to the brain, *J. Control. Rel.* 2010, *147*, 118–126.

[157]Han, H.; Zhang, Y.; Jin, S.; Chen, P.; Liu, S.; Xie, Z.; Jing, X.; Wang, W. Paclitaxel-loaded dextran nanoparticles decorated with RVG29 peptide for targeted chemotherapy of glioma: An: In vivo study, *New J. Chem*. 2020,*44*, 5692–5701.

[158]Tian, Y.; Mi, G.; Chen, Q.; Chaurasiya, B.; Li, Y.; Shi, D.; Zhang, Y.; Webster, T.J.; Sun, C.; Shen, Y. Acid-Induced Activated Cell-Penetrating Peptide-Modified Cholesterol-Conjugated Polyoxyethylene Sorbitol Oleate Mixed Micelles for pH-Triggered Drug Release and Efficient Brain Tumor Targeting Based on a Charge Reversal Mechanism, *ACS Appl. Mater. Interfaces*. 2018, *10*, 43411–43428.

[159]Zhang, Y.; Xiao, Y.; Huang, Y.; He, Y.; Xu, Y.; Lu, W.; Yu, J. Poly(ethylene glycol) shell-sheddable TAT-modified core cross-linked nano-micelles: TAT-enhanced cellular uptake and lysosomal pH-triggered doxorubicin release, *Colloids Surf B Biointerfaces.* 2020, *188*, 110772.

[160]Niu, J.; Wang, L.; Yuan, M.; Zhang, J.; Zhang, Y. Dual-targeting nanocarrier based on glucose and folic acid functionalized pluronic P105 polymeric micelles for enhanced brain distribution, *J. Drug Deliv. Sci. Tech.* 2020, *57*, 101343.

[161]Suzuki, K.; Miura, Y.; Mochida, Y.; Miyazaki, T.; Toh, K.; Anraku, Y.; Melo, V.; Liu, X.; Ishii, T.; Nagano, O. Glucose transporter 1-mediated vascular translocation of nanomedicines enhances accumulation and efficacy in solid tumors, *J. Control. Rel.* 2019, *301,* 28–41.

[162]Sun, P.; Xiao, Y.; Di, Q.; Ma, W.; Ma, X.; Wang, Q.; Chen, W. Transferrin receptor-targeted peg-pla polymeric micelles for chemotherapy against glioblastoma multiforme, *Int. J. Nanomed*. 2020, *15,* 6673–6688.

[163]Guo, Q.; Xu, S.; Yang, P.; Wang, P.; Lu, S.; Sheng, D.; Qian, K.; Cao, J.; Lu, W.; Zhang, Q. A dual-ligand fusion peptide improves the brain-neuron targeting of nanocarriers in Alzheimer's disease mice, *J. Control. Rel*. 2020, *320,* 347–362.

[164]Gao, H.; Qian, J.; Yang, Z.; Pang, Z.; Xi, Z.; Cao, S.; Wang, Y.; Pan, S.; Zhang, S.; Wang, W.; Jiang, X.; Zhang, Q. Whole-cell SELEX aptamer-functionalised poly(ethyleneglycol)-poly(ε-caprolactone) nanoparticles for enhanced targeted glioblastoma therapy, *Biomaterials*. 2012, *33,* 6264–6272.

[165]Mu, C.; Dave, N.; Hu, J.; Desai, P.; Pauletti, G.; Bai, S.; Hao, J. Solubilization of flurbiprofen into aptamer-modified PEG-PLA micelles for targeted delivery to brain-derived endothelial cells in vitro, *J. Microencapsul*. 2013, *30,* 701–708.

[166]Hoosain, F.G.; Choonara, Y.E.; Tomar, L.K.; Kumar, P.; Tyagi, C.; du Toit, L.C.; Pillay, V. Bypassing P-Glycoprotein Drug Efflux Mechanisms: Possible Applications in Pharmacoresistant Schizophrenia Therapy, *BioMed Res. Int*. 2015, *2015,* 484963.

[167]Van Assema, D.M.E.; Lubberink, M.; Boellaard, R.; Schuit, R.C.; Windhorst, A.D.; Scheltens, P.; Lammertsma, A.A.; Van Berckel, B.N.M. P-glycoprotein function at the blood-brain barrier: Effects of age and gender, *Mol. Imaging. Biol.* 2012, *14,* 771–776.

[168]Wang, X.; Huang, S.; Jiang, Y.; Liu, Y.; Song, T.; Li, D.; Yang, L. Reactive astrocytes increase the expression of P-gp and Mrpl via TNF-α and NF-κB signaling, *Mol. Med. Rep.* 2018, *17,* 1198–1204.

[169]Aryal, M.; Fischer, K.; Gentile, C.; Gitto, S.; Zhang, Y.Z.; McDannold, N. Effects on P-glycoprotein expression after blood-brain barrier disruption using focused ultrasound and microbubbles, *PLoS ONE*. 2017, *12,* 1–15.

[170]Schinkel, A.H. P-Glycoprotein, a gatekeeper in the blood–brain barrier, *Adv. Drug. Deliv. Rev.* 1999, *36,* 179–194.

[171]Choi, H.J.; Lee, E.H.; Han, M.; An, S.H. J. Park, Diminished Expression of P-glycoprotein Using Focused Ultrasound Is Associated With JNK-Dependent Signaling Pathway in Cerebral Blood Vessels, *Front. Neurosci.* 2019, *13,* 1–12.

[172]Burgess, A.; Shah, K.; Hough, O.; Hynynen, K. Focused ultrasound-mediated drug delivery through the blood- brain barrier, *Exp. Rev. Neurother.* 2016, *15,* 477–491.

[173]Erdo, F.; Krajcsi, P. Age-related functional and expressional changes in efflux pathways at the blood-brain barrier, *Front. Aging Neurosci.* 2019, *10,* 1–8.

[174]Bartels, A.L.; Van Berckel, B.N.M.; Lubberink, M.; Luurtsema, G.; Lammertsma, A.A.; Leenders, K.L. Blood brain barrier P-glycoprotein function is not impaired in early Parkinson' s disease, *Parkinsonism Relat Disord.* 2008, *14,* 505-508.

[175]Fromm, M.F. Importance of P-glycoprotein at blood-tissue barriers, *Trends. Pharmacol. Sci*. 2004, *25,* 423–429.

[176]Waghray, D.; Zhang, Q. Inhibit or Evade Multidrug Resistance P-Glycoprotein in Cancer Treatment, *J. Med. Chem*. 2018, *61,* 5108–5121.

[177]Föger, F.; Schmitz, T.; Bernkop-Schnürch, A. In vivo evaluation of an oral delivery system for P-gp substrates based on thiolated chitosan, *Biomaterials.* 2006, *27,* 4250–4255.

[178]Hugger, E.D.; Audus, K.L.; Borchardt, R.T. Effects of poly(ethylene glycol) on efflux transporter activity in Caco-2 cell monolayers, *J. Pharm. Sci.* 2002, *91,* 1980–1990.

[179]Dintaman, J.M.; Silverman, J.A. Inhibition of P-glycoprotein by D-alpha-Tocopheryl Polyethylene glycol 1000 succinate (TPGS), *Pharm. Res.* 1999, *16,* 1550-6.

[180]Rege, B.D.; Kao, J.P.Y.; Polli, J.E. Effects of nonionic surfactants on membrane transporters in Caco-2 cell monolayers, *Eur. J. Pharm. Sci*. 2002, *16,* 237–246.

[181]Psimadas, D.; Georgoulias, P.; Valotassiou, V.; Loudos, G. Molecular Nanomedicine Towards Cancer. *J. Pharm. Sci*. 2012, *101*, 2271–80.

[182]Batrakova, E.V.; Li, S.; Miller, D.W.; Kabanov, A.V. Pluronic P85 increases permeability of broad spectrum of drugs in polarized BBMEC and Caco-2 cell and monolayers, *Pharm. Res.* 1999, *16*, 1366-72

[183]Bromberg, L.; Alakhov, V. Effects of polyether-modified poly(acrylic acid) microgels on doxorubicin transport in human intestinal epithelial Caco-2 cell layers, *J. Control. Rel*. 2003, *88*, 11–22.

[184]Kim, J.Y.; Choi, W.I.; Kim, Y.H.; Tae, G. Brain-targeted delivery of protein using chitosan- and RVG peptide-conjugated, pluronic-based nano-carrier, *Biomaterials.* 2013, *34*, 1170–1178.

[185]Pascual, J.M.; Liu, P.; Mao, D.; Kelly, D.I.; Hernandez, A.; Sheng, M.; Good,L.B.; Ma, Q.; Marin-Valencia, I.; Zhang, X.; Park, J.Y.; Hynan, L.S.; Stavinoha, P.; Roe, C.R.; Lu, H. Triheptanoin for Glucose Transporter Type I Deficiency (G1D), *JAMA Neurol.* 2014, 71, 1255.

[186]Yi X, Kabanov, A.V. Brain delivery of proteins via their fatty acid and block copolymer modifications, *J. Drug. Target*. 2008, *23*, 1–7.

[187]Batrakova, E.V.; Li, S.; Alakhov, V.Y.; Miller, D.W.; Kabanov, A.V. Optimal structure requirements for Pluronic block copolymers in modifying P-glycoprotein drug efflux transporter activity in bovine brain microvessel endothelial cells, *J. Pharmacol. Exp. Thera.* 2003, *304*, 845–854.

[188] Miller, D.; Batrakova, E.V.; Waltner, T.O.; Alakhov, V.Y.; Kabanov, A.V. Interactions of pluronic block copolymers with brain microvessel endothelial cells: Evidence of two potential pathways for drug absorption, *Bioconjug. Chem*. 1997, *8*, 649–657.

[189]Sotoudegan, F.; Amini, M.; Faizi, M.; Aboofazeli, R. Nimodipine-loaded Pluronic® block copolymer micelles: Preparation, characterization, in-vitro and in-vivo studies, *Iran. J. Pharm. Res.* 2016, *15*, 641–661.

[190]Nour, S.A.; Abdelmalak, N.S.; Naguib, M.J.; Rashed, H.M.; Ibrahim, A.B. Intranasal brain-targeted clonazepam polymeric micelles for immediate control of status epilepticus: in vitro optimization, ex vivo determination of cytotoxicity, in vivo biodistribution and pharmacodynamics studies, *Drug Deliv*. 2016, *23*, 3681–3695.

[191]Seth, A.; Katti, D.S. A one-step electrospray-based technique for modulating morphology and surface properties of poly(lactide-co-glycolide) microparticles using Pluronics®, *Int. J. Nanomed*. 2012, *7*, 5129–5136.

[192]Frozza, R.L.; Lourenco, M.V.; de Felice, F.G. Challenges for Alzheimer’s disease therapy:

Insights from novel mechanisms beyond memory defects, *Front. Neurosci*. 2018, *12*, 1–13.

[193]Fonseca-Santos, B.; Gremião, M.P.D.; Chorilli, M. Nanotechnology-based drug delivery systems for the treatment of Alzheimer's disease, *Int. J. Nanomed.* 2015, *10*, 4981–5003.

[194]Morris, M.; Maeda, S.; Vossel, K.; Mucke, L. The Many Faces of Tau, *Neuron*. 2011, *70*, 410–426.

[195]Clarke, J.R.; Lyra e Silva, N.M.; Figueiredo, C.P.; Frozza, R.L.; Ledo, J.H.; Beckman, D.; Katashima, C.K.; Razolli, D.; Carvalho, B.M.; Frazão, R.; Silveira, M.A.; Ribeiro, F.C.; Bomfim, T.R.; Neves, F.S.; Klein, W.L.; Medeiros, R.; LaFerla, F.M.; Carvalheira, J.B.; Saad, M.J.; Munoz, D.P.; Velloso, L.A.; Ferreira, S.T..; De Felice, F.G. Alzheimer-associated Aβ oligomers impact the central nervous system to induce peripheral metabolic deregulation, *EMBO Mol. Med*. 2015, *7*, 190–210.

[196]Stevanovic, K.; Yunus, A.; Joly-Amado, A.; Gordon, M.; Morgan, D.; Gulick, D.; Gamsby, J. Disruption of normal circadian clock function in a mouse model of tauopathy, *Exp. Neurol*. 2017, *294*, 58–67.

[197]Nobili, A.; Latagliata, E.C.; Viscomi, M.T.; Cavallucci, V.; Cutuli, D.; Giacovazzo, G.; Krashia, P.; Rizzo, F.R.; Marino, R.; Federici, M.; De Bartolo, P.; Aversa, D.; Dell'Acqua, M.C.; Cordella, A.; Sancandi, M.; F. Keller, Petrosini, L.; Puglisi-Allegra, S.; Mercuri, N.B.; Coccurello, R.; Berretta, N.; D'Amelio, M. Dopamine neuronal loss contributes to memory and reward dysfunction in a model of Alzheimer's disease, *Nat. Commun*. 2017, *8*, 14727.

[198]Alyautdin, R.; Khalin, I.; Nafeeza, M.I.; Haron, M.H.; Kuznetsov, D. Nanoscale drug delivery systems and the blood-brain barrier, *Int. J. Nanomed*. 2014, *9*, 795–811.

[199]Agwa, M.M.; Abdelmonsif, D.A.; Khattab, S.N.; Sabra, S. Self- assembled lactoferrin-conjugated linoleic acid micelles as an orally active targeted nanoplatform for Alzheimer's disease, *Int. J. Biol. Macromol*. 2020, *162*, 246–261.

[200]Glynn-Servedio, B.E.; Ranola, T.S. AChE inhibitors and NMDA receptor antagonists in advanced Alzheimer's disease, *Consult. Pharm*. 2017, *32*, 511–518.

[201]Korkmaz, O.T.; Ay, H.; Aytan, N.; Carreras, I.; Kowall, N.W.; Dedeoglu, A.; Tuncel, N. Vasoactive Intestinal Peptide Decreases β-Amyloid Accumulation and Prevents Brain Atrophy in the 5xFAD Mouse Model of Alzheimer's Disease. *J. Mol. Neurosci.* 2019, *68*, 389–96.

[202]Navarro, G.; Pan, J.; Torchilin, V.P. Micelle-like nanoparticles as carriers for DNA and siRNA,

Mol. Pharm. 2015, *12*, 301–313.

[203]Zahir-Jouzdani, F.; Mottaghitalab, F.; Dinarvand, M.; Atyabi, F. siRNA delivery for treatment of degenerative diseases, new hopes and challenges, *J. Drug. Deliv. Sci. Technol.* 2018, *45*, 428–441.

[204]Zheng, X.; Pang, X.; Yang, P.; Wan, X.; Wei, Y.; Guo, Q.; Zhang, Q.; Jiang, X. A hybrid siRNA delivery complex for enhanced brain penetration and precise amyloid plaque targeting in Alzheimer's disease mice, *Acta Biomaterialia*. 2017, *49*, 388–401.

[205]Yang, P.; Sheng, D.; Guo, Q.; Wang, P.; Xu, S.; Qian, K.; Li, Y.; Cheng, Y.; Wang, L.; Lu, W.; Zhang, Q. Neuronal mitochondria-targeted micelles relieving oxidative stress for delayed progression of Alzheimer's disease, *Biomaterials*. 2020, *238*, 119844.

[206]Scialabba, C.; Rocco, F.; Licciardi, M.; Pitarresi, G.; Ceruti, M.; Giammona, G. Amphiphilic polyaspartamide copolymer-based micelles for rivastigmine delivery to neuronal cells, *Drug. Deliv.* 2012, *19*, 307–316.

[207]Ren, J.; Jiang, F.; Wang, M.; Hu, H.; Zhang, B.; Chen, L.; Dai, F. Increased cross-linking micelle retention in the brain of Alzheimer's disease mice by elevated asparagine endopeptidase protease responsive aggregation, *Biomater. Sci.* 2020, *8*, 6533–6544.

[208]Sánchez-López, E.; Ettcheto, M.; Egea, M.A.; Espina, M.; Cano, A.; Calpena, A.C.; Camins, A.; Carmona, N.; Silva, A.M.; Souto, E.B.; García, M.L. Memantine loaded PLGA PEGylated nanoparticles for Alzheimer's disease: In vitro and in vivo characterization, *J. Nanobiotechnol.* 2018, *16*, 1–16.

[209]Lohan, S.; Sharma, T.; Saini, S.; Swami, R.; Dhull, D.; Beg, S.; Raza, K.; Kumar, A.; Singh, B. QbD-steered development of mixed nanomicelles of galantamine: Demonstration of enhanced brain uptake, prolonged systemic retention and improved biopharmaceutical attributes, *Int. J. Pharm.* 2021, *600*, 120482.

[210]Zeng, H.; Xu, L.; Zou, Y.; Wang, S. Romidepsin and metformin nanomaterials delivery on streptozocin for the treatment of Alzheimer ' s disease in animal model, *Biomed. Pharmacother.* 2021, *141*, 111864.

[211]Gao, X.; Wu, B.; Zhang, Q.; Chen, J.; Zhu, J; Zhang, W.; Rong, Z.; Chen, X.; Jiang, X. Brain delivery of vasoactive intestinal peptide enhanced with the nanoparticles conjugated with wheat germ agglutinin following intranasal administration, *J. Control. Rel.* 2007, *121*, 156–167.

[212]Liu, Z.; Jiang, M.; Kang, T.; Miao, D.; Gu, G.; Song, Q.; Yao, L.; Hu, Q.; Tu, Y.; Pang, Z.;

Chen, H.; Jiang, X.; Gao, X.; Chen, J. Lactoferrin-modified PEG-co-PCL nanoparticles for enhanced brain delivery of NAP peptide following intranasal administration, *Biomaterials*. 2013, *34*, 3870–3881.

[213]Shyam, R.; Ren, Y.; Lee, J.; Braunstein, K.E.; Mao, H.Q.; Wong, P.C. Intraventricular delivery of siRNA nanoparticles to the central nervous system, *Mol. Ther. Nucelic acid*. 2015, *4*, e242.

[214]Guo, Q.; Zheng, X.; Yang, P.; Pang, P.; Qian, K.; Wang, P.; Xu, S.; Sheng, D; Wang, L.; Cao, J.; Lu, W.; Zhang, Q.; Jiang, X. Small interfering RNA delivery to the neurons near the amyloid plaques for improved treatment of Alzheimer′s disease, *Acta Pharm. Sin B.* 2019, *9*, 590–603.

[215]Lu, X.; Ji, C.; Xu, H.; Li, X.; Ding, H.; Ye, M.; Zhu, Z.; Ding, D.; Jiang, X.; Ding, X.; Guo, X. Resveratrol-loaded polymeric micelles protect cells from Aβ-induced oxidative stress, *Int. J. Pharm.* 2009, *375*, 89–96.

[216]Cheng, K.K.; Yeung, C.F.; Ho, S.W.; Chow, S.F.; Chow, A.H.L.; Baum, L. Highly stabilized curcumin nanoparticles tested in an in vitro blood-brain barrier model and in alzheimer’s disease Tg2576 Mice, *AAPS J*. 2013, *15*, 324–336.

[217]Aghajanzadeh, M.; Andalib, S.; Danafar, H.; Rostamizadeh, K.; Sharafi, A. The effect of baicalein-loaded Y-shaped miktoarm copolymer on spatial memory and hippocampal expression of DHCR24, SELADIN and SIRT6 genes in rat model of Alzheimer, *Int. J. Pharm.* 586, 119546.

[218]Carboni, E.; Lingor, P. Insights on the interaction of alpha-synuclein and metals in the pathophysiology of Parkinson’s disease, *Metallomics.* 2015, *7*, 395–404.

[219]Stoker, T.B.; Torsney, K.M.; Barker, R.A. Emerging treatment approaches for Parkinson’s disease, *Front. Neurosci.* 2018, *12*, 1–10.

[220]Lotharius, J.; Brundin, P. Pathogenesis of Parkinson's Disease Parkinson's Disease: Dopamine, Vesicles and, α-synuclein, *Nat. Rev. Neurosci*. 2002, *3*, 932–942.

[221]Krishnan, U.M. Biomaterials in the treatment of Parkinson’s disease, *Neurochem. Int.* 2021, *145*, 105003.

[222]Teller, E. Paralysis Agitans: A Disclaimer. *British Med. J.* 1946, *1*, 815.

[223]Smith, Y.; Wichmann, T.; Factor, S.A.; Delong, M.R. Parkinson ’ s Disease Therapeutics : New Developments and Challenges Since the Introduction of Levodopa, *Neuropsychopharmacol.*

2011, *37*, 213–246.

[224]Silva, S.; Almeida, J. Importance of Nanoparticles for the Delivery of Antiparkinsonian Drugs, *Pharmaceutics*. 2021, *13*, 508.

[225]Ahmad, Z.; Shah, A.; Siddiq, M.; Kraatz, H.B. Polymeric micelles as drug delivery vehicles, *RSC Adv*. 2014, *4*, 17028–17038.

[226]Bi, C.C.; Wang, A.P.; Chu, Y.C.; Liu, S.; Mu, H.J.; Liu, W.H.; Wu, Z.M.; Sun, K.X.; Li, Y.X. Intranasal delivery of rotigotine to the brain with lactoferrin-modified PEG-PLGA nanoparticles for Parkinson's disease treatment, *Int. J. Nanomed.* 2016, *11*, 6547–6559.

[227]Vong, L.B.; Sato, Y.; Chonpathompikunlert, P.; Tanasawet, S.; Hutamekalin, P.; Nagasaki, Y. Self-assembled polydopamine nanoparticles improve treatment in Parkinson's disease model mice and suppress dopamine-induced dyskinesia, *Acta Biomateria*. 2020, *109*, 220–228.

[228]Wang, F.; Yang, Z.; Liu, M.; Tao, Y.; Li, Z.; Wu, Z.; Gui, S. Facile nose-to-brain delivery of rotigotine-loaded polymer micelles thermosensitive hydrogels: In vitro characterization and in vivo behavior study, *Int. J. Pharm*. 2020, *577*, 119046.

[229]Brynskikh, A.M.; Zhao, Y.; Mosley, R.L.; Li, S.; Boska, M.D.; Klyachko, N.L.; Kabanov, A.V.; Gendelman, H.E.; Batrakova, E.V. Macrophage delivery of therapeutic nanozymes in a murine model of Parkinsons disease, *Nanomed*. 2010, *5*, 379–396.

[230]Saeed, N.M.; El-naga, R.N.; El-bakly, E.W.; Abdel-rahman, H.M.; El-demerdash, E. Epigallocatechin-3-gallate pretreatment attenuates doxorubicin-induced cardiotoxicity in rats: A mechanistic study, *Biochem. Pharmacol.* 2015, *95*, 145-55

[231]Xue, Y.; Wang, N.; Zeng, Z.; Huang, J.; Xiang, Z.; Guan, Y.Q. Neuroprotective effect of chitosan nanoparticle gene delivery system grafted with acteoside (ACT) in Parkinson's disease models, *J. Mater. Sci. Technol.* 2020, *43*, 197–207.

[232]Hu, K.; Y. Shi, W. Jiang, J. Han, S. Huang, Jiang, X. Lactoferrin conjugated PEG-PLGA nanoparticles for brain delivery: Preparation, characterization and efficacy in Parkinsons disease, *Int. J. Pharm*. 2011, *415*, 273–283.

[233]Wen, Z.; Yan, Z.; Hu, K.; Pang, Z.; Cheng, X.; Guo, L.; Zhang, Q.; Jiang, X.; Fang, L.; Lai, R. Odorranalectin-conjugated nanoparticles: Preparation, brain delivery and pharmacodynamic study on Parkinson's disease following intranasal administration, J. Control. Rel. 2011, *151*, 131–138.

[234]Huang, R.; Ke, W.; Liu, Y.; Wu, D.; Feng, L.; Jiang, C.; Pei, Y. Gene therapy using lactoferrin-modified nanoparticles in a rotenone-induced chronic Parkinson model, *J. Neurol. Sci.* 2010, *290*, 123–130.

[235]Huang, R.; Ma, H.; Guo, Y.; Liu, S.; Kuang, Y.; Shao, K.; Li, J.; Liu, Y.; Han, L.; Huang, S.; An, S.; Ye, L.; Lou, J.; Jiang, C. Angiopep-conjugated nanoparticles for targeted long-term gene therapy of parkinson's disease, *Pharm. Res*. 2013, *30*, 2549–2559.

[236]Liu, Y.Y.; Yang, X.Y.; Li, Z.;Liu, Z.L.; Cheng, D.; Wang, Y.; Wen, X.J.; Hu, J.Y.; Liu,J.; Wang, L.M.; Wang, H.J. Characterization of polyethylene glycol-polyethyleneimine as a vector for alpha-synuclein siRNA delivery to PC12 cells for Parkinson's disease, *CNS Neurosci. Thera*. 2014, *20*, 76–85.

[237]Sánchez-Giraldo, V.; Monsalve, Y.; Palacio, J.; Mendivil-Perez, M.; Sierra, L.; Velez-Pardo, C.; López, B.L.; Jiménez-Del-Rio, M. Role of a novel (−)-epigallocatechin-3-gallate delivery system on the prevention against oxidative stress damage in vitro and in vivo model of Parkinson's disease, *J. Drug Deliv. Sci. Technol*. 2020, *55*, 101466.

[238]Liu, H.; Zhang, J.; Chen, X.; Du, X.S.; Zhang, J.L.; Liu, G.; Zhang, W.G. Application of iron oxide nanoparticles in glioma imaging and therapy: From bench to bedside, *Nanoscale.* 2016, *8*, 7808–7826.

[239]Cancer, T.; G. Atlas, Comprehensive genomic characterization defines human glioblastoma genes and core pathways, *Nature.* 2008, *455*, 1061–1068.

[240]Sturm, D.; Bender, S.; Jones, D.T.W.; Lichter, P.; Grill, J.; Becher, O.; Hawkins, C.; Majewski, J.; Jones, C.; Costello, J.F.; Lavarone, A.; Aldape, K.; Brennan, C.W.; Jabado, N.; Pfister, S.M. Paediatric and adult glioblastoma : multiform (epi) genomic culprits emerge, *Nat. Rev. Cancer.* 2014, *14*, 92–107.

[241]Maher, E.A.; Furnari, F.B.; Bachoo, R.M.; Furnari, F.B.; Bachoo, R.M.; Rowitch, D.H.; Louis, D.N.; Cavenee, W.K.; Depinho, R.A. Malignant glioma : genetics and biology of a grave matter Malignant glioma : genetics and biology of a grave matter, *Genes. Dev*. 2001, *15*, 1311–1333.

[242]Davis, M.E. Glioblastoma: Overview of Disease and Treatment, *Clin. J. Oncol. Nurs*. 2016, *20*, 33–44.

[243]Durand, M.; Lelievre, E.; Chateau, A.; Berquand, A.; Laurent, G.; Carl, P.; Roux, S.; Chazee, L.; Bazzi, R.; Eghiaian, F.; Jubreaux, J.; Ronde, P.; Barberi-Heyob, M.; Chastagner, P.; Devy, J.;

Pinel, S. The detrimental invasiveness of glioma cells controlled by gadolinium chelate-coated gold nanoparticles, *Nanoscale*. 2021, *13,* 9236–9251.

[244]Morshed, R.A.; Cheng, Y.; Auffinger, B.; Wegscheid, M.L.; Lesniak, M.S. The potential of polymeric micelles in the context of glioblastoma therapy, *Front. Pharmacol.* 2013, *4,* 1–15.

[245]Liu, Y.J.; Ma, Y.C.; Zhang, W.J.; Yang, Z.Z.; Liang, D.S.; Wu, Z.F.; Qi, X.R. Combination therapy with micellarized cyclopamine and temozolomide attenuate glioblastoma growth through Gli1 down-regulation, *Oncotarget.* 2017, *8,* 42495–42509.

[246]Li, Y.; Baiyang, L.; Leran, B.; Zhen, W.; Yandong, X.; Baixiang, D.; Dandan, Z.; Yufu, Z.; Jun, L.; Rutong, Y.; Hongmei, L. Reduction-responsive petoz-ss-pcl micelle with tailored size to overcome blood–brain barrier and enhance doxorubicin antiglioma effect, *Drug Deliv*. 2017, *24,* 1782–1790.

[247]Meng, L.; Chu, X.; Xing, H.; Liu, X.; Xin, X.; Chen, L.; Jin, M.; Guan, Y.; Huang, W.; Gao, Z. Improving glioblastoma therapeutic outcomes via doxorubicin-loaded nanomicelles modified with borneol, *Int. J. Pharm*. 2019, *567*, 118485.

[248]Zhan, C.; Gu, B.; Xie, C.; Li, J.; Liu, Y.; Lu, W. Cyclic RGD conjugated poly(ethylene glycol)-co-poly(lactic acid) micelle enhances paclitaxel anti-glioblastoma effect, *J. Control. Rel.* 2010, *143,* 136–142.

[249]Ran, D.; Mao, J.; Shen, Q.; Xie, C.; Zhan, C.; Wang, R.; Lu, W. GRP78 enabled micelle-based glioma targeted drug delivery, *J. Control. Rel*. 2017, *255,* 120–131.

[250]Chen, X.; Tai, T.; Gao, J.; Qian, J.; Zhang, M.; Li, B.; Xie, C.; Lu, L.; Lu, W.; Lu, W. A stapled peptide antagonist of MDM2 carried by polymeric micelles sensitizes glioblastoma to temozolomide treatment through p53 activation, *J. Control. Rel.* 2015, *218,* 29–35.

[251]Zhan, C.; Wei, X.; Qian, J.; Feng, L.; Zhu, J.; Lu, W. Co-delivery of TRAIL gene enhances the anti-glioblastoma effect of paclitaxel in vitro and in vivo, *J. Control. Rel.* 2012, *160,* 630–636.

[252]Qian, X.; Long, L.; Shi, Z.; Liu, C.; Qiu, M.; Sheng, J.; Pu, P.; Yuan, X.; Ren, Y.; Kang, C. Star-branched amphiphilic PLA-b-PDMAEMA copolymers for co-delivery of miR-21 inhibitor and doxorubicin to treat glioma, *Biomaterials*. 2014, *35,* 2322–2335.

[253]Oh,B.; Han, J.; Choi, E.; Tan, X.; Lee, M. Peptide Micelle-Mediated Delivery of Tissue-Specific Suicide Gene and Combined Therapy with Avastin in a Glioblastoma Model, *J. Pharm. Sci.* 2015, *104,* 1461–1469.

[254]Peng, Y.; Huang, J.; Xiao, H.; Wu, T.; Shuai, X. Codelivery of temozolomide and sirNa with polymeric nanocarrier for effective glioma treatment, *Int. J. Nanomed.* 2018, *13,* 3467–3480.

[255]Sarisozen, C.; Dhokai, S.; Tsikudo, E.G.; Luther, E.; Rachman, I.M.; Torchilin, V.P. Nanomedicine based curcumin and doxorubicin combination treatment of glioblastoma with scFv-targeted micelles: In vitro evaluation on 2D and 3D tumor models, *Eur. J. Pharm. Biopharm.* 2016, *108*, 54–67.

[256]Wang, G; Wang, J.J.; Li, F.; Tony To, S.S. Development and Evaluation of a Novel Drug Delivery: Pluronics/SDS Mixed Micelle Loaded with Myricetin in Vitro and in Vivo, *J. Pharm. Sci.* 2016, *105*, 1535–1543.

[257]Gao, X.; Yu, T.; Xu, G.; Guo, G.; Liu, X.; Hu, X.; Wang, X.; Liu, Y.; Mao, Q.; You, C.; Zhou, L. Enhancing the anti-glioma therapy of doxorubicin by honokiol with biodegradable self-assembling micelles through multiple evaluations, *Sci. Rep.* 2017, *7,* 1–19.

[258]Li, A.J.; Zheng, Y.H.; Liu, G.D.; Liu, W.S.; Cao, P.C.; Bu, Z.F. Efficient delivery of docetaxel for the treatment of brain tumors by cyclic RGD-tagged polymeric micelles, *Mol. Med. Rep*. 2015, *11*, 3078–3086.

[259]Nguyen, J.; Cooke, J.R.N.; Ellis, J.A,; Deci, M.; Emala, C.W.; Bruce, J.N.; Bigio, I.J.; Straubinger, R.M.; Joshi, S. Cationizable lipid micelles as vehicles for intraarterial glioma treatment, *J. Neuro-Oncol*. 2016,*128,* 21–28.

[260]Guo, X.; Wu, G.; Wang, H.; Chen, L. Pep-1&borneol–Bifunctionalized Carmustine-Loaded Micelles Enhance Anti-Glioma Efficacy Through Tumor-Targeting and BBB-Penetrating, *J. Pharm. Sci.* 2019, *108,* 1726–1735.

[261]Zhang, H.; Liu, X.; Xu, K.; Du, B.; Zhu, C.; Li, Y. Biodegradable polyurethane PMeOx-PU(SS)-PMeOx micelles with redox and pH-sensitivity for efficient delivery of doxorubicin, *Eur. Polym. J*. 2020, *140*, 110054.

[262]Jimenez-Sanchez, M.; Licitra, F.; Underwood, B.R.; Rubinsztein, D.C. Huntington's Disease: Mechanisms of Pathogenesis and Therapeutic Strategies, *Cold Spring Harb Perspect Med.* 2017, *7*, a024240.

[263]Palareti, G.; Legnani, C.; Cosmi, B.; Antonucci, E.; Erba, N.; Poli, D.; Testa, S.; Tosetto, S. Comparison between different D-Dimer cutoff values to assess the individual risk of recurrent venous thromboembolism: Analysis of results obtained in the DULCIS study. *Int. J. Lab. Hematol.* 2016, *38,*

42–9.

[264]Reiner, A.; Albin, R.L.; Anderson, K.D.; D'Amato, C.J.; Penney, J.B.; Young, A.B. Differential loss of striatal projection neurons in Huntington disease, *PNAS*. 1988, *85*, 5733–5737.

[265]Sales, T.A.; Prandi, I.G.; De Castro, A.A.; Leal, D.H.S.; da Cuncha, E.F.F.; Kuca, K.; Ramalho, T.C. Recent Developments in Metal-Based Drugs and Chelating Agents for Neurodegenerative Diseases Treatments, *Int. J. Mol. Sci*. 2019, *20*, 1829.

[266]Relaño-Ginés, A.; Lehmann, S.; Brillaud, E.; Belondrade, M.; Casanova, D.; Hamela, C.; Vincent, C.; Poupeau, S.; Sarniguet, J; Alvarez, T.; Arnaud, J.D.; Maurel, J.C.; Crozet, C. Lithium as a disease-modifying agent for prion diseases, *Transl. Psychiatry.* 2018, *8*, 163.

[267]Xue, R.; Han, Y.; Xiao, Y.; Huang, J.; Tang, B.Z.; Yan, Y. Lithium Ion Nanocarriers Self-Assembled from Amphiphiles with Aggregation-Induced Emission Activity, *ACS Appl. Nano Mater.* 2018, *1*, 122–131.

[268]Medić, B.; Stojanović, M.; Stimec, B.V.; Divac, N.; Vujović, K.S.; Stojanović, R.; Čolović, M.; Krstić, D.; Prostran, M. Lithium-Pharmacological and Toxicological Aspects: The Current State of the Art, *Curr. Med. Chem.* 2018, *27*, 337–351.

[269]Duggirala, N.K.; Smith, A.J.; Wojtas, L.; Shytle, R.D.; Zaworotko, M.J. Physical stability enhancement and pharmacokinetics of a lithium ionic cocrystal with glucose, *Cryst. Growth. Des.* 2014, *14*, 6135–6142.

[270]Pepe, G.; Calce, E.; Verdoliva, V.; Saviano, M.; Maglione, V.; Di Pardo, A.; De Luca, S. Curcumin-loaded nanoparticles based on amphiphilic hyaluronan-conjugate explored as targeting delivery system for neurodegenerative disorders, *Int. J. Mol. Sci.* 2020, *21*, 1–13.

[271]Van den Bos, M.A.J.; Geevasinga, N.; Higashihara, M.; Menon, P.; Vucic, S. Pathophysiology and diagnosis of ALS: Insights from advances in neurophysiological techniques, *Int. J. Mol. Sci*. 2019, *20*, 2818.

[272]Poppe, L.; Rué, L.; Robberecht, W.; Van Den Bosch, L. Translating biological findings into new treatment strategies for amyotrophic lateral sclerosis (ALS), *Exp. Neurol*. 2014, *262*, 138–151.

[273]Hardiman, O.; Al-Chalabi, A.; Chio, A.; Corr, E.M.; Logroscino, G.; Robberecht, W.; Shaw, P.J.; Simmons, Z.; Van Den Berg, L.H. Amyotrophic lateral sclerosis, *Nat. Rev. Dis. Primers.* 2017, *3*, 1-18.

[274]Oskarsson, B.; Gendron, T.F.; Staff, N.P. Amyotrophic Lateral Sclerosis: An Update for 2018, *Mayo Clinic Proceedings*. 2018, *93*, 1617–1628.

[275]Ragagnin, A.M.G.; Shadfar, S.; Vidal, M.; Jamali, M.S.; Atkin, J.D. Motor neuron susceptibility in ALS/FTD, *Front. Neurosci*. 2019, *13*, 532.

[276]Dharmadasa, T.; Kiernan, M.C. Riluzole, disease stage and survival in ALS, *The Lancet Neurol.* 2018, *17*, 385–386.

[277]Blanco, E.; Shen,H.; Ferrari, M. Principles of nanoparticle design for overcoming biological barriers to drug delivery, *Nat. Biotechnol.* 2015, *33*, 941–951.

[278]Tripodo, G.; Chlapanidas, T.; Perteghella, S.; Vigani, B.; Mandracchia, D.; Trapani, A.; Galuzzi, M/.; Tosca, M.C.; Antonioli, B.; Gaetani, P.; Marazzi, M.; Torre, M.L. Mesenchymal stromal cells loading curcumin-INVITE-micelles: A drug delivery system for neurodegenerative diseases, *Colloids Surf B Biointerfaces*. 2015, *125*, 300–308.

[279]Jin, Q.; Cai, Y.; Li, S.; Liu, H.; Zhou, X.; Lu, C.; Gao, X.; Qian, J.; Zhang, J.; Ju, S.; Li, C. Edaravone-encapsulated agonistic micelles rescue ischemic brain tissue by tuning blood-brain barrier permeability, *Theranostics.* 2017, *7*, 884–898.

[280]Suksiriworapong, J.; Rungvimolsin, T.; Agomol, A.; Junyaprasert, V.B.; Chantasart, D. Development and Characterization of Lyophilized Diazepam-Loaded Polymeric Micelles, *AAPS. Pharm. Sci. Tech.* 2014, *15*, 52–64.

[281]Liu, J.; He, Y.; Zhang, J.; Li, J.; Yu, X.; Cao, Z.; Meng, F.; Zhao, Y.; Wu, X.; Shen, T.; Hong, Z. Functionalized nanocarrier combined seizure-specific vector with P-glycoprotein modulation property for antiepileptic drug delivery, *Biomaterials*. 2016, *74*, 64–76.

[282]Yu, A.; Lv, J.; Yuan, F.; Xia, Z.; Fan, K.; Chen, G.; Ren, J.; Lin, C.; Wei, S.; Yang, F. mPEG - PLA/TPGS mixed micelles via intranasal administration improved the bioavailability of lamotrigine in the hippocampus, *Int. J. Nanomed*. 2017, *12*, 8353–8362.

[283]Singla, P.; Garg, S.; Bhatti, R.; Peeters, M.; Singh, O.; Mahajan, R.K. Solubilization of hydrophobic drugs clozapine and oxcarbazepine in the lower and higher molecular weight pluronic mixed micelles-a physicochemical, In vitro release and In vitro anti-oxidant study, *J. Mol. Liq*. 2020, *317*, 113816.

[284]Muthu, M.S.; Sahu, K.; Sonali, Abdulla, A.; Kaklotar, D.; Rajesh, C.V.; Singh, S.; Pandey, B.L. Solubilized delivery of paliperidone palmitate by d- alpha-tocopheryl polyethylene glycol 1000

succinate micelles for improved short-term psychotic management, *Drug Deliv*. 2016, *23*, 230–237.

[285]Patil, P.H.; Wankhede, P.R.; Mahajan, H.S.; Zawar, L.R. Aripiprazole-Loaded Polymeric Micelles: Fabrication, Optimization and Evaluation using Response Surface Method, *Recent Pat Drug Deliv. Formul*. 2018, *12*, 53–64.

[286]Pokharkar, V.; Suryawanshi, S.; Dhapte-Pawar, V. Exploring micellar-based polymeric systems for effective nose-to-brain drug delivery as potential neurotherapeutics, *Drug Deliv. Transl. Res.* 2020, *10*, 1019–1031.

[287]Yokoyama, M. Clinical Applications of Polymeric Micelle Carrier Systems in Chemotherapy and Image Diagnosis of Solid Tumors. *J. Exp. Clin. Med.* 2011, *3*, 151–8.

[288] Pomara, C.; Pascale, N.; Maglietta, F.; Neri, M.; Riezzo, I.; Turillazzi, E. Use of contrast media in diagnostic imaging: medico-legal considerations, *Radiol. Med*. 2015, *120*, 802–809.

[289]Torchilin, V.P. PEG-based micelles as carriers of contrast agents for different imaging modalities, Adv. Drug Deliv. Rev. 2002, *54*, 235–252.

[290]Yin, T.; Liu, X.; J. Wang, Y. An, Z. Zhang, L. Shi, Thermosensitive mixed shell polymeric micelles decorated with gold nanoparticles at the outmost surface: Tunable surface plasmon resonance and enhanced catalytic properties with excellent colloidal stability, *RSC Adv.* 2015, *5*, 47458–47465.

[291]Varela-Moreira, A.; Shi, Y.; Fens, M.H.AM.; Lammers, T.; Hennink, W.E.; Schiffelers, R.M. Clinical application of polymeric micelles for the treatment of cancer, *Mater. Chem. Front*. 2017, *1*, 1485–1501.

[292]Liang, Y.; Huo, Q.; Lu, W.; Jiang, L.; Gao, W.; Xu, L.; Han, S.; Cao, J.; Zhang, T.; Sun, Y.; He, B. Fluorescence resonance energy transfer visualization of molecular delivery from polymeric micelles, *J. Biomed. Nanotechnol*. 2018, *14*, 1308–1316.

[293]Xiao, Y.; Hong, H.; Javadi, A.; Engle, J.W.; Xu, W.; Yang, Y.; Zhang, Y.; Barnhart, T.E.; Cai, W.; Gong, S. Multifunctional unimolecular micelles for cancer-targeted drug delivery and positron emission tomography imaging, *Biomaterials.* 2012, *33*, 3071–3082.

[294]Chen, G.; Wang, L.; Cordie, T.; Vokoun, C.; Eliceiri, K.W.; Gong, S. Multi-functional self-

fluorescent unimolecular micelles for tumor-targeted drug delivery and bioimaging, *Biomaterials*. 2015, *47*, 41–50.

[295]Zhou, Q.; Mu, K.; Jiang, L.; Xie, H.; Liu, W.; Li, Z.; Qi, H.; Liang, S.; Xu, H.; Zhu, Y.; Zhu, W.; Yang, X. Glioma-targeting micelles for optical/magnetic resonance dual-mode imaging, *Int. J. Nanomed*. 2015, *10*, 1805–1818.

[296]Garello, F.; Pagoto, A.; Arena, F.; Buffo, A.; Blasi, F.; Alberti, D.; Terreno, E. MRI visualization of neuroinflammation using VCAM-1 targeted paramagnetic micelles, *Nanomed. Nanotechnol. Biol. Med.* 2018, *14*, 2341–2350.

[297]Shiraishi, K.; Wang, Z.; Kokuryo, D.; Aoki, I.; Yokoyama, M. A polymeric micelle magnetic resonance imaging (MRI) contrast agent reveals blood–brain barrier (BBB) permeability for macromolecules in cerebral ischemia-reperfusion injury, *J. Control. Rel.* 2017, *253*, 165–171.

[298]Wu, B.; Deng, K.; Lu, S.; Zhang, C.; Ao, Y.; Wang, H.; Mei, H.; Wang, C.; Xu, H.; Hu, B.; Huang, S. Reduction-Active Fe3O4-loaded micelles with Aggregation- Enhanced MRI Contrast for Differential Diagnosis of Neroglioma, *Biomaterials*, 2021, *268*, 120531.

[299] Patents.google.com[a], https://patents.google.com/patent/CA2319057C/en?oq=CA2319057C, Accessed on 15 August, 2021

[300]Patents.google.com[b],https://patents.google.com/patent/EP1652512A1/en?oq=Reverse+micelle+composition+for+delivery+of+metal+cations+comprising+a+diglyceride+and+a+phytosterol+and+method+of+preparation, Accessed on 15 August 2021

[301]Patents.google.com[c],https://patents.google.com/patent/CA2756581A1/en?oq=CA2756581A1, Accessed on 15 August 2021

[302] Patents.google.com[d], https://patents.google.com/patent/CN102614105A/en?oq=CN102614105A, Accessed on 15 August 2021

[303] Patents.google.com[e], https://patents.google.com/patent/CN102212116B/en?oq=CN102212116B, Accessed on 15 August 2021

[304] Patents.google.com[f], https://patents.google.com/patent/CN103182087B/en?oq=CN103182087B, Accessed on 15 August 2021

[305] Patents.google.com[g], https://patents.google.com/patent/CN104586765A/en?oq=CN104586765A, Accessed on 15 August 2021

[306] Patents.google.com[h], https://patents.google.com/patent/US9393308B2/en?oq=US9393308B2, Accessed on 15 August 2021

[307] Patents.google,com[i], https://patents.google.com/patent/US10758484B2/en?oq=US10758484B2, Accessed on 15 August 2021

[308] Patents.google.com[j], https://patents.google.com/patent/CN108339124B/en?oq=CN108339124B, Accessed on 15 August 2021

[309]Raval, N.; Maheshwari, R.; Shukla, H.; Kalia, K.; Torchilin, V.P.; Tekade, R.K. Multifunctional polymeric micellar nanomedicine in the diagnosis and treatment of cancer, *Mater. Sci. Eng C.* 2021, *126*, 112186.

[310]He, Z.; Wan, X.; Schulz, A.; Bludau, H.; Dobrovolskaia, M.A.; Stern, S.T.; Montgomery,S.A.; Yuan, H.; Li, Z.; Alakhova, D.; Sokolsky, M.; Darr, D.B.; Perou, C.M.; Jordan, R.; Kabanov, A.V. A High Capacity Polymeric Micelle of Paclitaxel: Implication of High Dose Drug Therapy to Safety and In Vivo Anti-Cancer Activity, *Biomaterials.* 2017, *101*, 296–309.

[311]Caster, J.M.; Patel, A.N.; Zhang, T.; Wang, A. Investigational nanomedicines in 2016 : a review of nanotherapeutics currently undergoing clinical trials, *Wiley Interdiscip. Rev. Nanomed. Nanobiotechnol.* 2017, *9*, 1416.

[312]Szunerits, S.; Melinte, S.; Voronova, A.; Abderrahmani, A. The impact of chemical engineering and technological advances on managing diabetes : present and future concepts, *Chem. Soc. Rev.* 2020, *50*, 2102-2146.

[313]Bobo, D.; Robinson, K.J.; Islam, J.; Thurecht, K.J.; Corrie, S.R. Nanoparticle-Based Medicines : A Review of FDA-Approved Materials and Clinical Trials to Date, *Pharm. Res.* 2016, *33*, 2373–2387.

[314] Lu, Y.; Zhang, E.; Yang, J.; Cao, Z. Strategies to improve micelle stability for drug delivery, *Nano. Res*. 2017, *176*, 139–148.